ESD-TR-71-362

MTR-2143

RECURSIVE NAVIGATION: PROGRAM DESCRIPTION AND CHARACTERISTIC PERFORMANCE, AS INDICATED BY SIMULATION AND ANALYSIS

R. C. Snodgrass

OCTOBER 1971

Prepared for

DEPUTY FOR PLANNING AND TECHNOLOGY
ELECTRONIC SYSTEMS DIVISION
AIR FORCE SYSTEMS COMMAND
UNITED STATES AIR FORCE
L. G. Hanscom Field, Bedford, Massachusetts

Project 5170

Prepared by
THE MITRE CORPORATION
Bedford, Massachusetts

Contract F19(628)-71-C-0002

ESD-TR-71-362

MTR-2143

RECURSIVE NAVIGATION: PROGRAM DESCRIPTION AND CHARACTERISTIC PERFORMANCE, AS INDICATED BY SIMULATION AND ANALYSIS

R. C. Snodgrass

OCTOBER 1971

Prepared for

DEPUTY FOR PLANNING AND TECHNOLOGY
ELECTRONIC SYSTEMS DIVISION
AIR FORCE SYSTEMS COMMAND
UNITED STATES AIR FORCE
L. G. Hanscom Field, Bedford, Massachusetts

Project 5170

Prepared by

THE MITRE CORPORATION
Bedford, Massachusetts

Contract F19(628)-71-C-0002

ABSTRACT

This document provides a current program description of, and shows the capabilities indicated by, the recursive navigation simulation. Two sets of simulation data are examined in some detail; one resembling the PLRACTA Demonstration testbed and one characteristic of a large tactical area with many aircraft. It will be shown that performance can be predicted with some confidence for certain specific situations.

ACKNOWLEDGMENTS

I wish to thank those associated with the PLRACTA project who through encouragement and hearty discussion participated in the development of the recursive navigation algorithm. I am especially indebted to the computer programming support provided by Messrs. Lewis C. Corey and Charles LaRosa. Mr. Corey programmed the early models and carried the simulation development through essentially to its present structure. Mr. LaRosa, who also participated in that development, has patiently recompiled at least thirty sets of program modifications. Their help in processing some three hundred and fifty simulation "runs" has been invaluable. Finally, I must thank Miss Mary Stewart for her assistance in putting together this technical report.

TABLE OF CONTENTS

LIST OF ILLUSTRATIONS

LIST OF ILLUSTRATIONS, Continued

LIST OF ILLUSTRATIONS, Concluded

SECTION I

INTRODUCTION

The development of the recursive navigation simulation, begun in January of 1969, has been evolutionary in nature. Starting with a very simple model, the scope and complexity of the simulation was increased only as confidence in the recursive navigation algorithm warranted. The course of the development was full of surprises and frustrations, though generally solutions were just around the corner. However it is not intended in this document to give a history of that development but rather to provide a current program description of, and to show the capabilities indicated by, the recursive navigation simulation. The latter will be accomplished by examining in some detail results of some of the latest simulation "runs." It will be shown that tracked position accuracy can be maintained at or better than the 100 foot measurement accuracy over a large portion of the navigation sector. It will also be shown that performance can be predicted with some confidence (and some reservation), at least for certain specific situations.

The document proper begins with a general, but brief, description of the recursive navigation simulation program in Section II. In Section III, the recursive operations are examined in considerable detail. These include observation, error estimation, smoothing and prediction. The expected performance of a system member is the subject of Section IV. This is treated in terms of the transient and steady state response characteristics of an α - β tracker. In Section V results of recent simulations of the PLRACTA Demonstration are presented. The organization of this section follows a typical start-up sequence: initial synchronization of a reference site, steady state reference operation, initial synchronization and position location of the ground mobile unit and subsequent steady state operation, and then, entry of an airborne unit into the system and subsequent interaction with the ground unit. The section closes with an example of airborne extension of coverage to a remote ground unit. Much of the foregoing is expanded in Section VI to the large tactical area with many aircraft. Additional topics include: the maintenance of synchronization at a remote reference station, and navigation capability of aircraft with--and without--instrument inputs. Finally, the capability of aircraft to navigate while relying solely on airborne data sources is demonstrated.

SECTION II

GENERAL DESCRIPTION

This program simulates a cyclic, time-slotted communication and navigation system consisting of one stationary ground master station, two or more stationary ground reference stations, ground units and airborne units. There exists a repeating frame time which is divided into consecutively numbered transmission slots. Each slot contains a guard time sufficient to prevent interference over an area of approximately 300 to 400 nautical miles square. Each unit transmits a message containing position, status, and data priority at the estimated start time of his assigned slot--ground and airborne units, once per frame, master and reference stations, several times (as desired) per frame. Using the position reports from other system members as a basis for measurement, each unit "tracks" his own position and time variables. The simulation can accommodate from 2 to 50 units utilizing up to 500 slots. There will be as many blank slots as necessary to fill the specified frame time.

UNIT TYPES

Unit types are specified in program input and remain constant throughout a problem run. A brief description of the four unit types and their functions follows.

Master	A stationary ground unit which provides the system time and position reference. Measures "apparent" system error and includes the information in position reports as feedback (TF, XF, YF).
Reference	A sited, stationary ground unit. Adjusts timing estimates (t, $\dot{t}$) only, since position is assumed known. Does not process feedback. Reference sites prevent the system from rotating about the master.
Ground	An unsited ground unit, stationary or quasi-stationary. Adjusts timing and position estimates (t, $\dot{t}$, x, y). Processes feedback. Assumes zero velocity.
Airborne	Any moving unit. Adjusts timing, position, speed, and heading estimates (t, $\dot{t}$, x, y, vp, h). Processes feedback.

STATUS

Airborne or ground units may be "active" or passive." Master or reference units must always be active. Only active units may be used as data sources (and then, only if they possess the appropriate data priority items). Airborne and ground units may follow one of five possible status histories during a run, depending on program input.

1. Active throughout.
2. Passive throughout.
3. Passive, changing (once) to active, after completion of n frames with successful least squares solution.
4. Active or passive, potentially changing status every frame depending on the "goodness" of data.
5. Same as 4, except remaining passive during turns.

DATA PRIORITY

There are four levels of data priority ranging from Priority 1, the best, to Priority 4, the worst. Each unit attempts to maintain its navigation capability using that set of data sources with the best possible priority. In turn, the unit establishes its own data priority based upon its data sources. By definition, the master is always Priority 1. The criteria for establishing the data priority is given in Table 1 following.

TABLE 1

DATA PRIORITY CRITERIA

Data Priority	Ground or Airborne Unit	Reference Station
1	Receiving master and use only Priority 1 sources.	If master in sight, use only master data. If master not in sight, use only Priority 1 sources.
2	Use only Priority 1 sources but not receiving master.	Use only Priority 2 sources, Priority 1 not available.
3	Use both Priority 1 and 2, as there are insufficient Priority 1 sources.	Use only Priority 3 sources, Priority 1 or 2 not available.

TABLE 1, Continued

DATA PRIORITY CRITERIA

Data Priority	Ground or Airborne Unit	Reference Station
4	Use any source, as there are insufficient Priority 1 and 2 sources.	Use only Priority 4 sources, Priority 1, 2, and 3 not available.

If a unit fails to get a navigation solution due to insufficient or inappropriate data, its priority is increased by one step (up to 4), opening up a larger set of inputs for the next cycle and removing the unit as a source for certain other units. Similarly, as long as a unit is getting a good solution at data priority levels above 1, a potential count is maintained to see if it would be possible to operate as a lower (better) data priority source. Whenever the potential count so indicates, the priority is lowered by one step (down to 1) adding the unit as a source for units of appropriate priority. In the simulation, airborne and ground units are given initial priorities of 4 if the master is not in sight; otherwise, an initial priority of 1 is assigned.

SIMULATION

The program simulates both the true world, which includes the ground master station's clock and position, and the assumed world, as seen from each unit's point of view. Each unit is considered to have a velocity vp, h, ż and to be at an altitude z above the point x, y on a flat plane. Realism is added by screening out reports from transmitters that would be beyond the line-of-sight of the receiver.

An airborne unit may follow a straight line path, or a maneuver made up of an alternating series of straight lines and arcs of a circle, and in turn, the arcs may alternate or maintain a constant direction. Two types of tracking are available for airborne units. "Data tracking" is based solely on range measurements--the computer is not made aware of any intended speed and heading changes. "Instrument tracking" makes use of known heading changes.

Program inputs include the mean bias and standard deviation (gaussian) of errors in clock setting, clock rate, time measurement, transmission time, position, altitude, speed, heading, and altitude rate. Additionally, for a maneuvering unit, leg time, turn time,

turn size, and direction are specified.

Assumed initial positions and clock settings are perturbed by a random deviate at the start of a run. True velocity is perturbed by a random deviate at the start of each frame. Under input control, this perturbation may be about the input bias (FIXED) or about the previous value (RANDOM)--the latter produces shakier tracks. Transmission time is perturbed with each transmission and time of arrival measurement is perturbed with each measurement.

At the end of each frame, the true and assumed conditions, the errors, and the adjustments made to estimates are available for output purposes, on each unit.

A run consists of a stated number of frames. A problem may consist of one or more runs--iterations over the same set of conditions differing only by the starting random number.

SECTION III

TRACKING

Tracking is a recursive operation including observation, error estimation, smoothing, and prediction. It is applied to the time and position variables which describe the state of each unit. Each unit monitors available position reports. Upon receipt of an active transmission from an appropriate unit, the time elapse with respect to start slot is measured to determine the one-way "measured range." A "computed range" is determined by differencing the position data contained in the message with the receivers own currently updated position estimate. The difference between measured range and computed range is called the "range discrepancy" and represents an observation. Observations are collected, over the period of a frame, in the form of running sums, representing matrix elements. At the end of the frame, these sums are used to obtain least squares, linear, unbiased estimates of errors in assumptions of time and position. The method of obtaining the estimates varies with unit type and status as will be shown in the following sections. These error estimates are then entered into difference equations (α and α - β trackers) which derive, recursively, estimates of timing (t, $\dot{t}$), position (x, y), speed and heading (vp, h), as applicable.

OBSERVATION

The key to recursive navigation is the periodic position report which each unit transmits in its assigned slot(s). This report always contains position, no matter how poorly known, status (active or passive) and data priority. If the latter two items indicate that this is an appropriate message to add to the data set, the "measured" range is determined. In a "live" system this is simply the product of propagation velocity and elapsed time, the latter being message receipt time less start slot time. In the simulation, however, it is necessary to construct the true range and add the effect of the joint timing errors between sender and receiver, to arrive at the measured range, Rm. The receiving unit then extrapolates its own position estimate up to the message arrival time and determines the "computed range." The x, y, and z components of computed range to the j^{th} unit are:

$$\begin{aligned} \delta x &= x_j - x' \\ \delta y &= y_j - y' \\ \delta z &= z_j - z' \end{aligned} \qquad (1)$$

where the primed coordinates represent the receiving units updated position. The computed range, P, then is given by

$$P = \sqrt{\delta x^2 + \delta y^2 + \delta z^2} \tag{2}$$

The observation then is the measured range minus the computed range. It has been termed the "range discrepancy" and is given by

$$\Delta R = Rm - P \tag{3}$$

Now, the assumption is that the range discrepancy is made up of components of time (range) error, er, and position error, ex, ey, and ez, at the receiving unit; that is

$$\Delta R = \begin{bmatrix} 1 & \beta x & \beta y & \beta z \end{bmatrix} \cdot \begin{bmatrix} er \\ ex \\ ey \\ ez \end{bmatrix} \tag{4}$$

where the direction cosine terms are given by

$$\begin{aligned} \beta x &= \delta x / P \\ \beta y &= \delta y / P \\ \beta z &= \delta z / P \end{aligned} \tag{5}$$

However, since no attempt is made to correct for altitude error, ez, the effect of altitude error is diminished by projecting the measurement onto the horizontal plane. Computing the horizontal direction cosine, βh, by

$$\beta h = \sqrt{\beta x^2 + \beta y^2} = \sqrt{1 - \beta z^2} \tag{6}$$

the horizontal component of the range discrepancy is given by

$$\Delta R \cdot \beta h = \begin{bmatrix} \beta h & \frac{\beta x}{\beta h} & \frac{\beta y}{\beta h} \end{bmatrix} \cdot \begin{bmatrix} er \\ ex \\ ey \end{bmatrix} \tag{7}$$

The above observation on the j^{th} unit is now in the standard form

$$\theta_j = A_j \cdot b \tag{8}$$

as given by Deutsch (Reference 1), where the elements A_j are the direction cosines and b is the error vector.

SUMMATION

The series of observations made during a frame have the form

$$\theta = A \cdot b \tag{9}$$

which contains the elements

$$\begin{bmatrix} \Delta R_1 \cdot \beta h_1 \\ \Delta R_2 \cdot \beta h_2 \\ \vdots \\ \Delta R_n \cdot \beta h_n \end{bmatrix} = \begin{bmatrix} \beta h_1 & \frac{\beta x_1}{\beta h_1} & \frac{\beta y_1}{\beta h_1} \\ \beta h_2 & \frac{\beta x_2}{\beta h_2} & \frac{\beta y_2}{\beta h_2} \\ \vdots & \vdots & \vdots \\ \beta h_n & \frac{\beta x_n}{\beta h_n} & \frac{\beta y_n}{\beta h_n} \end{bmatrix} \cdot \begin{bmatrix} er \\ ex \\ ey \end{bmatrix}$$

The least squares linear estimate, $\hat{b}$, of the error vector, b, where

$$b = \begin{bmatrix} er \\ ex \\ ey \end{bmatrix} \tag{10}$$

is given by

$$\hat{b} = [A^T A]^{-1} A^T \theta \tag{11}$$

according to Deutsch (Reference 1). The solution, $\hat{b}$, can be obtained in a straight-forward manner by use of Cramer's rule. It is not necessary to save all of the (4 x n) elements in order to obtain the least squares solution; only the elements making up the $A^T A$ matrix and the $A^T \theta$ matrix need be saved.

$$\text{Because } A^T \theta = \begin{bmatrix} \Sigma \Delta R_j \cdot \beta h^2{}_j \\ \Sigma \Delta R_j \cdot \beta x_j \\ \Sigma \Delta R_j \cdot \beta y_j \end{bmatrix} \tag{12}$$

$$\text{and } A^TA = \begin{bmatrix} \Sigma\beta h^2_j & \Sigma\beta x_j & \Sigma\beta y_j \\ \Sigma\beta x_j & \Sigma\beta x^2_j/\beta h^2_j & \Sigma\beta x_j \cdot \beta y_j/\beta h^2_j \\ \Sigma\beta y_j & \Sigma\beta x_j \cdot \beta y_j/\beta h^2_j & \Sigma\beta y_j{}^2/\beta h^2_j \end{bmatrix} \quad (13)$$

It is only necessary to accumulate nine sums regardless of the sample size n. For convenience of notation in the following discussions these summation elements will be represented as

$$A^T\theta = \begin{bmatrix} dr \\ dx \\ dy \end{bmatrix} \quad (14)$$

$$\text{and } A^TA = \begin{bmatrix} cp & cx & cy \\ cx & CX2 & cxy \\ cy & cxy & CY2 \end{bmatrix} \quad (15)$$

At the start of a frame, the nine items (sums) are set to zero. Then as observations are made, appropriate data are added to the sums. At the end of a frame of data gathering then, these sums are available for determining error estimates.

SOLUTIONS AND RESTRICTIONS

The simultaneous solutions for three independent unknowns in time and position tends to contain large amplification factors. It is sensitive to noisy inputs and source errors, and therefore cannot be used without restriction.

In fact, the independent solution for three unknowns cannot be used by interacting system elements. Passive units can use this solution, however, and at least for a few frames, it does provide the best estimate of time and position error.

In fact, if there are just three data sources, the position solution is identical with loran. For this reason, the method of solution may be referred to as hyperbolation, whether referring to position or time.

Due to the steady nature of clocks, however (even crystal clocks do not maneuver violently) advantage can be taken of clock stability after several frames of pure hyperbolation. Continuing to obtain time estimates independent of position error and integrating over a long period--that is, smoothing the error estimates heavily, position estimates are then obtained dependent on time error. That is, time is assumed known and direct ranging measurements are made.

Another solution is used by reference units where position is assumed known. This is a time solution dependent upon position error.

There are then, three methods of solution to equation (11). The first is

$$1.\quad \begin{bmatrix} \hat{er} \\ \hat{ex} \\ \hat{ey} \end{bmatrix} = \begin{bmatrix} cp & cx & cy \\ cx & CX2 & cxy \\ cy & cxy & CY2 \end{bmatrix}^{-1} \cdot \begin{bmatrix} dr \\ dx \\ dy \end{bmatrix} \qquad (16)$$

This is used by passive airborne and ground units to obtain independent time (range) and position error estimates. it is also used by active airborne and ground units to obtain an independent time error estimate. There are three restrictions on this solution:

Precision Check	The magnitude of the determinant A^TA must be sufficiently large to avoid solution attempts in areas of extremely poor geometric dilution of precision.
Solution Check	The sign of the estimated range error, $\hat{er}$, must agree with the sign of dr, the sum of the range discrepancies. This avoids spurious solutions due to source bias and measurement noise. If the signs differ, $\hat{er}$ is set to zero.
Solution Clamp	Active units (which are assumed to be synchronized) restrict the magnitude of $\hat{er}$ to dampen time adjustments due to gross source or measurement error. Magnitudes of $\hat{er}$ greater than a program input MTA are limited to that value.

Solution failures due to the precision check will alter the data priority. Solution failures due to either the precision check or the solution check will alter the effective smoothing parameters used in "tracking" the clock, as will be seen in the following section.

A geometric dilution factor is also computed for use in tracking the clock. This is

$$g = \sqrt{\frac{|A^T A|}{CX2 \cdot CY2 - cxy^2}} \tag{17}$$

which is actually the inverse of the geometric dilution of precision along the time axis.

The second solution is

$$2. \begin{bmatrix} \hat{e}x \\ \hat{e}y \end{bmatrix} = \begin{bmatrix} CX2 & cxy \\ cxy & CY2 \end{bmatrix}^{-1} \cdot \begin{bmatrix} dx \\ dy \end{bmatrix} \tag{18}$$

This is used by active ground and airborne units to obtain the dependent position error estimates (direct ranging). It is also used by the master to estimate mean system position error for use in feedback. A precision check is also imposed on this solution, as in 1. above, failure of which will alter data priority.

The third solution is simply

$$3. \quad \hat{e}r = dr/cp \tag{19}$$

This is used by reference stations to compute time error estimates. (Position error is assumed to be zero.) It is also used by master to estimate mean system time error for use in feedback. In both cases, a solution clamp is imposed, as in 1. above, to dampen time adjustments due to gross source or measurement error. Reference units are limited to program input MTG, the master to MTA.

For units that automatically activate and deactivate status, the sum of the magnitudes of $\hat{e}r$, $\hat{e}x$, and $\hat{e}y$ is compared with program input BAD DATA to see if action should be taken.

FEEDBACK

Left on its own, a system, made up of active members using the least squares solutions described above, would tend to drift in time and position depending on the current net velocity error of its members and on the current net effect of measurement noise. One system member, however, has neither time error nor position error, by definition--the master station. Measurements made by the master indicate the apparent error of the master with respect to the system.

They are used to estimate the mean system error with respect to the master. These estimates, lightly smoothed are termed feedback and are transmitted once per frame in addition to, or included in, the position report. Receiving units, other than reference stations, subtract these feedback items from their own estimates of time and position error. In this manner, the net system time and position error tends to be driven to zero. The three feedback items, all in nautical miles, computed at the master unit are

$$\begin{aligned} TF &= ktm \cdot \hat{e}r \\ XF &= kpm \cdot \hat{e}x \\ YF &= kpm \cdot \hat{e}y \end{aligned} \qquad (20)$$

where the smoothing factors are input parameters selected especially for use by the master station.

It has been said that reference sites dampen the tendency of the system to rotate about the master. However, just as it was found that the master must function actively, through feedback, so may it be desirable for the references to function in an active manner. The concept of reference feedback has been added as an option to the simulation, but it has not yet been suitably tested to determine its worth or necessity.

Reference site feedback would work in the following manner. Essentially, each reference site determines apparent system x, y error, takes the component orthogonal to the direction toward master and converts this to an angular correction factor. This angular correction factor is transmitted along with the periodic position report, in a manner similar to master feedback. Non-reference units, air or ground, with data priority one, use the average of all such correction factors received and apply this orthogonally to their own direction toward master.

SMOOTHING

Smoothing is the process of converting an error estimate, $\hat{e}u$, into adjustments, Δu and $\Delta \dot{u}$, to be applied to the variable u and its first time derivative, $\dot{u}$. It is identical with the smoothing process that takes place in the simple α - β tracker. In fact, if the foregoing processes of observation and error estimation were reduced in complexity to simple coordinate measurements, the entire process of recursive navigation would be an α - β tracker in the dimensions of time and position. The α - β tracker is not a new idea--dating back to the middle fifties when it was applied to radar track-while-scan guidance schemes. See Page and Bridgeman, Reference 2 and Nemerever, Reference 3.

Having determined an error estimate, eu, for the variable, u, the smoothing equations are simply

$$\Delta u = \alpha \cdot \hat{e}u$$
$$\Delta \dot{u} = \beta \cdot \hat{e}u/\tau \qquad (21)$$

where τ is the frame time. Selection α and β is a compromise between suppression of noise and obtaining good transient response. According to Nelson (Reference 4) while the area of selection of α and β is relatively limited, there is no sharp optimum point for best noise and transient response.

In this program a simple α - β tracker is employed for the time variables t and $\dot{t}$, with equations of the form

$$\Delta t = kt \cdot \hat{e}r/c$$
$$\Delta \dot{t} = kd \cdot \Delta t/\tau \qquad (22)$$

where c is electromagnetic propagation velocity. The rate adjustment factor $\Delta \dot{t}$ is not computed for the first few frames; after that, it is limited in magnitude to program input DMAX.

Reference units use fixed values of the kt and kd so that the tracker has constant values of α = kt and β = kt · kd.

Airborne and ground units select the basic smoothing constant kt by unit type and status, and then further alter the value to consider changes in geometric dilution of precision, effective solution rate, and the passage of time. The history is maintained in item ΣG, and proceeds, once each frame, recursively

$$\Sigma G = (1\text{-}kt)\ \Sigma G$$
$$\text{If } \hat{e}r \neq 0, \text{ set } \Sigma G = \Sigma G + g \cdot kt \qquad (23)$$
$$kt' = g \cdot kt/\Sigma G, \text{ keeping } kt' \leq 1$$

The simulation is initialized so that a passive unit will start with $kt' \leq 1$, subsequently progressing through smaller values toward a steady state value near kt. Active units are initialized with the steady state value. The time adjustment factors are then computed as

in (22) except that

$$\Delta t = kt'(\hat{e}r - TF)/c \qquad (24)$$

where the feedback factor is zero if the unit cannot "see" the master. Airborne and ground units use a kd according to the relation

$$kd = kt/(2-kt) \qquad (25)$$

When in steady state, the tracker has values $\alpha = kt$ and $\beta = kt^2/(2-kt)$. This is the so-called optimum response according to Benedict and Bordner, Reference 5. When $kt' \neq kt$ the response is of course "sub optimum," but for $kt' > kt$ when adjustments Δt tend to be large, it is under responsive--a safe approach. While for $kt' < kt$, even though it is over responsive, the adjustments are small.

For position and velocity smoothing, an x, y α tracker is combined with a vp, h (speed and heading) β tracker. The latter, of course, applying only to airborne units. Ground and airborne units have a position smoothing constant dependant on unit type and status. The position adjustment factors are determined by

$$\begin{aligned} \Delta x &= kp(\hat{e}x - XF) \\ \Delta y &= kp(\hat{e}y - YF) \end{aligned} \qquad (26)$$

where the feedback factors XF and YF apply only if the unit has the master in sight.

Airborne units use speed and heading smoothing with constants kv and kh. After the first few frames in which velocity smoothing is omitted, an apparent velocity change is computed.

$$\begin{aligned} \Delta v &= (\Delta x \cdot u + \Delta y \cdot v)/(\tau \cdot vp) \text{ knots} \\ \Delta h &= -180(\Delta x \cdot v - \Delta y \cdot u)/(\pi \cdot \tau \cdot vp^2) \text{ degrees} \\ &\text{(where } \Delta h \text{ is in the range } -180 \leq \Delta h \leq 180) \end{aligned} \qquad (27)$$

the magnitudes of Δv and Δh are limited to program input values VMAX and HMAX. The parameters u and v are the west and north components of velocity--speed vp and heading h. For a "data track," which has

no instrument input this is the velocity computed last frame and in use during the current frame for position extrapolation. For "instrument tracks," in which the computer is advised of (apparent) heading changes, the velocity terms u, v, vp and h represent that just obtained for end of frame processing and is thus "current" with respect to any recent changes in heading. The smoothed velocity then is

$$\begin{aligned} vp &= vp - hv \cdot \Delta v && \text{knots} \\ h &= h - kh \cdot \Delta h && \text{degrees} \\ &\text{(where h is in the range } 0 \leq h \leq 360) \end{aligned} \tag{28}$$

the west and north components of the velocity correction are

$$\begin{aligned} \Delta u &= u + vp \sin h \\ \Delta v &= v - vp \cos h \end{aligned} \tag{29}$$

These factors are necessary only for units on instrument tracking, which have been integrating velocity to maintain a current position. They permit the velocity correction to be applied over the past frame, as will be seen in the section following covering prediction.

The west and north components of the smoothed velocity as of the end of frame are

$$\begin{aligned} u &= -vp \sin h \\ v &= +vp \cos h \end{aligned} \tag{30}$$

PREDICTION

The final step in the tracking process is now to apply the adjustments just computed to the variables of state, and predict the time for and the position to be contained in the next position report.

All units except the master determine a new estimate of clock running rate, with respect to master. This is

$$\dot{t} = \dot{t} + \Delta\dot{t} \tag{31}$$

the time for transmitting the next position report then is

$$t = t + \Delta t + \tau \cdot \dot{t} \tag{32}$$

Airborne units will assume an extrapolation time of

$$\tau a = \tau(1 + \dot{\Delta t}) + \Delta t \tag{33}$$

to move their reported position forward one frame.

In the simulation, the variables t and $\dot{t}$ are carried only implicitly. So too are the true clock rate, $\dot{T}$, which is constant, and the proper transmit time T, which advances by a constant amount each frame. The true time model for each unit could be represented as

$$\begin{aligned} \dot{T} &= \dot{T} \\ T &= T + \tau \cdot \dot{T} \end{aligned} \tag{34}$$

What is carried in the program is the time error, which is equation (34) minus equations (31) and (32), which results in

$$\begin{aligned} d &= d - \dot{\Delta t} && \text{rate error, or drift} \\ e &= e - \Delta t + \tau \cdot d && \text{setting error} \end{aligned} \tag{35}$$

Airborne units using data tracking determine their new position from

$$\begin{aligned} x &= x + u \cdot \tau a - \Delta x \\ y &= y + v \cdot \tau a - \Delta y \end{aligned} \tag{36}$$

Ground units also use equations (36) with u and v set to zero.

Airborne units using instrument tracking, however, have already moved position forward by the time interval τa. This has occurred, however, with the "old" value of velocity u and v. Therefore an additional velocity correction factor must be applied. If the changes in x and y, due to integration of u and v over the frame are represented by

$$\delta x = \int_0^{\tau a} u\,dt \tag{37}$$

$$\delta y = \int_0^{\tau a} v\,dt$$

Then the new end of frame position estimate is

$$\begin{aligned} x &= x + \delta x - \Delta x - \Delta u \cdot \tau a \\ y &= y + \delta y - \Delta y - \Delta v \cdot \tau a \\ z &= z + w \cdot \tau a \end{aligned} \tag{38}$$

(altitude, z, and altitude rate, w, are obtained external to the tracking process)

The simulation must also maintain the path of the true position. In this case the true extrapolation interval is

$$\tau x = \tau(1-d+\Delta d) + \Delta t \tag{39}$$

differing from the assumed frame interval by $d \cdot \tau$, the unresolved clock rate error. The west and north components, U and V (both time variant) of the true speed and heading, VP and H, are integrated over the true frame interval, τx, to obtain the end of frame true position

$$\begin{aligned} X &= X + \int_0^{\tau x} U dt \\ Y &= Y + \int_0^{\tau x} V dt \end{aligned} \tag{40}$$

Since the true altitude rate, W, remains constant over a one frame interval, the true altitude is simply

$$Z = Z + W \cdot \tau x \tag{41}$$

Position and velocity errors, in addition to the time errors, equations (35) are made available for simulation output as of the end of each frame. These are

$$\begin{aligned} ex &= x - X \\ ey &= y - Y \\ ez &= z - Z \\ evp &= vp - VP \\ eh &= h - H \\ eu &= u - U \\ ev &= v - V \end{aligned} \tag{42}$$

SECTION IV

EXPECTED PERFORMANCE

Before looking at simulation results, it is best to consider some of the factors affecting performance. Predictions, both qualitative and quantitative, can be made as to what performance to expect under specific sets of conditions. Those particular sets of conditions may actually never occur, but as they are approached we should expect some meaningful connection between prediction and performance.

UNBIASED SOLUTION

The error estimates derived from equations (16), (18), and (19) assume that measurements are being made on transmissions from zero error sources. Of course, they are not; nor, in general, will source errors be statistically distributed about a mean zero--unbiased. On any given measurement, the source position error in line with the receiver and the source timing error will add to the measurement error. Source position errors perpendicular to line of sight will have no effect.

To the degree that source, position, and timing errors are unbiased, they will contribute, along with measurement error, to the position error variance, about a zero mean, at the receiver. This variance can be reduced, at the receiver, by integrating over successive measurements. The amount of reduction--the noise reduction factor--is precisely determined by the particular set of smoothing constants used in the tracking process. That part of source position and timing error which is biased will, in turn, contribute to a position error bias at the receiver about which the variance is centered. Integration, at the receiver can have no effect on this error. (Integration at the master, however, can and does have an effect on net system bias, as will be shown in discussions on feedback.)

The effect of measurement and source error depends on the geometry of the receiver with respect to his sources--the system. Essentially, these errors are multiplied by a factor termed geometric dilution of precision, GDoP ($\mathring{g}p$ or $\mathring{g}t$) which is geometry sensitive. Apparently, all errors are treated equally, whether biased or unbiased.

STEADY STATE POSITION ERROR

The steady state variance, zero bias, in a single fix time and position estimate obtained by hyperbolation (pseudo ranging), as given by equation (11) or (16) is given by

$$\psi(t,x,y) = \sigma_m^2 (A^T A)^{-1} \tag{43}$$

where σ_m^2 is the variance of the measurement error on zero error sources, for equally weighted, independent observations. In terms of the present paper, equation (43) can be written

$$\begin{bmatrix} \sigma_t^2 & \sigma_{tx}^2 & \sigma_{ty}^2 \\ . & \sigma_x^2 & \sigma_{xy}^2 \\ . & . & \sigma_y^2 \end{bmatrix} = \sigma_m^2 \cdot \begin{bmatrix} cp & cx & cy \\ . & CX2 & cxy \\ . & . & CY2 \end{bmatrix}^{-1} \tag{44}$$

where the matrics are symmetrical. The elements in the righthand matrix are the sums of direction cosines, more explicitly detailed in equation (13). The sum, cp, approaches the sample size N for systems with little altitude differential.

For a symmetrical distribution of sources, taking x as the dimension along the direction to the center of those sources, and y perpendicular, the time and position error variances become

$$\begin{bmatrix} \sigma_t^2 & \sigma_{tx}^2 & 0 \\ . & \sigma_x^2 & 0 \\ . & . & \sigma_y^2 \end{bmatrix} = \sigma_m^2 \cdot \begin{bmatrix} CX2/\nabla & -cx/\nabla & 0 \\ . & cp/\nabla & 0 \\ . & . & 1/CY2 \end{bmatrix} \tag{45}$$

where $\nabla = cp \cdot CX2 - (cx)^2$

The uppermost line of Figure 1 depicts solutions to equation (45) for a three source, flat system, in terms of the ratio

$$\sqrt{\sigma_x^2 + \sigma_y^2}/\sigma_m$$

This is commonly called the geometric dilution of precision. I will label it $\dot{g}p$. It is the single fix accuracy of position determination by hyperbolation. The plot represents a unit distant d from a system with baseline width b.

If the position is integrated over several successive frames--that is, tracked in an α - β tracker, there will be a reduction in the position error variance, but not in bias. The variance in tracked position error, according to Benedict and Bordner (Reference 5) for an α - β tracker is given by

$$\sigma_{pt}^2 = \sigma_p^2\left[\frac{2\alpha^2 + \beta(2-3\alpha)}{\alpha(4-\beta-2\alpha)}\right] \tag{46}$$

taking $\sigma_p^2 = \sigma_x^2 + \sigma_y^2$ as position error variance.

Or, it could be said that the power of the tracker to reduce position error is given by the factor

$$rp = \sigma_p/\sigma_{pt} = \sqrt{\frac{\alpha(4-\beta-2\alpha)}{2\alpha^2 + \beta(2-3\alpha)}} \tag{47}$$

Expressing tracked position error, σ_{pt}, in terms of measurement error, σm, and geometric dilution of precision (position), $\dot{g}p$, this becomes

$$\sigma_{pt} = \sigma m \cdot \dot{g}p/rp \tag{48}$$

for hyperbolation. The tracked position accuracy for α = .18 and β = .018 is shown in Figure 1 as the upper dotted line. The noise reduction power of this tracker is rp = 2.67 that is, the upper, single fix curve is moved down by a factor of 2.67.

The above development holds strictly only for the theoretically "pure" α - β tracker in which the measurement occurs at the end of the tracking interval--that is, when speaking of the variance of a track history coincident with the measurement points. In fact, the "measurement" is generally spread over the frame, and the position of interest involves some small prediction beyond the last measurement. At worst, if the prediction is an entire frame, the variance will be increased by the factor $1/(1-\alpha)$ for a critically damped tracker, (compare x_k and xp_k in Table II, page 29. For the case above ($\alpha = .18$) this would increase the standard deviation of position error by 10%. However, it is likely that the effective prediction involved to be on the order of half a frame, and the increased position variance no more than 3%.

With the above qualification in mind, then the upper dotted line of Figure 1 represents the sort of steady state error performance to expect for passive units tracking successive position fixes obtained by hyperbolation.

If the clock is integrated over several (many) frames, using an α - β tracker there will be a reduction in the time error variance, as with position, similar to equation (46)

$$\sigma_{tt}^2 = \sigma_t^2 \left[\frac{2\alpha^2 + \beta(2-3\alpha)}{\alpha(4-\beta-2\alpha)}\right] \tag{49}$$

and we can talk of the power of the tracker to reduce time error, labeling the factor rt, where

$$rt = \sigma_t/\sigma_{tt} \tag{50}$$

The variance of the tracked clock error is given by equations (45) and (49). It is

$$\sigma_{tt}^2 = \sigma_m^2 \cdot CX2/rt^2 \cdot \nabla \tag{51}$$

If now, the clock is assumed true and direct ranging measurements are used to obtain position error estimates then the position error variance, for the symmetric case becomes

$$\sigma_p^2 = \sigma_x^2 + \sigma_y^2 = \sigma_m^2 \left[\frac{1}{CX2} + \frac{rt^2 \cdot (cx)^2}{\nabla \cdot CX2} + \frac{1}{CY2}\right] \tag{52}$$

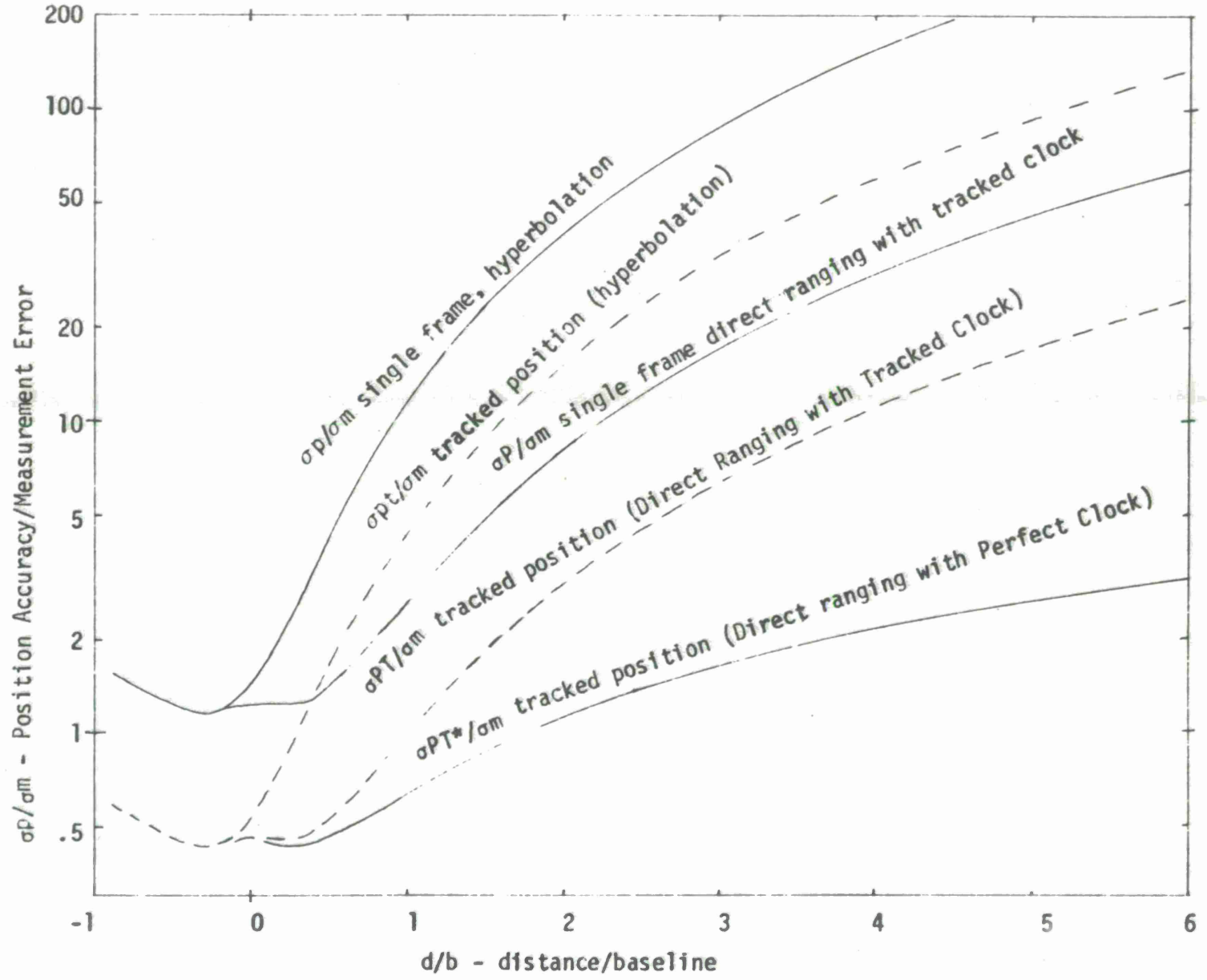

Figure 1 - Position Accuracy versus Distance from Baseline

Note that the cross track term σ_y^2 is the same as before, but the long track terms now incorporate time error. A solution to (52) is shown in Figure 1 (the middle solid line) for $\alpha_t = 0.044$ and $\beta_t = 0.001$, which were values used in some of the simulation runs. This is now the direct ranging, single fix position error with tracked clock. Note that for small distances d it is the same or nearly the same as hyperbolation, however as distance from the source is increased the improvement factor approaches rt. For the α, β's chosen, rt = 5.48.

The same qualification applied to position variance concerning measurement and prediction must also be applied to time. However, for the smoothing constants shown, this factor, something between 1 and $1/(1-\alpha)$, will have an effect 2% at most, and more likely less than 1%.

Finally, now, if the direct ranging position fixes are tracked, the position error will be reduced by the factor rp. This curve is shown as the lower dotted line in Figure 1. As the distance from the baseline is increased, the improvement factor, or the power of the trackers approaches rp · rt = 2.67 x 5.48 = 14.62. That is, a standard deviation of position error 14.62 times lower than single fix hyperbolation.

Without changing the position tracker, the best that can be done--i.e., perfect clock--is shown as the lowest curve on Figure 1. By integrating over longer time periods, this curve can be approached--limited only by the transient response problem.

Recalling that tracking is improved by the factor rp and part of the factor rt, it is possible to express an efficiency factor, eff. as a function of rt and the geometric dilution of precision (time),

$$\dot{g}t = \sigma_t/\sigma_m$$

This efficiency factor states how much of the factor rt will be applied to noise reduction. It is now possible to express the total tracking improvement as

$$\frac{\sigma p}{\sigma_{PT}} = rp\left[1 + eff(rt-1)\right] \qquad (53)$$

Or, in terms of the original measurement error, the tracked position accuracy obtainable by direct ranging can be expressed as

$$\sigma_{PT} = \sigma m * \dot{g}p / \left[rp(1+eff[rt-1]) \right] \qquad (54)$$

Figure 2 plots eff versus the geometric dilution of precision, $\dot{g}t = \sigma_t/\sigma_m$ for three values of rt, the larger being an extremely long integration interval. Part of Figure 2 is expanded and reproduced in Figure 3 and curves have been added to cover most of values of α and β that have been used in the simulation.

There are some additional factors in the tracking process which will effect the steady state solution that have yet to be discussed. The solution clamp MTA or MTG restricts the magnitude of time error estimates prior to smoothing. After the smoothing operation, DMAX limits the magnitude of time rate adjustments and VMAX and HMAX limit the velocity adjustments. The effects of these clamps and limits have not been determined analytically. However they tend to improve steady state response by reducing reaction to noisy measurements. Conversely, they tend to have a deleterious effect on transient response and must therefore be used with caution--if at all! Discussion of these factors is deferred to the following section.

TRANSIENT RESPONSE

The transient response of the damped linear oscillator is not a new subject, and it is directly applicable to the α - β tracker. This topic has been covered extensively in the literature. In this section the standard curves for Impulse, Position Step and Velocity Step response will be shown. Then the departure from standard, caused by the peculiarities of the recursive navigation algorithm will be discussed.

The position step response is indicative of the initial time synchronization or position location problem; it starts with a unit clock or position bias, but no rate error. The velocity step response starts with a unit error in time rate or velocity, from a point of zero clock or position bias. It is also indicative of the initialization process, in that rate error must be determined before a steady state condition with zero bias can be reached. It is also useful in considering departures from steady state and the nature of the return that might occur due to changes, e.g. in the relative clock running rates due to temperature changes. The impulse responses perhaps more properly belongs to the steady state considerations. It assumes a zero position and rate error followed by a measurement one unit in error--a noise spike.

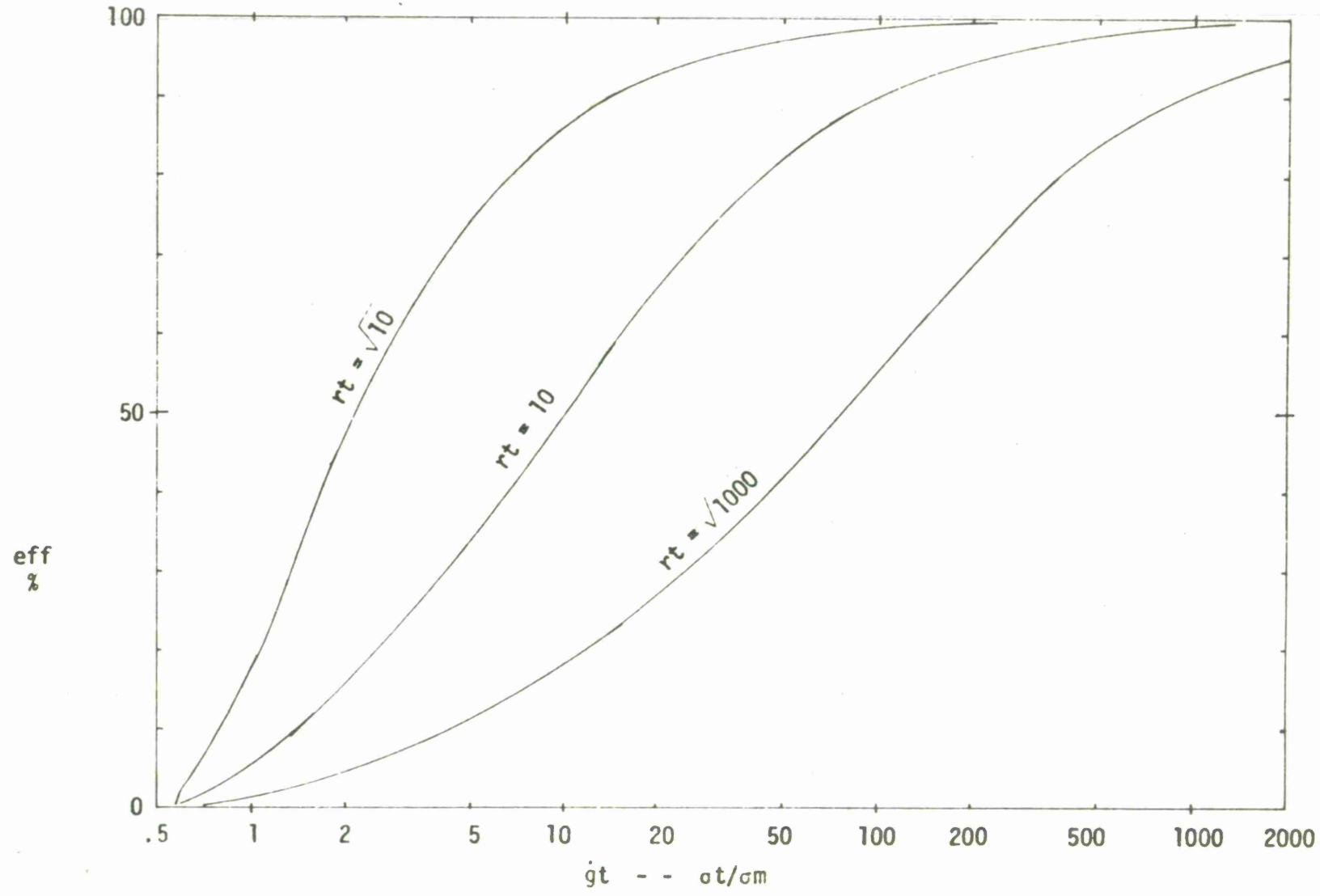

Figure 2. Efficiency Factor versus Geometric Dilution of Precision (Time)

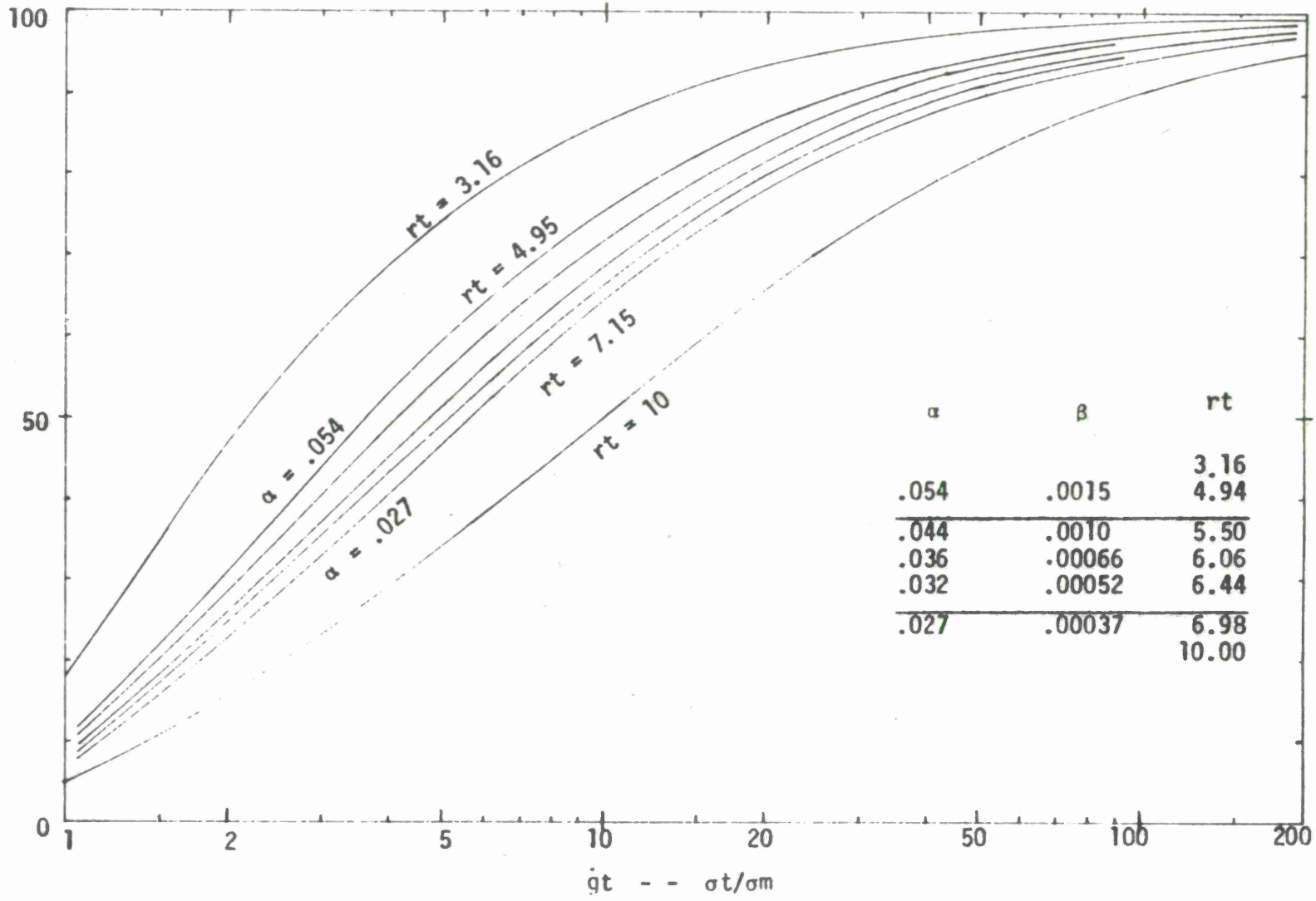

Figure 3. Efficiency Factor, Expanded

The transient solution, given by Nelson, Reference 4, for the underdamped oscillator, on the k^{th} frame, is

$$x_k = \rho^k (C_1 \cos \phi k + C_2 \sin \phi k) \tag{55}$$

where

$$\rho = \sqrt{1-\alpha} \quad \text{and} \quad \phi = \tan^{-1} \sqrt{\frac{4(1-\alpha)}{(2-\alpha-\beta)^2} - 1} \tag{56}$$

The left hand member, x_k, may be interpreted as predicted position, xp_k, smoothed position x_k, or velocity, $\dot{x}_k$, as desired as all three have the same characteristic equation

$$\lambda^2 + (\alpha+\beta-2)\lambda + (1-\alpha) = 0 \tag{57}$$

The arbitrary constants, C_1 and C_2 are determined by the initial conditions. The values of these constants for the position step, velocity step, and impulse function are shown in Table II following.

The oscillator can be pictured in terms of the half-period, the decrement and the envelope. The envelope decays by a factor $\rho = 1-\alpha$ with each passing frame. It contains the oscillations. The half-period is the number of frames from a maximum to the following minimum. Since the angle covered in one frame is ϕ, equation (56), the half period is simply

$$T/2 = \pi/\phi \tag{58}$$

The decrement, δ, tells how much the magnitude of oscillation has decreased in one half-period, (or how much the envelope has decreased). It is

$$\delta = \rho^{\pi/\phi} \tag{59}$$

The characteristics of the oscillator as determined by particular values of α and β are pictured in Figure 4 (high values) and Figure 5 (low values). The former might be applicable to the position and velocity track of an aircraft, while the latter is more applicable to clock tracking. The figures show values of δ (equation 59) in terms of per cent overshoot; the half-period (equation 58); and the reduction of variance in the steady state (equation 49). The

TABLE II

CONSTANTS FOR EQUATION (55)

Unit Position Step

(xp_k)	$C_1 = 1/(1-\alpha)$	$C_2 = -(\alpha-\beta)/(1-\alpha)\zeta$
(x_k)	$C_1 = 1$	$C_2 = -(\alpha-\beta)/\zeta$
$(\dot{x}_k)$	$C_1 = 0$	$C_2 = -2\beta/\zeta$

Unit Velocity Step

(xp_k)	$C_1 = 0$	$C_2 = 2/\zeta$
(x_k)	$C_1 = 0$	$C_2 = 2(1-\alpha)/\zeta$
$(\dot{x}_k)$	$C_1 = 1$	$C_2 = (\alpha-\beta)/\zeta$

Unit Impulse (negative)

(xp_k)	$C_1 = \alpha/(1-\alpha)$	$C_2 = [2\beta-\alpha(\alpha+\beta)]\ /(1-\alpha)\zeta$
(x_k)	$C_1 = \alpha$	$C_2 = [2\beta-\alpha(\alpha+\beta)]/\zeta$
$(\dot{x}_k)$	$C_1 = \beta$	$C_2 = -(\alpha+\beta)/\zeta$

where $\zeta = \sqrt{4(1-\alpha) - (2-\alpha-\beta)^2}$ in all of the above

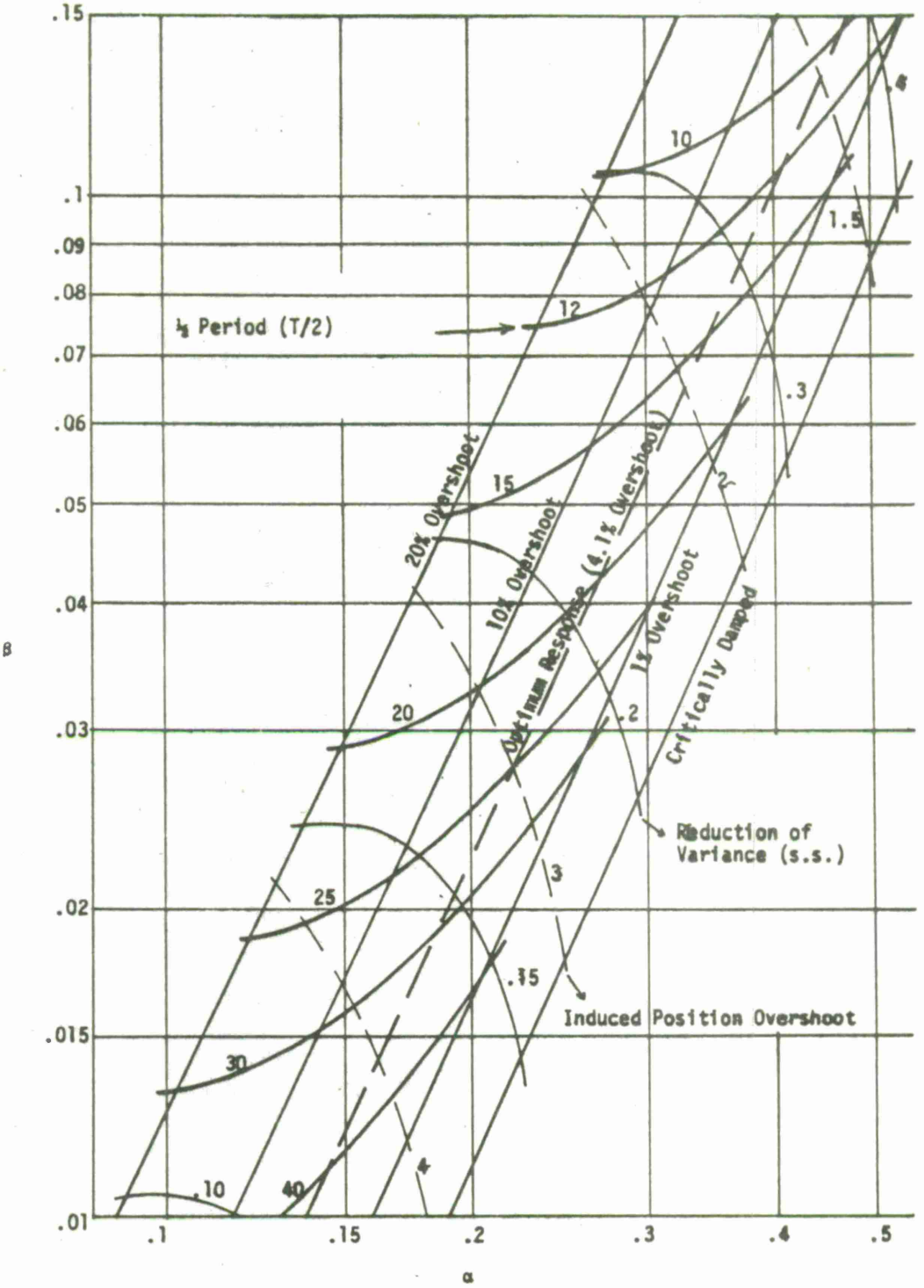

Figure 4. Response Characteristics of the α - β Tracker (high α)

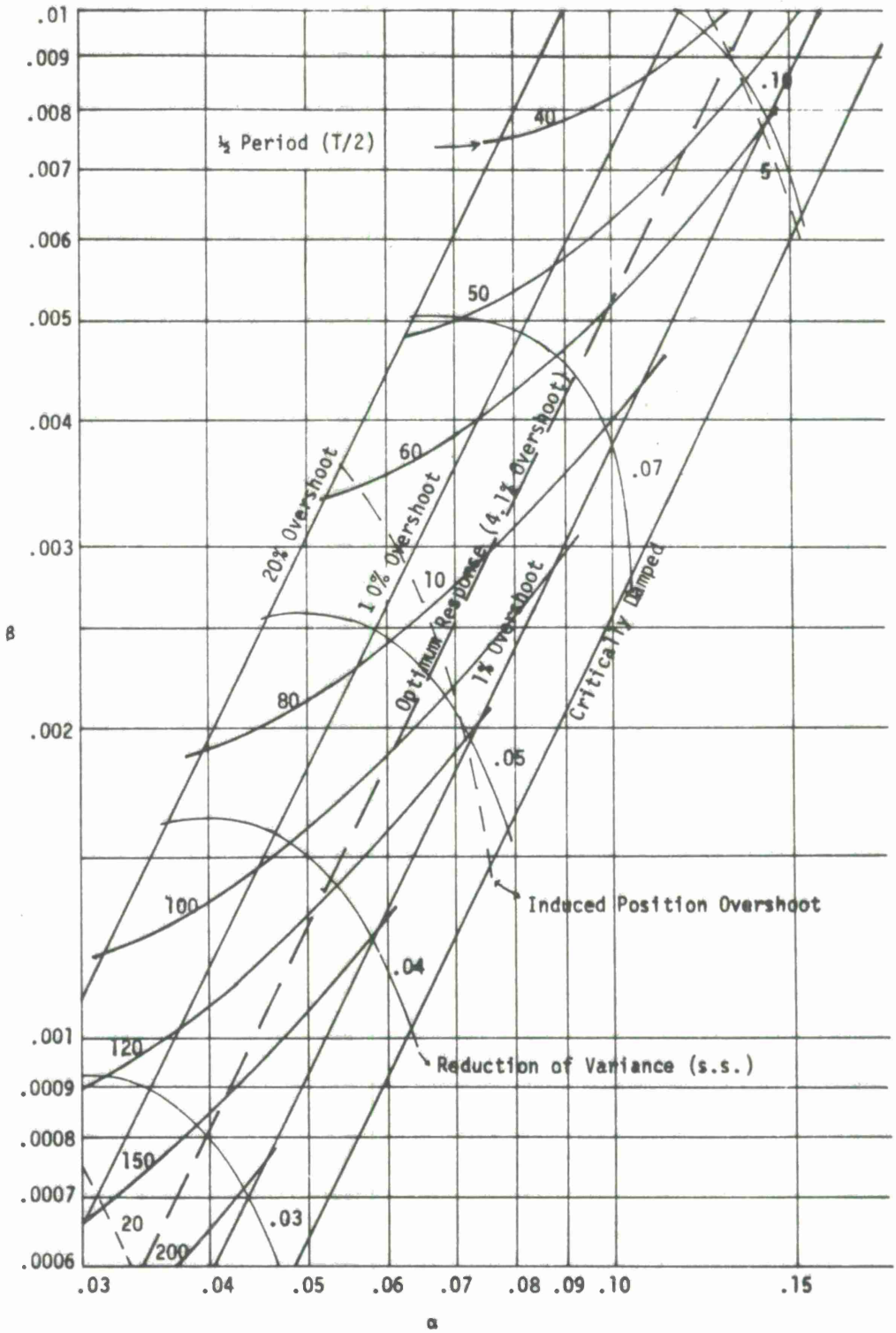

Figure 5. Response Characteristics of the α - β Tracker (low α)

critically damped curve is for $4(1-\alpha) = (2-\alpha-\beta)$. Also shown is the induced position overshoot, given a unit velocity step input. This number becomes quite large for small α and β which are slow to adjust out the initial error.

Solutions to equation (55) have been plotted in Figure 6a for the unit negative impulse and in Figure 6b for the unit position step. Shown are the smoothed position x, and the velocity x. The dotted curves are for the ideal α - β tracker with measurement at end of frame, and zero computation delay. The solid curves show the departure from ideal if the measurement occurs mid-frame. The unit position step response can be taken as any optimum tracker with $\beta = \alpha^2/(2-\alpha)$, which has about a .04 decrement, where the half period is given by equations (56) and (58). The impulse response of Figure 6a can be taken only as the optimum tracker with -- in this case $\alpha = .4$ and $\beta = .1$, which were the computed values from which the plot was made.

The response to the unit velocity step is shown in Figure 7. The dotted curve of the ideal tracker clearly shows the decrement of $\delta = .041$, that is, with successive position or velocity peaks of .99, -.041, .0017. The solid curve shows a considerably greater decrement and a very slightly shortened period. The successive peaks show a decrement on the order of .085. The initial peak is determined by the particular α and β used (see Figures 4 and 5). In this case, $\alpha = .4$ and $\beta = .1$ were plotted. These values give a half period, T/2 of 12.4 frames.

The α - β tracker, as pictured above, is used by reference units for time adjustment (equation 22) and by airborne units for position adjustment (equations 26-28). A modified α - β tracker is used by air and ground units for time adjustment (equations 23-25) in which values of α and β can change with time, position, and data rate. In the steady state, with constant position and data rate, the two trackers behave the same, so that the impulse response of Figure 6 also applies to the modified tracker.

At initialization, the modified tracker starts with $\alpha = 1$ and progresses with time down to a steady state α_0. The rate constant starts with $\beta = \alpha \cdot \alpha_0/(2-\alpha_0)$ progressing down to $\beta = \alpha_0^2/(2-\alpha_0)$ which is optimum. Since $\alpha = 1$ in frame one, there is nothing to discuss concerning the unit step response; all bias, down to measurement uncertainty, is wiped out in frame one. The unit velocity step is meaningful however, and indicates the time to zero-in on a clock running rate. This is shown for the modified α - β tracker in Figure 8. The dotted curves representing measurement at end of frame, and

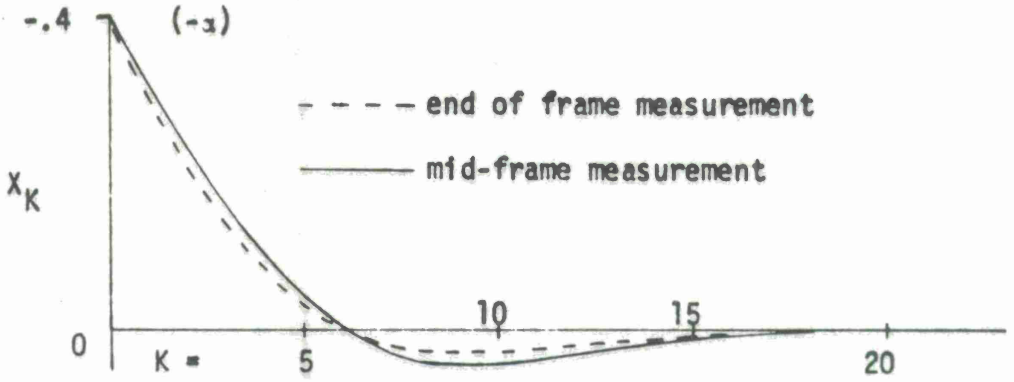

Figure 6a. Unit Negative Impulse Response

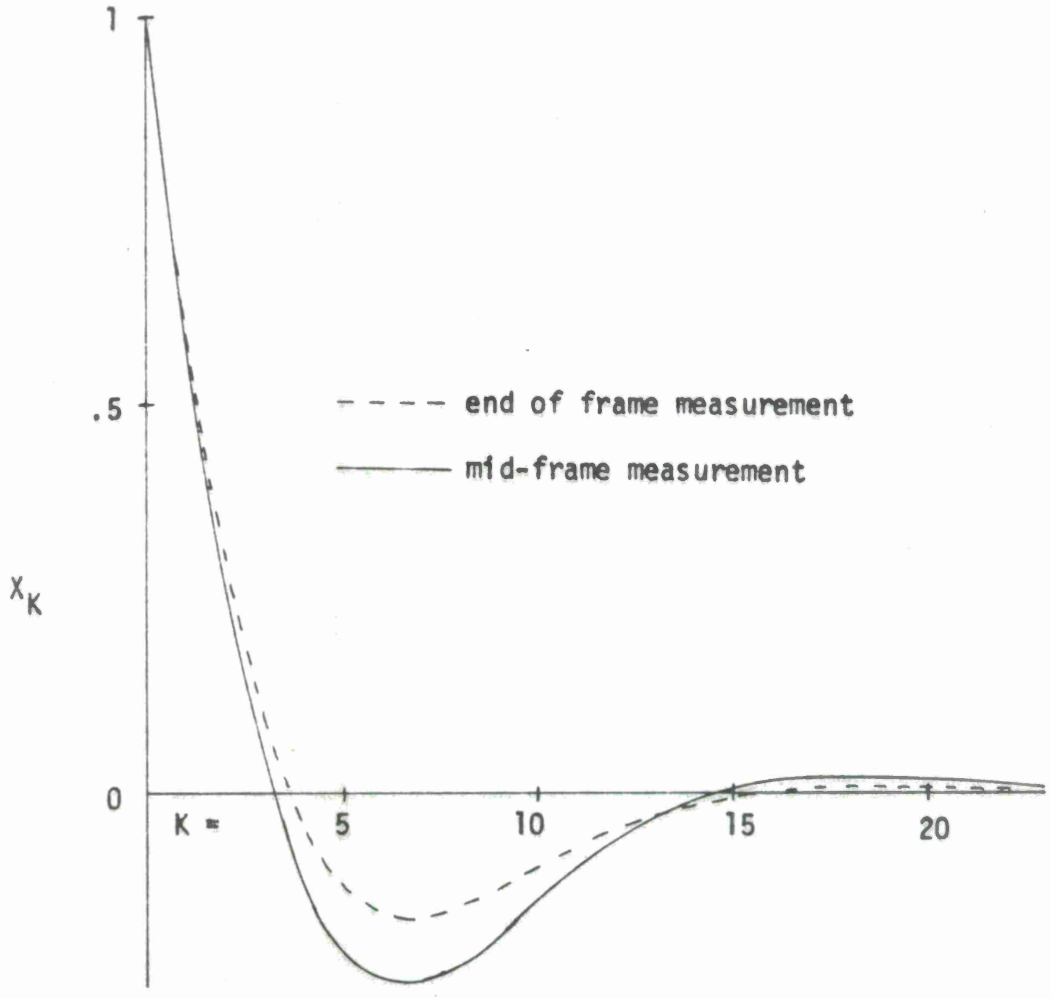

Figure 6b. Unit Position Step Response

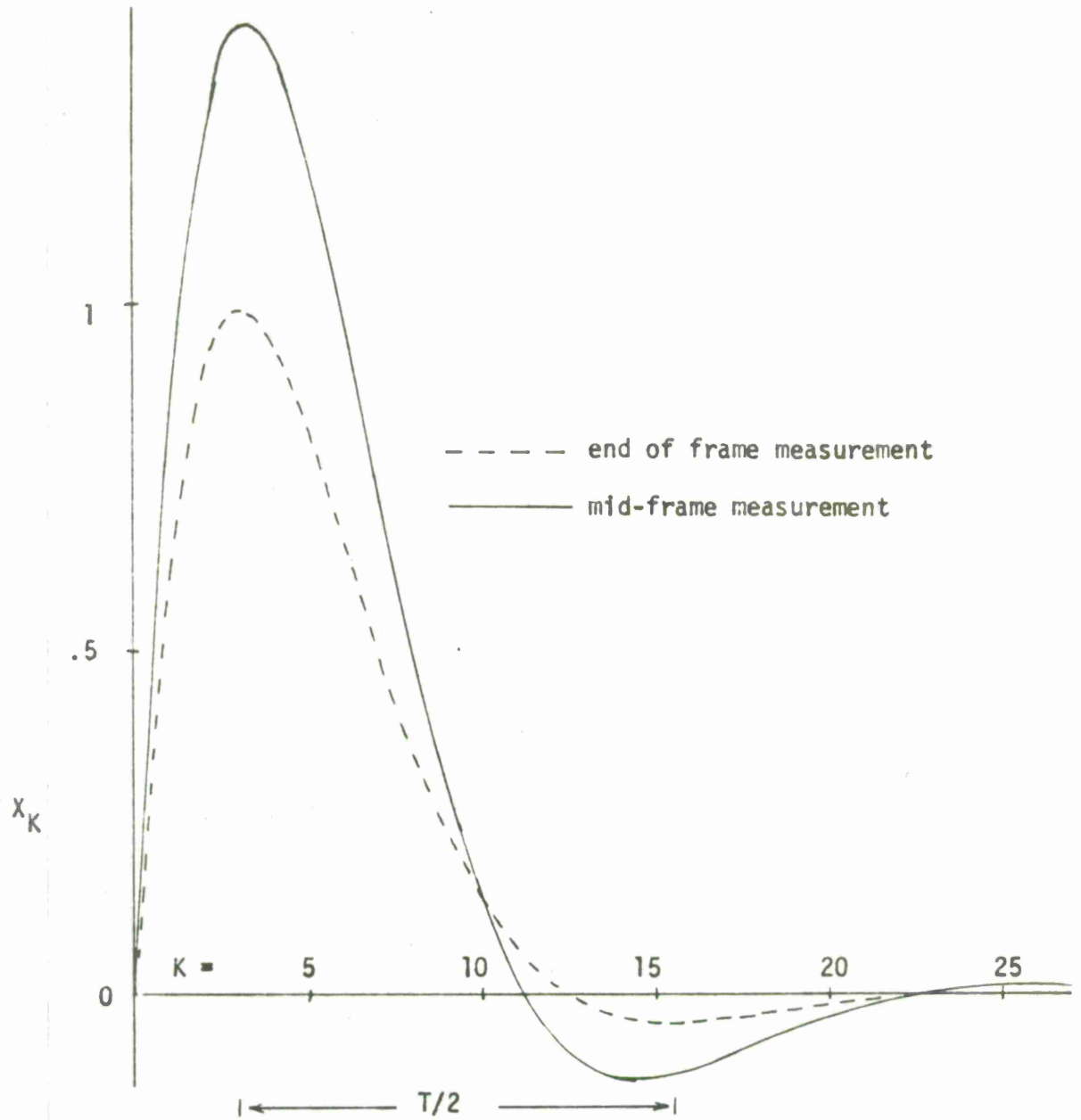

Figure 7. Unit Velocity Step Response

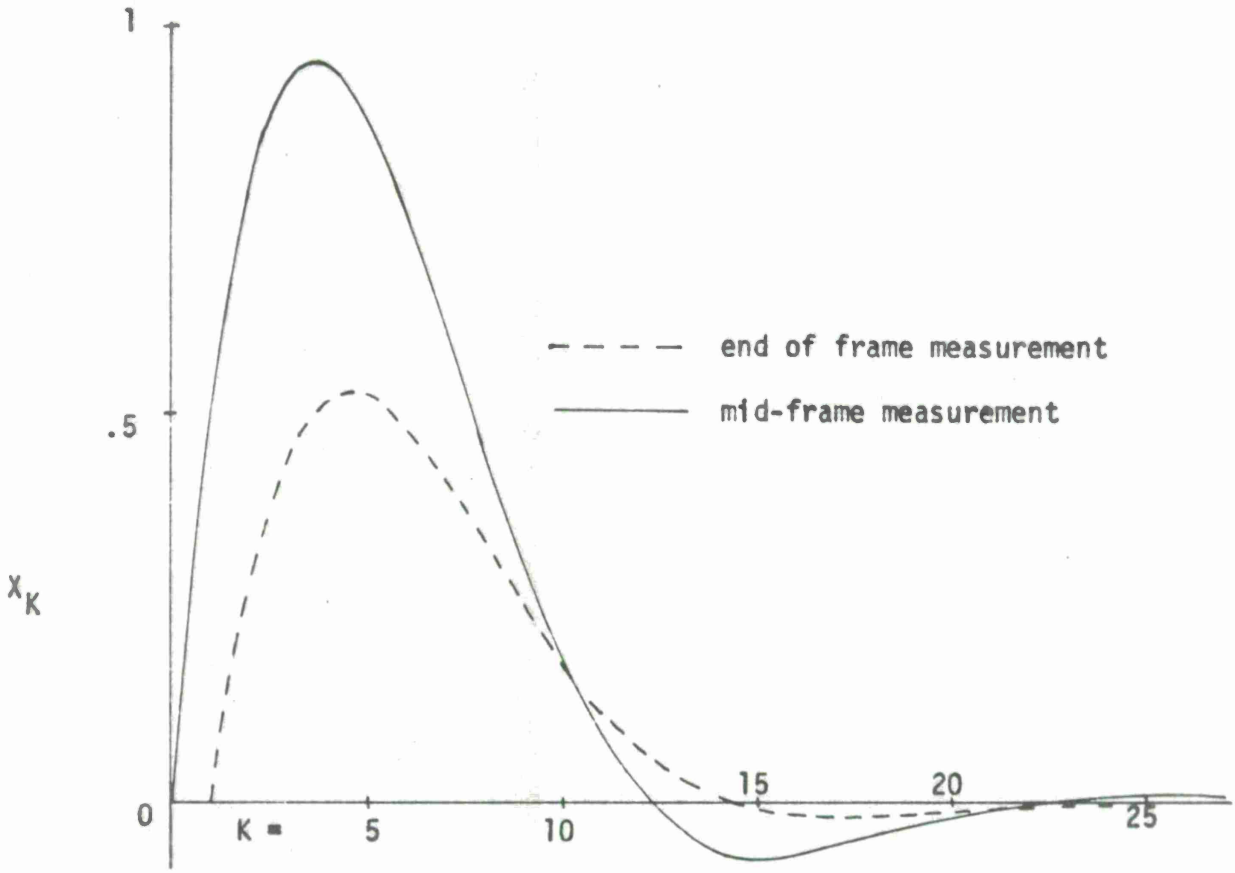

Figure 8. Modified α - β Tracker, Unit Velocity Step Response

the solid curve, the departure due to measurement at mid-frame. The same values of α and β were used as in Figure 7, that is $\alpha = .4$ and $\beta = .1$. In fact, these values are not far from those which might be desirable for use in an initial synchronization phase. For steady state operation, however, much smaller values should be used.

In the recursive navigation algorithm, additional restraints are placed on the α - β tracker, which singly and collectively cause departures from standard operation. These restraints are:

a) initial delay of rate adjustment,
b) solution clamp, MTG or MTA,
c) rate limits, DMAX, VMAX, and HMAX.

The individual and combined effects of these restraints will now be shown.

In the start-up logic, a unit is permitted to delay rate smoothing for a specified number of frames. This means that the response initially will be purely exponential (an α tracker), then switch to an α - β tracker after the delay period. This effect is demonstrated in Figure 9 for the unit step response. The solid curve represents mid frame measurement with no delay (the same as in Figure 6). The dotted and dashed curves represent two and five frame delays in applying rate adjustment. The figure shows the obvious: if the initial error is all position, or clock setting, then delay of rate adjustment is most beneficial providing a smooth and orderly response. The unit velocity step response with delay is shown in Figure 10 for the straight tracker. Again the solid curve represents no delay, the dotted and dashed curves are for two and five seconds delay. Where the initial error is in rate, the delay is, of course, detrimental, producing larger excursions and taking longer to settle down. The effect is even more pronounced for the modified α - β tracker, which uses lighter smoothing initially, as shown in Figure 11. Here three delays are shown--one, two, and five frames. For the modified tracker, there appears to be no justification for a delay of more than one frame.

Rate limits are imposed singly in velocity correction and both singly and in conjunction with solution clamps in time adjustment. The effect of rate limits alone is shown in Figure 12a, for impulse response, in Figure 12b for the position step response, and in Figure 13, for the velocity step response. The limits shown are .05, .02, and .01 in terms of the unit input. Clearly, there is little effect on the steady state condition as indicated by the impulse response. The zero crossing occurs somewhat sooner, but with slightly more overshoot. The position step response shows

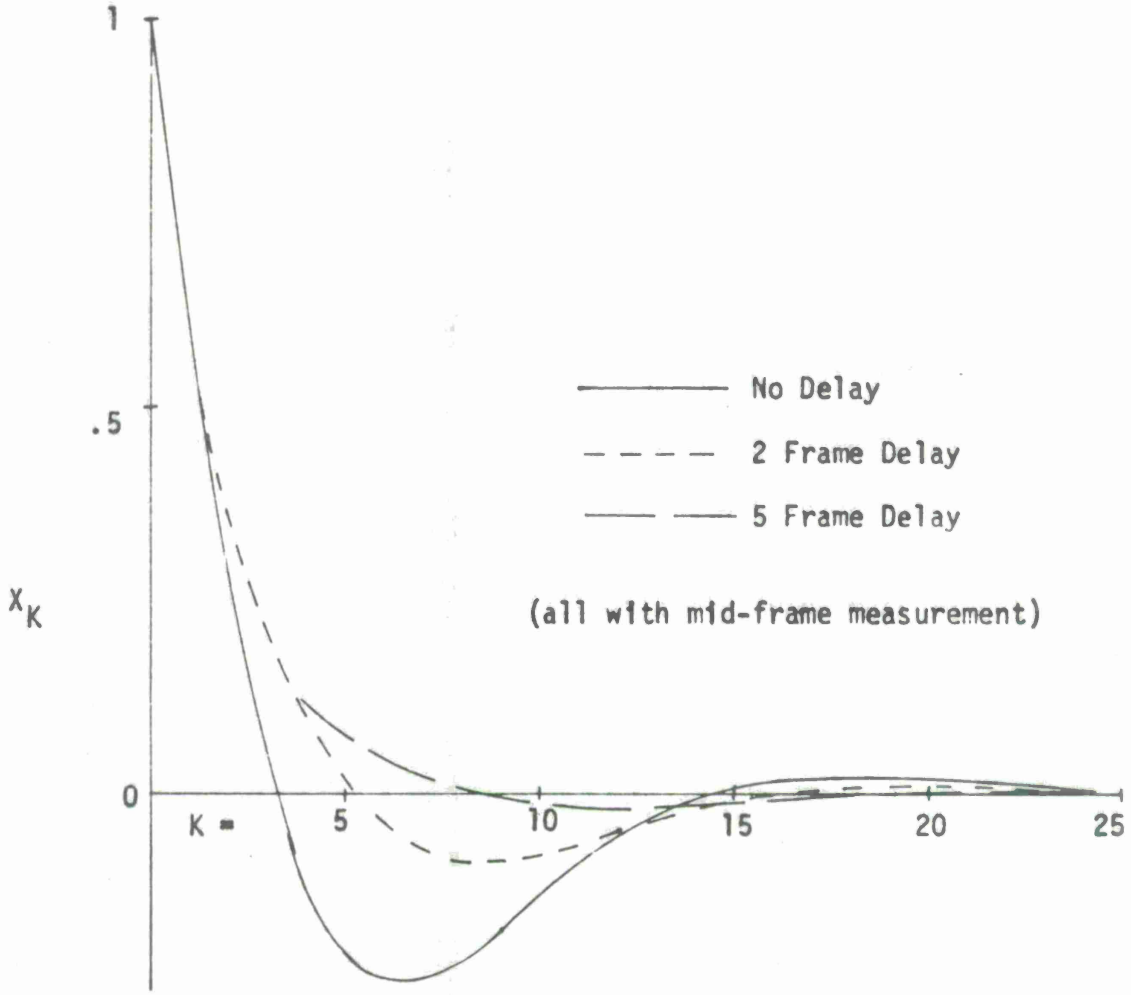

Figure 9. Effect of Delay in Rate Adjustment on Unit Position Step Response

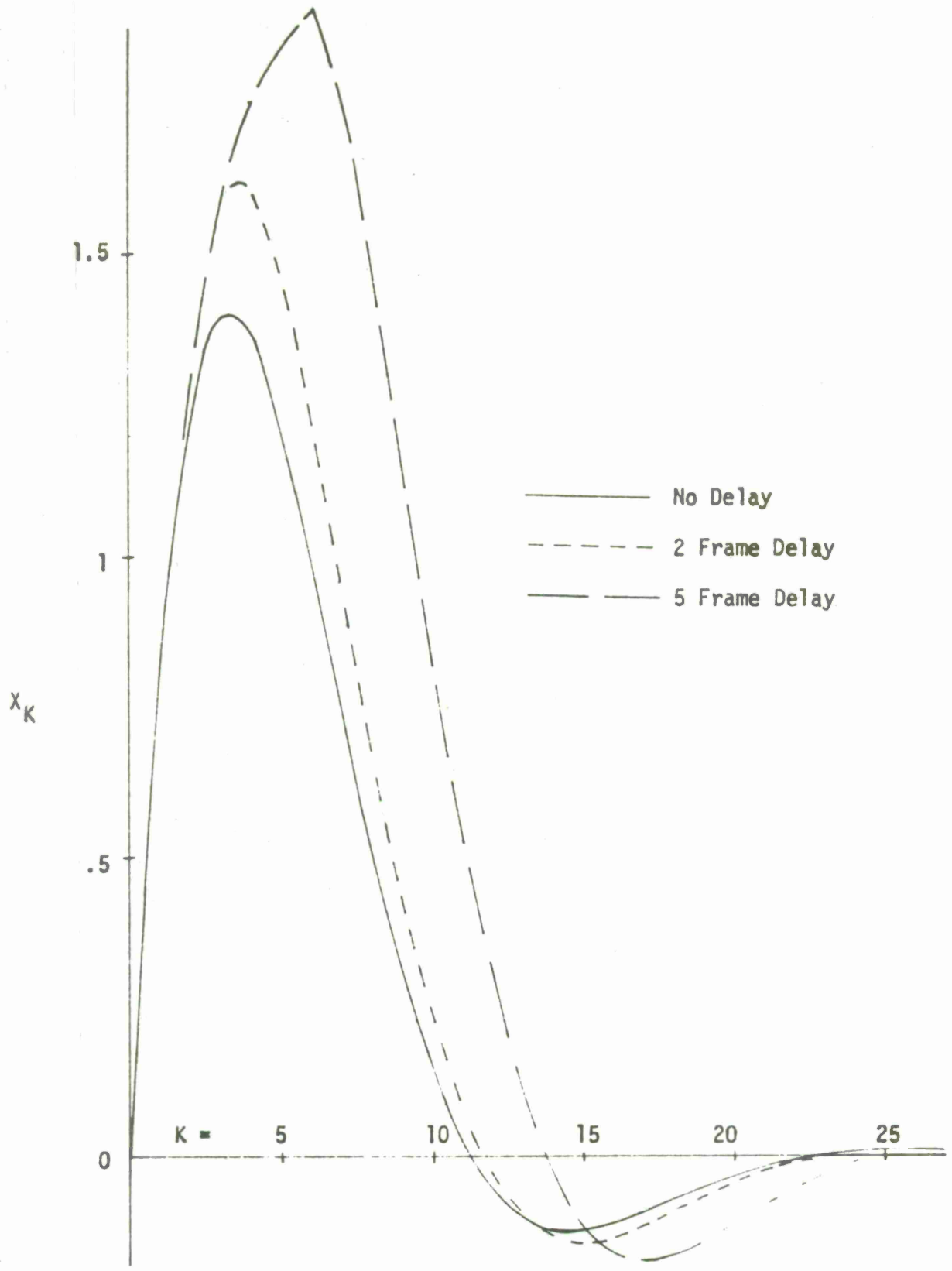

Figure 10. Effect of Delay in Rate Adjustment on Unit Velocity Step Response

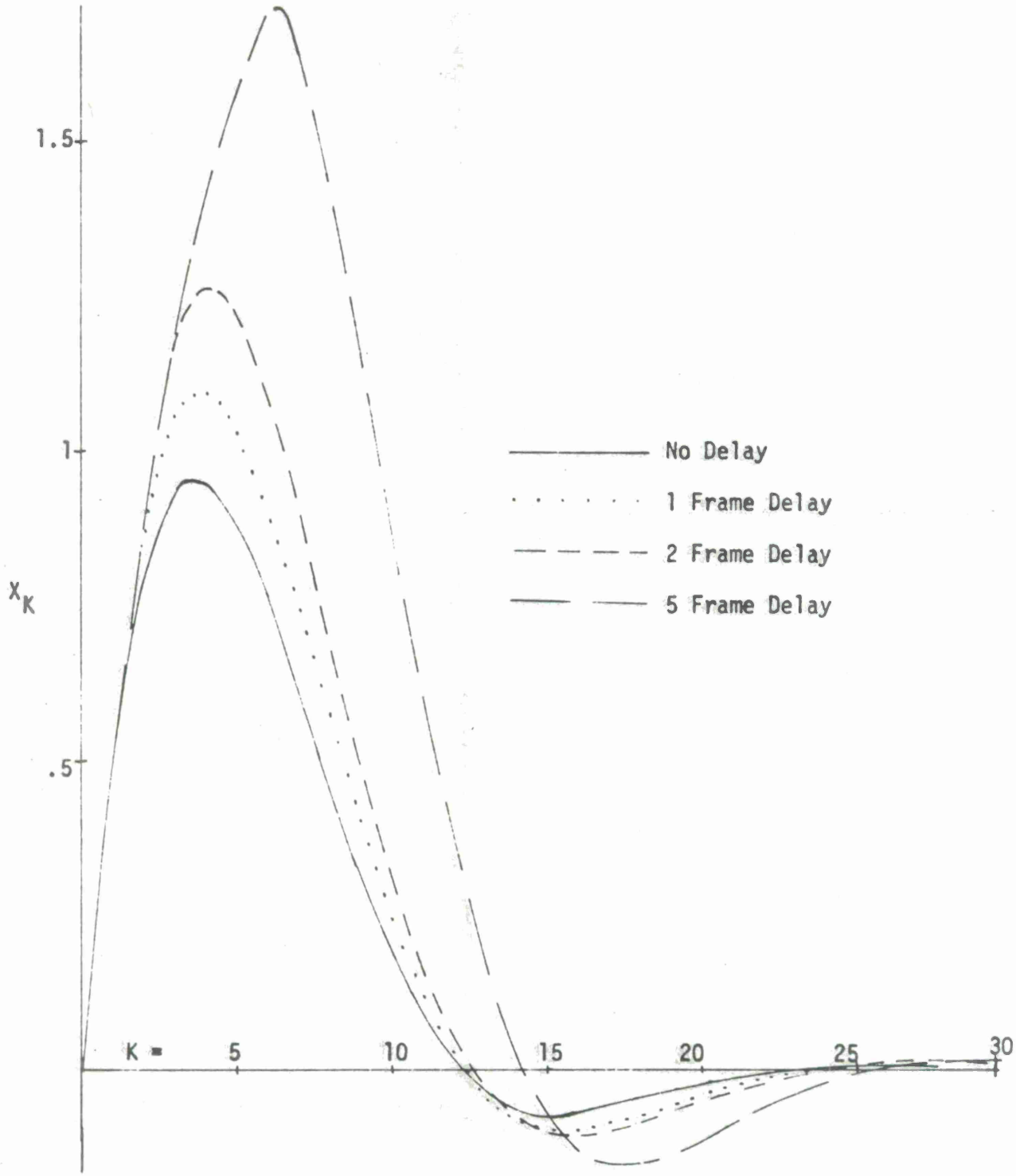

Figure 11. Effect of Delay in Rate Adjustment on Unit Velocity Step Response with Modified α - β Tracker

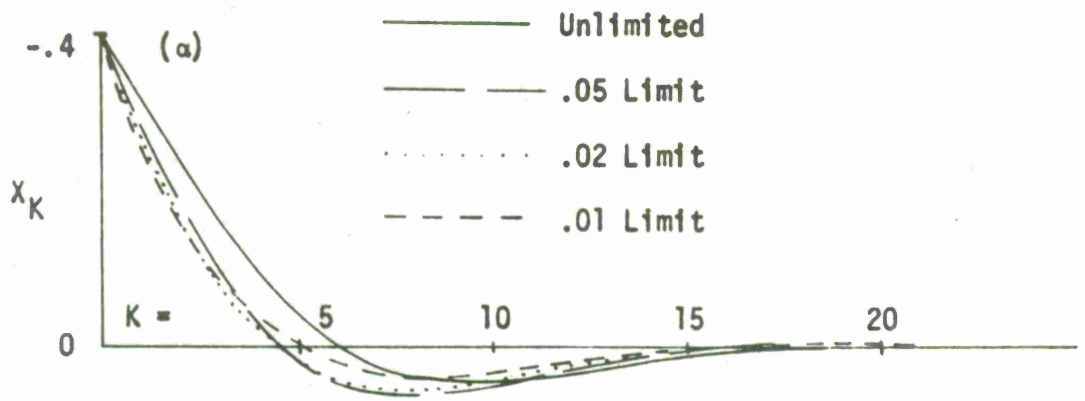

Figure 12a. Effect of Rate Limits on Unit Negative Impulse Response

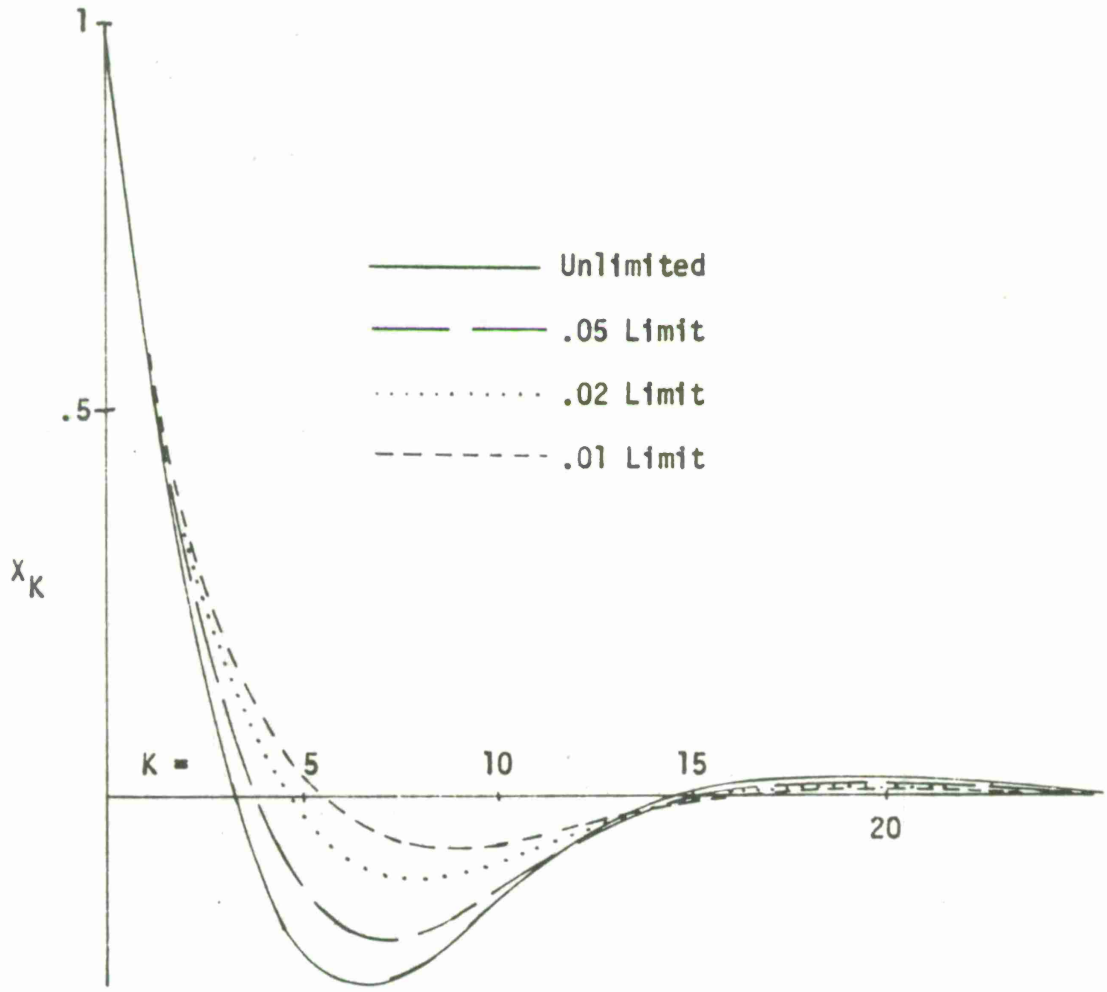

Figure 12b. Effect of Rate Limits on Unit Position Step Response

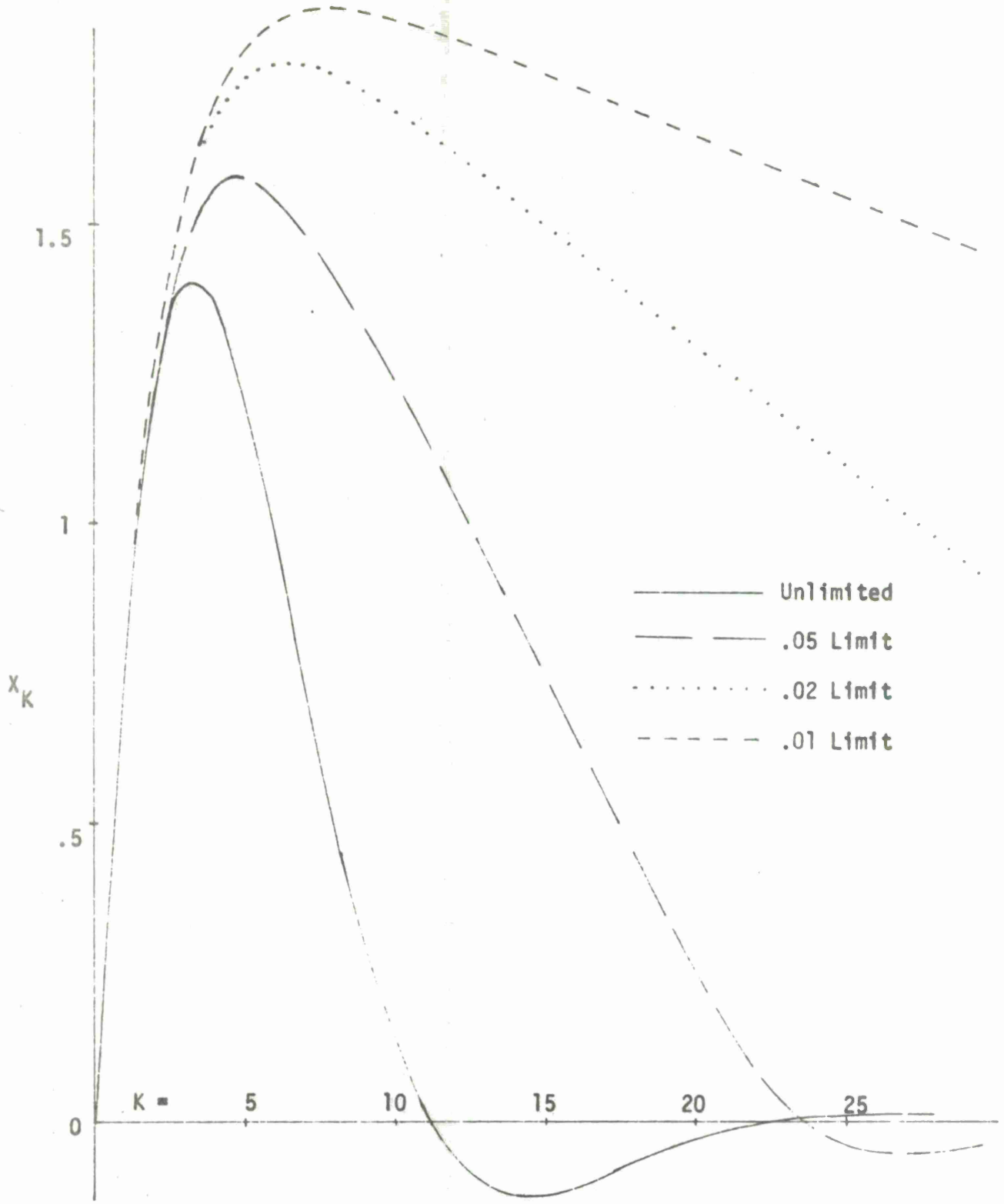

Figure 13. Effect of Rate Limits on Unit Velocity Step Response

the most beneficial effect of limiting rate adjustment when the error is all position. The velocity step response shows just as clearly the problems introduced in limiting rate adjustment. The initial overshoot is increased and a condition of steady transient is reached where the rate limit is applied each frame until zero is reached. This is demonstrated more clearly in Figure 14 which is a 4-1 scale reduction. It can be seen that the initial period is extended from about 24 frames to 36, 66, and 116 frames respectively for the limits of .05, .02, and .01 shown. Clearly, rate limits should not be imposed until after some initial transient period has elapsed.

The solution clamp is applied to time error estimates by units assumed to have already reached a steady state condition. By its nature, it also automatically imposes a rate limit smaller by a factor β/α. The effect of the solution clamp is shown in Figure 15a for the impulse response, in Figure 15b for the position step response, and in Figure 16 for the velocity step. The clamps shown are .2, .1, and .05 in terms of the unit, and the automatically induced rate limits, for $\alpha = .4$ and $\beta = .1$, are .05, .025, and .0125 respectively. The impulse response shows the beneficial effect on steady state behavior--the period is unchanged but the peak magnitudes are proportional to the clamp for clamps less than α. The clamp produces a delay in the position step response of 1, 3, and 9 frames respectively for the three clamps shown. The .05 clamp shows a significant broadening of the initial overshoot cycle. The real problem shows up in the velocity step response. Here, only the .2 clamp is shown--the lower values are disasterous. The induced position overshoot has grown by nearly a factor of five--from 1.4 to 6.8 and the initial period has been extended to 52 frames. The trouble is caused by limiting the position adjustment to .2 and the rate adjustment to .05--frame after frame--when, in fact, a much larger correction is needed in the early frames.

Finally now in addition to the solution clamp, the rate adjustment may be more severely limited. This is shown in Figures 17a, 17b, and 18 for a clamp of .2 and a limit of .02 (as opposed to the automatic .05). The additional rate limit has little effect on the impulse response, except to speed it up slightly. It has a beneficial effect on the position step response, as was shown before with rate limiting alone. In this instance, the period is slightly lengthened, say two frames, but the overshoot is cut in half. The effect on the velocity step response is pure disaster, however. The scale in Figure 18 has been cut now by a factor of 10 from the original in Figure 7. The initial period is now up to 125 frames and the induced position overshoot up to 16.4. As with rate limiting alone, the effect is not good on the velocity step. Lower values are not plotted for obvious reasons.

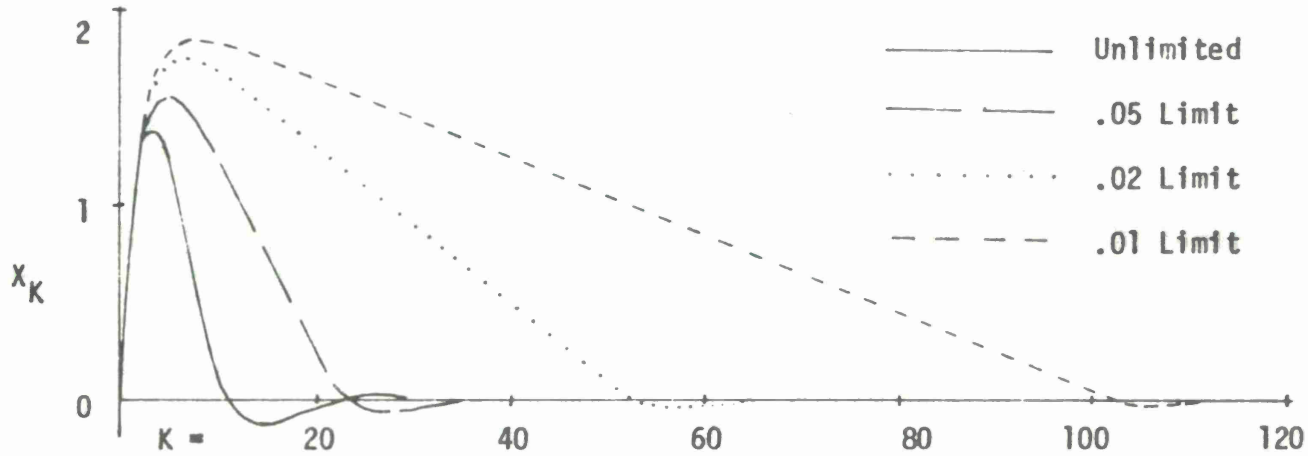

Figure 14. Effect of Rate Limits on Unit Velocity Step Response, 4 to 1 Scale Increase

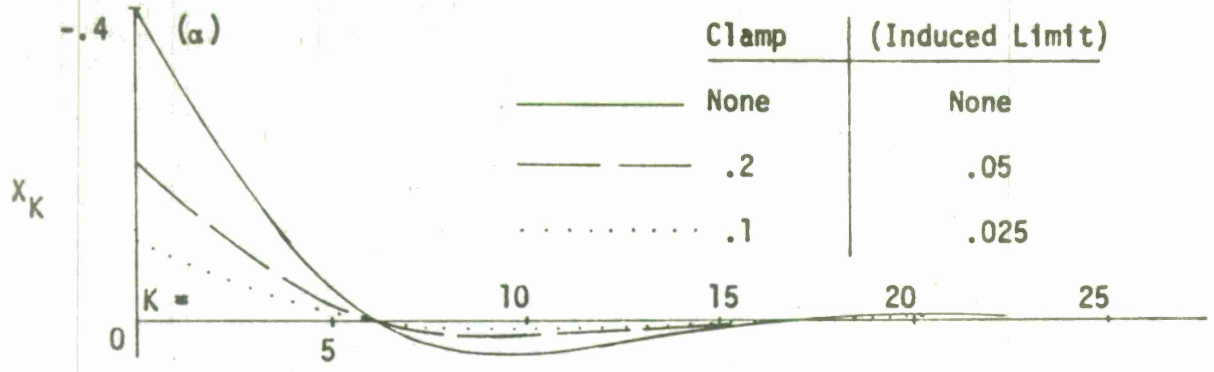

Figure 15a. Effect of Solution Clamp on Unit Negative Impulse Response

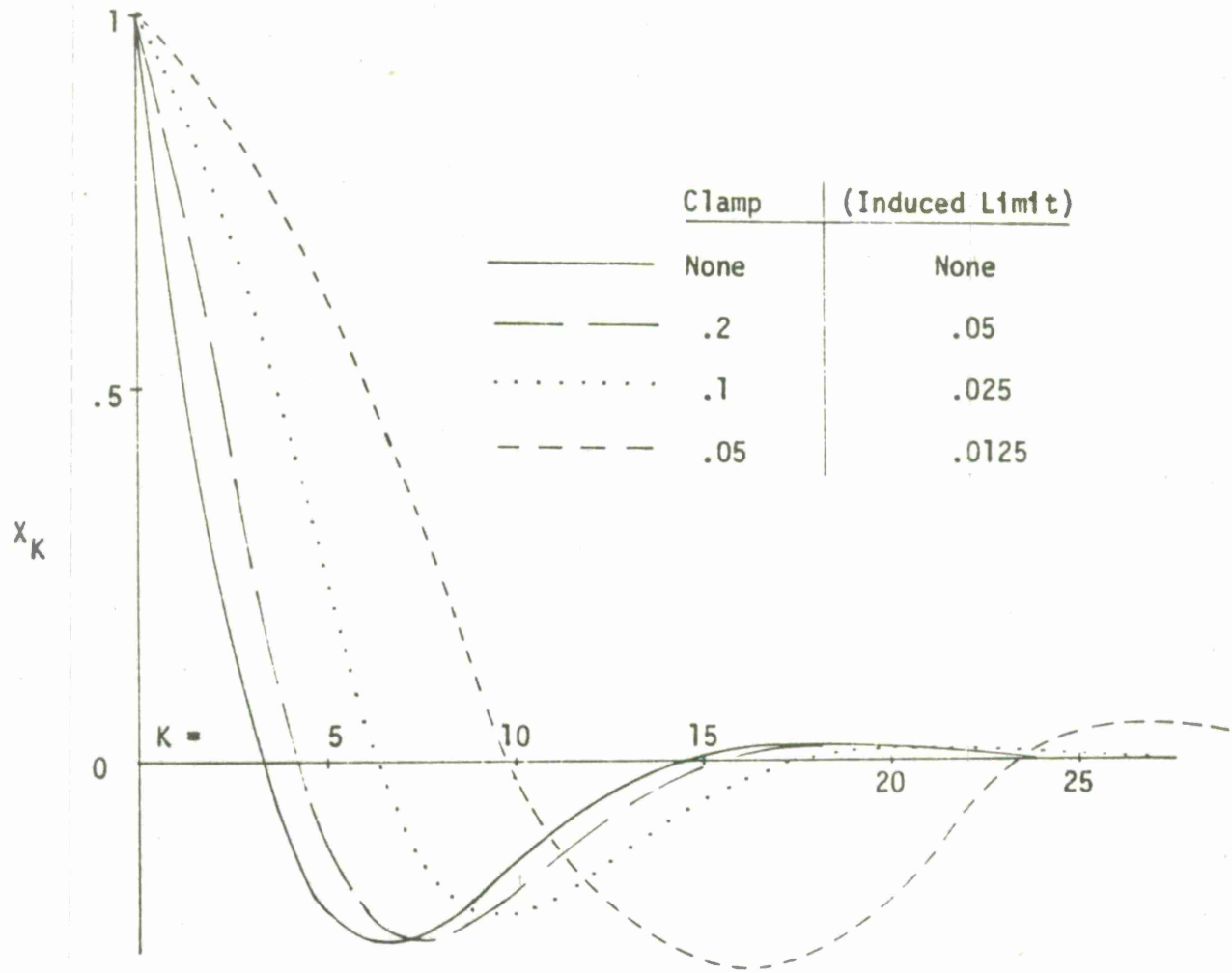

Figure 15b. Effect of Solution Clamp on Unit Position Step Response

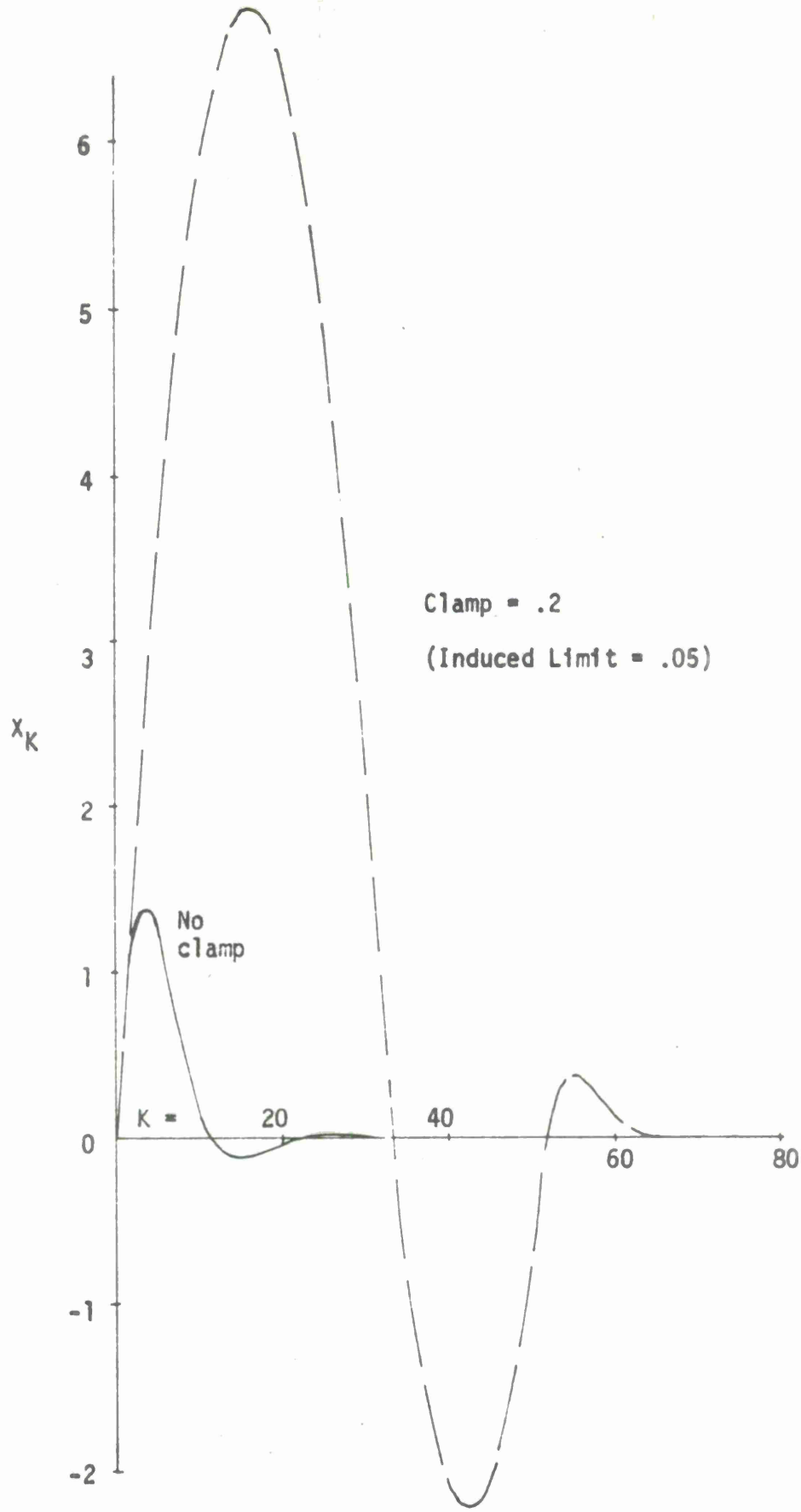

Figure 16. Effect of Solution Clamp on Unit Velocity Step Response

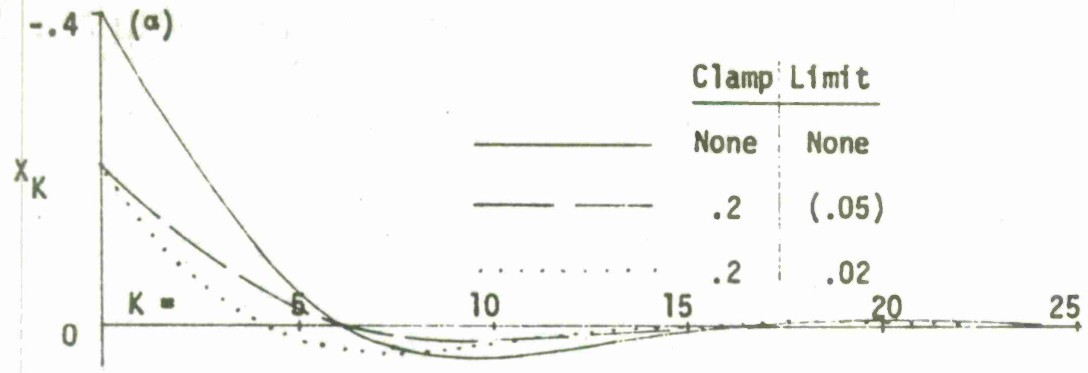

Figure 17.a. Solution Clamp and Rate Limit, Unit Negative Impulse Response

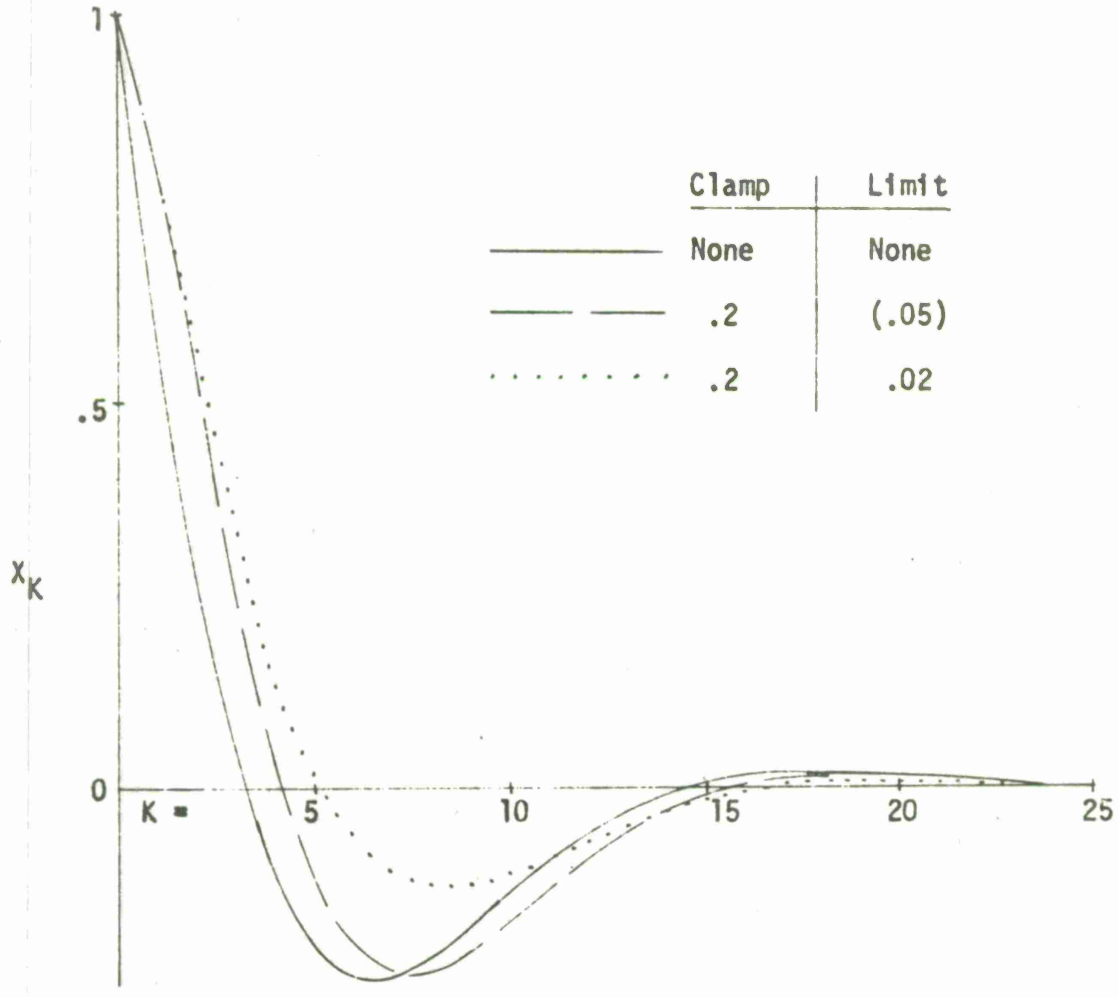

Figure 17.b. Solution Clamp and Rate Limit, Unit Position Step Response

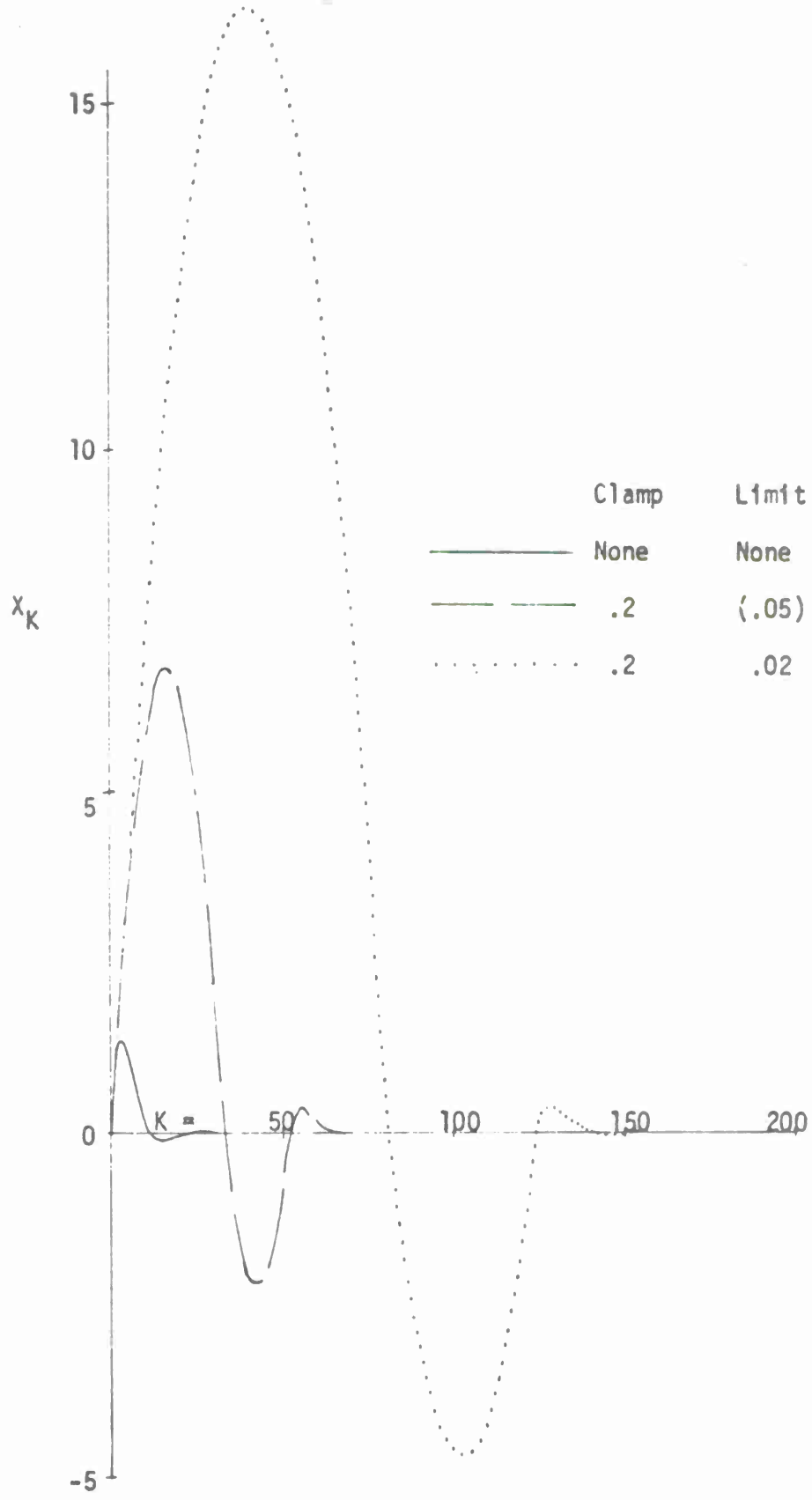

Figure 18. Solution Clamp and Rate Limit, Unit Velocity Step Response

Summarizing then, clamping improves the impulse response; rate limiting improves the position step response; while both have a deleterious effect on the velocity step response. They should be used with care, if at all.

SECTION V

SIMULATION OF THE PLRACTA DEMONSTRATION

A geographic view of the PLRACTA Demonstration test bed is shown in Figure 19. MITRE E Building, Boston Hill, and Millstone Hill will normally be the master and two references. Highways and hilltops are shown as some of the possible locations for the ground mobile unit. Baseline extensions are also shown. These are no solution areas for three station operation.

Several examples are taken from simulations of the test bed to illustrate the performance characteristics of PLRACTA. Specific cases to be shown include:

(a) synchronization of a reference site,
(b) synchronization and position location of a ground unit,
(c) entry of an airborne unit into an otherwise steady state system,
(d) steady state system operation with two aircraft,
(e) ground unit operating off extension provided by two aircraft and one reference site.

Certain parameters are common to all of the Demonstration examples. These are itemized in Table III following

Table III

COMMON PARAMETERS--DEMONSTRATION SIMULATION

τ	1 second	frame time
s	10 milliseconds	slot duration
σm	100 nanoseconds	measurement error
σt	50 nanoseconds	transmission error
Xt	1 frame	delay before time rate adjustment
Xv	1 frame	delay before velocity adjustment

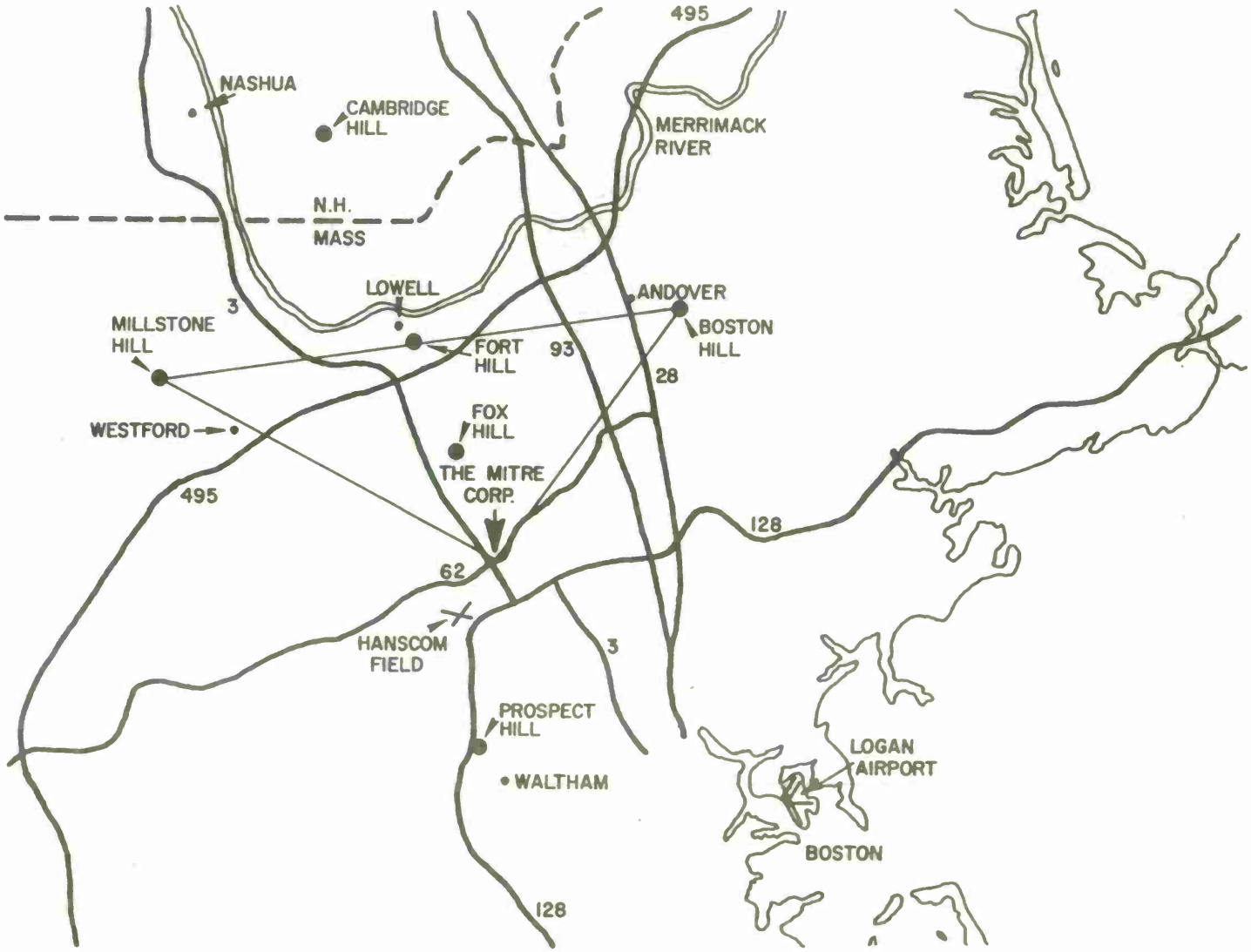

Figure 19. PLRACTA Demonstration Test Bed

In all of the runs simulating the PLRACTA Demonstration, the reference sites are within line-of-sight of the master, so that they process only master data and are unaffected by ground and airborne units, which is the case in the "live" test bed. It is assumed that all clocks run at a constant rate--though that rate may differ from the master clock. (This assumption is reasonable only for "Hot Clock" operation in the test bed.) Furthermore, it is assumed that aircraft are instrumented in such a way that accurate differential velocity information is provided to the on board computer.

REFERENCE--INITIAL SYNCHRONIZATION

The first problem to be considered is the initial synchronization of a reference site. In the PLRACTA Demonstration algorithm, an initial gross sync adjustment is made in frame one. This is followed by a "short" transition period in which relatively large smoothing constants (α and β) are used. After the transition period, small values for α and β are chosen. We are concerned here with the short transition phase which starts with essentially no clock setting bias, but possibly a large clock rate error. The unit velocity step response tells the story.

Two examples are considered. They are set in the same environment and differ only by the selected values of α and β. In both cases, an initial clock rate error of 1×10^{-6} seconds per second is applied. The environmental conditions and the expected performance as indicated by equations 55 to 59 are given in Table IV following. No solution clamps or rate limits are employed in these two examples.

In both cases, the measurement occurred 0.24 seconds prior to the end of frame. The simulation result is shown in Figure 20. The result is quite close to theory, as shown in the comparison in Table V.

In both cases the induced peak error in clock setting is about 12% lower than predicted. The decrement, whether observing peak to peak position or velocity, was also lower than predicted--more so in the case of the shorter period. The reason for these slight "improvements" is unknown, as a slight degradation was actually expected due to the 0.24 second delay between measurement and end of frame. At any rate, it can be seen that after little more than one period of operation, any transients due to an initial rate error of 1×10^{-6}seconds per second will have decayed. Figures 4 and 5 can be used to relate any selected set of smoothing constants, α and β, to the required transition period. (Caution: the current algorithm in the PLRACTA test bed computer uses β as a function of α, so that the optimum response curve must be followed.)

Table IV

REFERENCE, TRANSIENT ENVIRONMENT & EXPECTED PERFORMANCE

eo	-19 ns	initial clock setting error
do	1.0023 μs/second	initial clock rate error
exo	-23 feet	position error
eyo	-56 feet	position error
ezo	-8.5 feet	altitude error

	A - Case	B	
α	.18	.10	time smoothing constant
β	.026	.0055	time-rate smoothing constant
ϕ	7.2	3°	phase angle
T/2	25 frames	60 frames	half period
δ	.0835	.0425	decrement
C_1	0	0	constants for equation 53
C_2	8.06	20.2	constants for equation 53
K_p	7	15	frame in which position peak occurs
ρ_{kp}	.50	.454	envelope magnitude
$\sin\phi k$	.770	.706	Phase
e max	3.11 μs	6.48 μs	induced overshoot
e min	-.26	-.276	following minimum

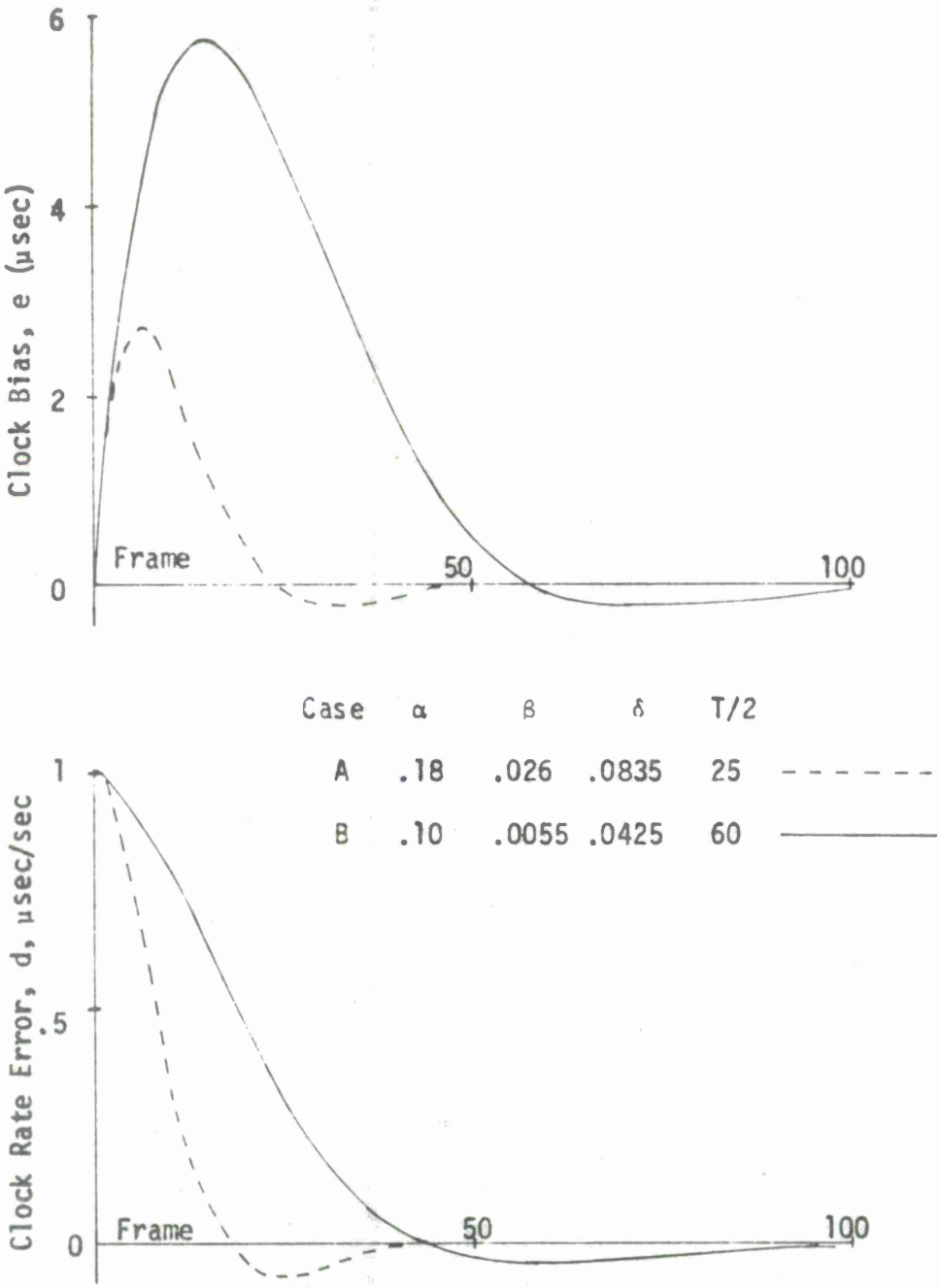

Figure 20. Reference Initial Synchronization

Table V

REFERENCE, TRANSIENT RESPONSE

	Case A		Case B	
	Theory	Sim	Theory	Sim
α	.18	.18	.10	.10
β	.026	.026	.0055	.0055
T/2	25	26	60	60
δ	.0835	.065 (rate)	.0425	.041
δ	.0835	.074 (setting)	.0425	.039
e max	3.11 μs	2.72 μs	6.49 μs	5.75 μs
e min	-.26 μs	-.20 μs	-.276 μs	-.224 μs

REFERENCE--STEADY STATE

The steady state variance of the α - β tracker is predicted by equation (46). It is assumed that there will also be steady state bias due to any position error in the direction toward the master station. Two sets of reference site data have been extracted from simulation runs to show the effect of α and β on variance and the effect of position error on bias. One set uses α = .14, which is rather coarse, while the other uses α = .036, which may be more realistic for steady state reference site operation. The initial conditions and the predicted steady state errors are shown in Table VI.

Table VI

REFERENCE, STEADY STATE ENVIRONMENT

Run #	301		303		319		320	
Site #	R1	R2	R1	R2	R1	R2	R1	R3
α	.14	.14	.14	.14	.036	.036	.036	.036
β	.0182	.0182	.0182	.0182	.00068	.00068	.00068	.00068
MTG (ns)	618*	618*	618*	618*	309*	309*	309*	309*
DMAX (ns/s)	1**	1**	1**	1**	.5*	.5*	.5*	.5*
eo (ns)	-5	-48	7	7	0	-4	-42	-38
do (ns/s)	2.3	-2.3	-1.7	.8	.5	-.9	-.8	-.2
exo (feet)	-23	-29	2.0	-18	-49	-61	-15	-41
eyo (feet)	-34	-3	-12	15	-10	-21	57	-18
ezo (feet)	-8	-32	-14	33	0	10	32	-34
position error in direction to master (feet)	12	27	23	9	-23	64	54	45
Predicted Standard Deviation (n.s)	40	40	40	40	20	20	20	20

* ineffective
** effective

The coarse group consists of two reference sites in each of two runs--301 and 303. A time history of clock setting error and clock rate error for 200 one second frames is plotted in Figure 21--the solid line for site R2 and the dotted line for site R3.

It was intended that the reference sites should start the run in the steady state condition, and this appears to be the case. Rate adjustment was limited to 1 nanosecond per second, and because of the large smoothing constants used, the adjustments were often up against the stops. A summary of the measured statistics on this group is given in Table VII following where the error data are given in nanoseconds.

Table VII

REFERENCE, STEADY STATE CLOCK ERROR (α = .14)

Run	Site	Predicted Bias	Measured Bias	Predicted Std. Dev.	Measured Std. Dev.	Measured r.m.s. error
301	G2	-12 ns	-23 ns	40.4	34.6	41.5
	G3	-27	-9.5	40.4	28.7	41.5
303	G2	-23	-15.2	40.4	32.2	35.8
	G3	-9	-7.5	40.4	36	36.8
Mean		-17.8	-13.8	40.4	33.0	39.1

Certainly, the simulated results are not far from predictions, though the measured standard deviation in clock setting error was about 20% less than predicted. The r.m.s. error appears closer, but this includes the bias error.

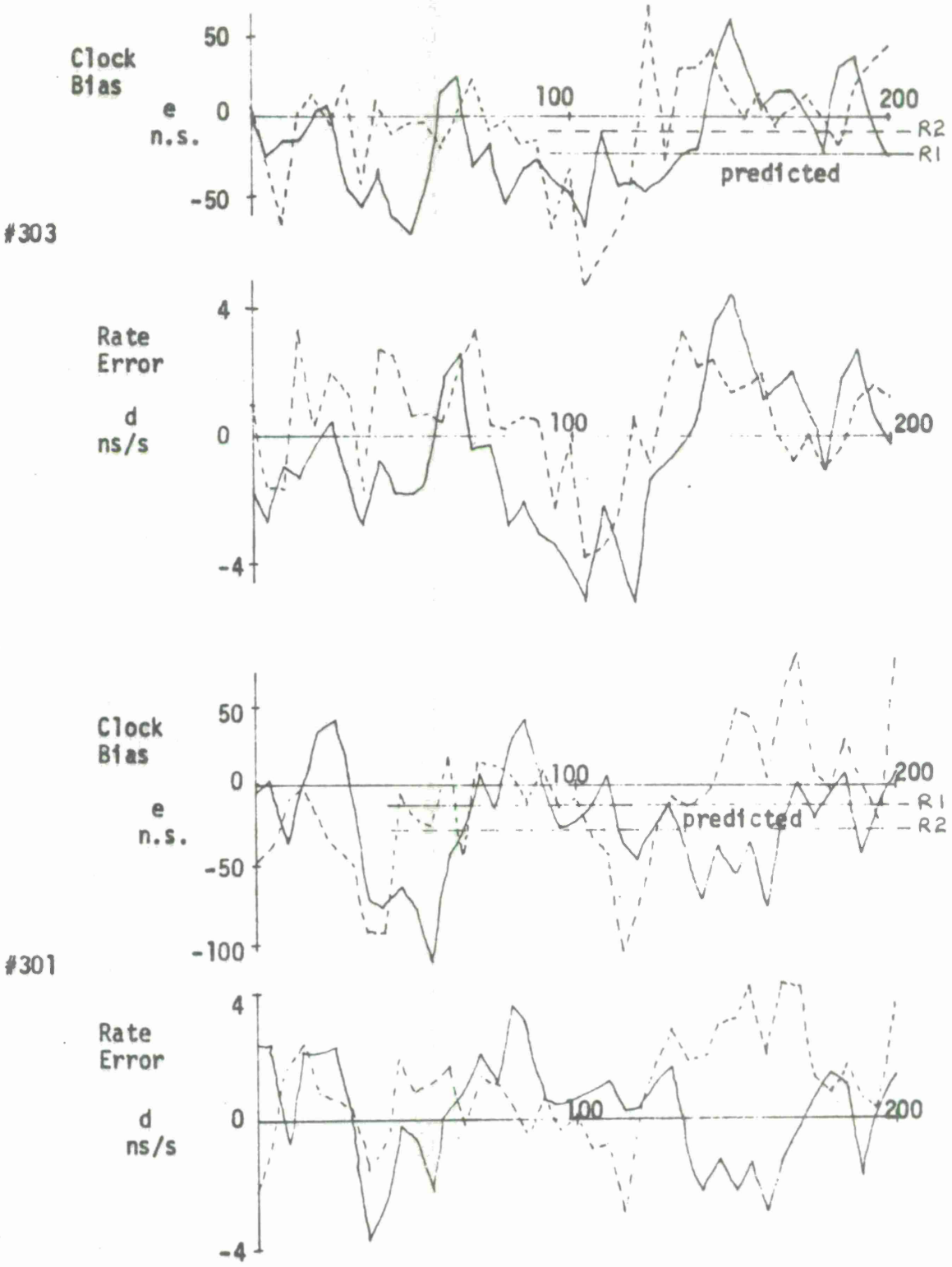

Figure 21. Reference--Steady State Clock Error for $\alpha = 0.14$, $\beta = .0182$

Similar data for small α (.036) is shown in Figure 22. The steady state condition is obviously much smoother, but the biases induced by position errors stand out much more clearly. It is also clear that the runs did not quite start in a steady state condition, as intended though this condition is achieved after about 25 frames. While solution clamps and rate limits were imposed, their setting was too high to effect the result. A summary of the measured statistics on this group is given in Table VIII, where again the error data are in nanoseconds.

Table VIII

REFERENCE, STEADY STATE CLOCK ERROR (α = .036)

Run	Site	Predicted Bias	Measured Bias	Predicted Std. Dev.	Pleasured Std. Dev.	Measurement r.m.s. error
319	R2	23 ns	28 ns	20.2 ns	14.1 ns	31 ns
	R3	-64	-62.8	20.2	23.8	66.2
320	R2	54	54.5	20.2	24	58.7
	R3	-45	-34.1	20.2	7.9	34.5
Mean		-8	-3.6	20.2	18.8	49.7
Mean Magnitude		46.5	44.8			

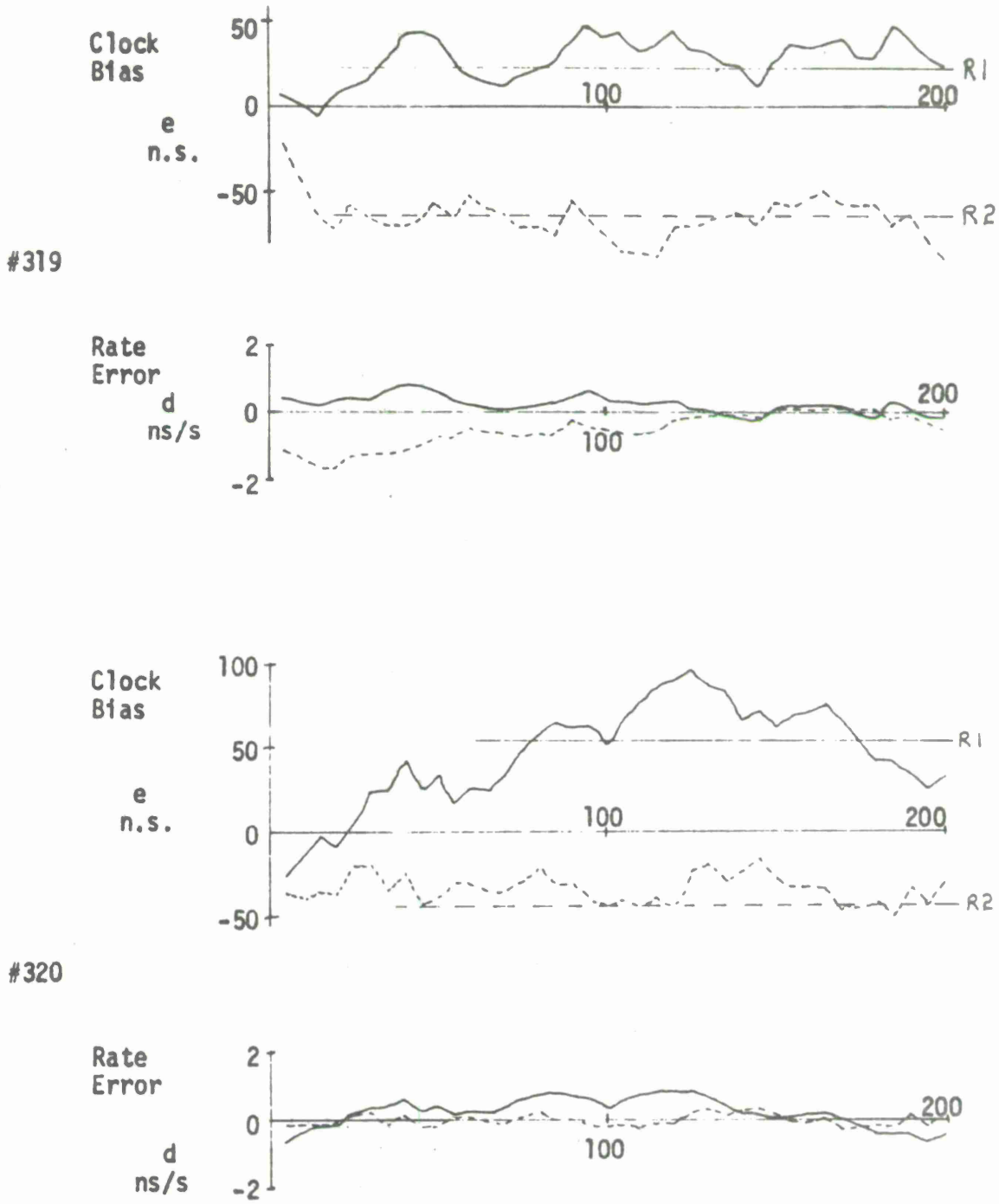

Figure 22. Reference Steady State Clock Error for $\alpha = 0.036$, $\beta = .00068$

In this group, the measured standard deviation comes closer to prediction. But the bulk of the error is due to the input position error of the reference sites. Thus, the efforts to reduce steady state error by heavy smoothing, in this case, were of little value.

Figures 4 and 5 show the relation between reduction in variance and the selected α and β. Some consideration must be given to the input measurement error and the probable site location error in arriving at the desired reduction in variance, and thus the value of α and β, for steady state operation. After a point, further decrease in α cannot reduce the r.m.s. clock error, but can only increase the response time.

GROUND--SYNCHRONIZATION AND POSITION LOCATION

Given now that there is a basic triad of one master and two reference sites operating in a steady state condition, the response of a ground unit entering the network will be considered.

In the transient state, successive positions, determined by hyperbolation are tracked with an α tracker. The response curve should be a pure exponential, at least down to the noise level. Times, also determined by hyperbolation, are tracked with the modified α - β tracker. Time error should jump down to the noise level in frame one. Time rate error should follow a response curve somewhat similar to the unit position step response. There may then follow some induced time error, due to rate error, as shown in Figure 8. The length of the transient period is variable because the solution check following equation (16) often discards results; and the algorithm requires a fixed number of successful solutions prior to changing state. The effective time smoothing constant is determined by equation (23) which considers this history.

In the (assumed) steady state, successive positions are determined by direct ranging while time continues to be determined by hyperbolation. Normally, much smaller smoothing constants will be used in steady state operation. The effective time smoothing constant, again, will depend upon the history of solution rejects.

The nature of the response is also dependent upon the location of the ground unit with respect to its data sources. The geometric dilution of precision (time) as given by equation (17) for the basic triad of the PLRACTA test facility is shown at a contour diagrams in Figure 23. This figure has been drawn to the same scale as the map of Figure 19 so that $\breve{g}t$ can be related to specific map location. The raw data from which this figure has been constructed was supplied by Mr. R. J. Kulpinski. Not shown is $\breve{g}p$, the geometric

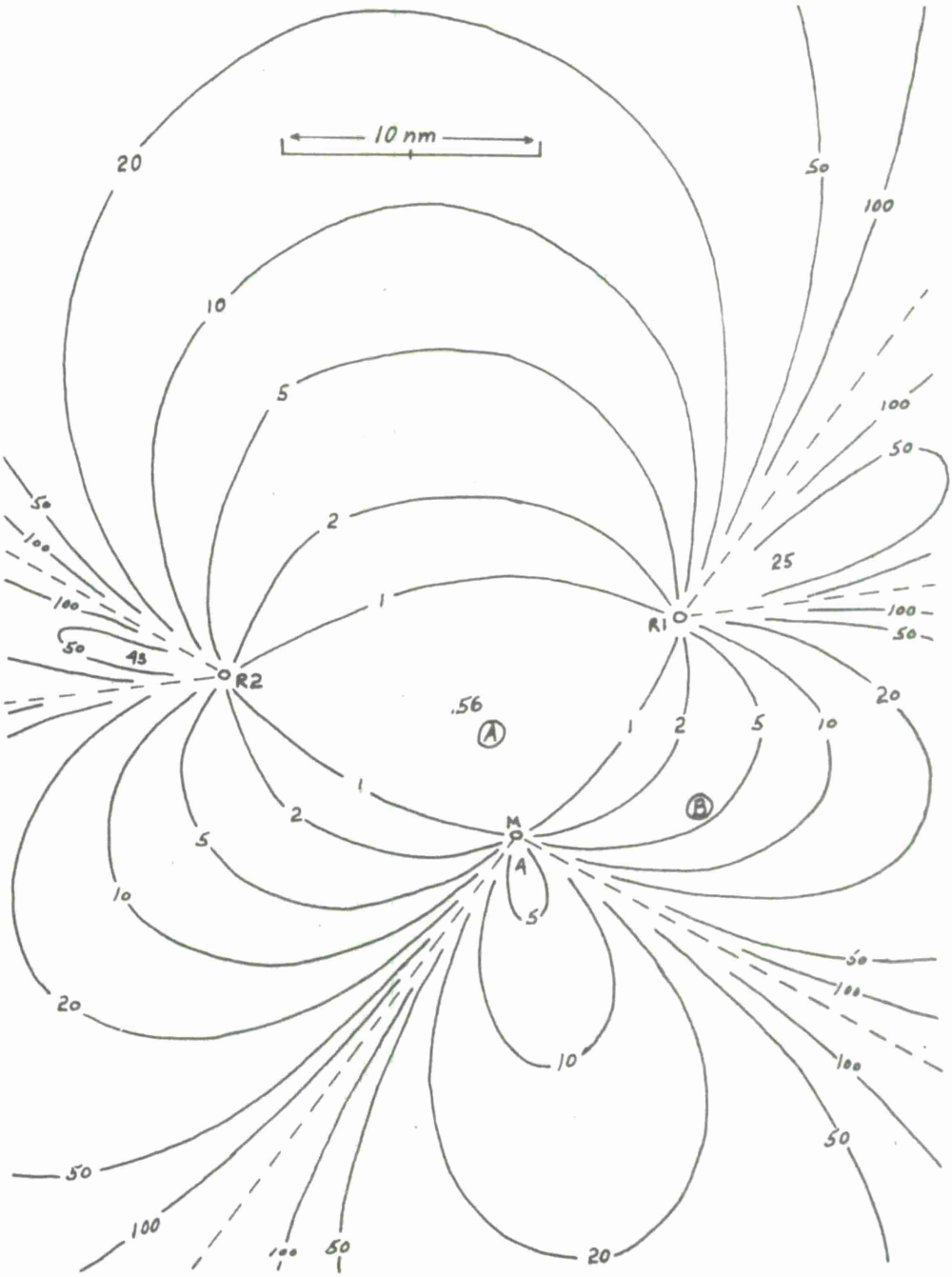

Figure 23. Geometric Dilution of Precision (Time) $\dot{g}t$ in the PLRACTA Demonstration Test Bed

dilution of precision (position) which is always slightly larger than $\dot{g}t$. The greatest difference occurs in close where $\dot{g}t$ reaches a minimum of 0.58, while $\dot{g}p$ is 1.15. As distance from the triad increases the two become nearly equal.

Two locations, A and B, are marked on Figure 23. At position A, the $\dot{g}t$ is .58--about as good as it can get. At position B, the $\dot{g}t$ is 3.76. The response of a ground unit located at each of these positions will be shown in some detail. The steady state condition of the reference triad has already been discussed, and is that pictured in Figure 21, Tables VI and VII. in which the reference sites used a rather coarse value of $\alpha(.14)$. The ground unit was in position A in run #301 and in position B in run #303. In both cases, a transient period of 25 successful time solutions was specified (according to the Solution check the following equation [16]). At location A this was accomplished in 27 frames, while at location B, this required 46 frames. The environmental conditions and expected performance for these two cases are itemized in Table IX.

In Table IX, β_t is computed internally to $\alpha_t^* \cdot \alpha_t/(2-\alpha_t)$, so that if the effective constant, α_t^* equals α_t, then β_t is optimum (reference 5), otherwise it is suboptimum. Generally, β_t will level off somewhat toward the critically damped curve (Figures 4 and 5). Also, items rp and rt--tracking power--are given by equation (47) and (50), and eff, the efficiency is computed by equation (53). The expected tracked position error, σ_p^* is given either by equation (48) in the transient state, or by equation (54) in the steady state.

Time history plots of position error are shown in Figure 24 and plots of time and time rate error are shown in Figure 25. The plots at least give the general picture. With site A, the exponential nature of the position response and the time jump are apparent. A near steady state condition had been reached by the end of the transient period, and ensuing logic switch. In the simulation, this logic switch is rather arbitrary with respect to existing conditions. For site A, it occurred at an opportune time.

At site B the response is much rougher due to the higher $\dot{g}t$. It also appears that a bad moment was chosen for switching to the steady state logic. However, bear in mind that the expected values of the standard deviation of position and time error in the transient state, σ_p^* and σ_t for site B were 200 feet (.033 nm) and 156 nanoseconds respectively (from Table IX). Thus, the fact that in frame 45, ex = .025 nm, ey = .031 nm (i.e. ep = .04 or 244 feet) and e = -375 nanoseconds, is not unreasonable. The errors are large however, and after the logic switch it takes some time for

Table IX

GROUND--ENVIRONMENT AND EXPECTED PERFORMANCE

MTA	.5 nm
DMAX	1 nanosecond/second

	Site A	Site B
eo	453 ns	614 ns
do	-1.26 ns/s	-1.09 ns/s
exo	0.024 nm	0.040 nm
eyo	0.076 nm	-0.030 nm
ezo	-18 feet	-94 feet
$\dot{g}t$	.58	3.76
$\dot{g}p$	1.17	4.80

	Transient	Steady State	Transient	Steady State
αt	.18	.032	.18	.032
βt	.0178	.00052	.0178	.00052
α_p	.18	.018	.18	.018
rp	2.36	7.45	2.36	7.45
rt	2.68	6.44	2.68	6.44
eff	0	0	0	.41
σ_p/σ_{pt}	2.36	7.45	2.36	24.3
σ_p*	55 ft	17.3 ft	200 ft	22 ft
σ_p*	.0089 nm	.0028nm	.0329 nm	.0036 nm
σ_t	24 ns	10 ns	156 ns	65 ns

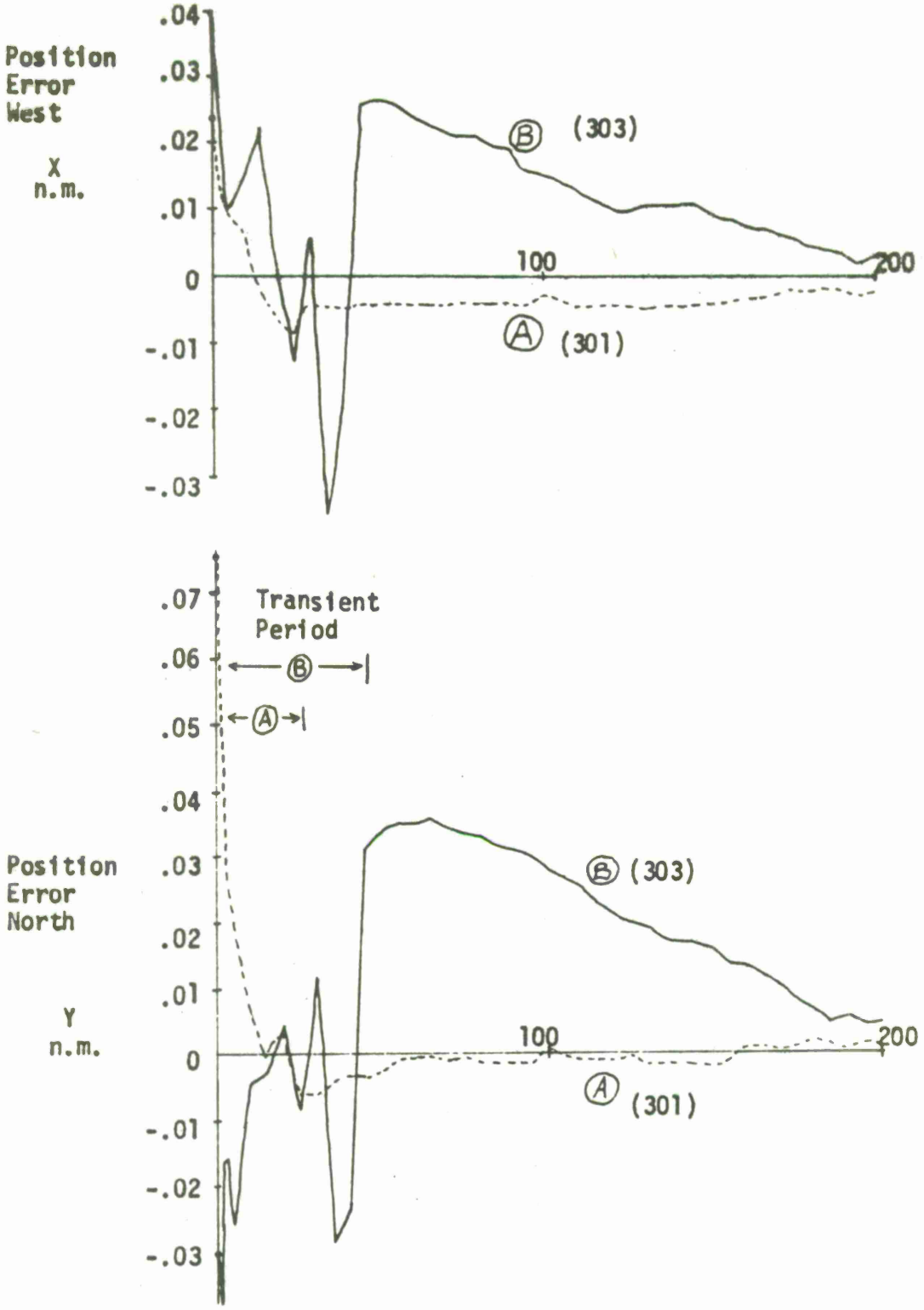

Figure 24. Ground Unit--Initial Position Location

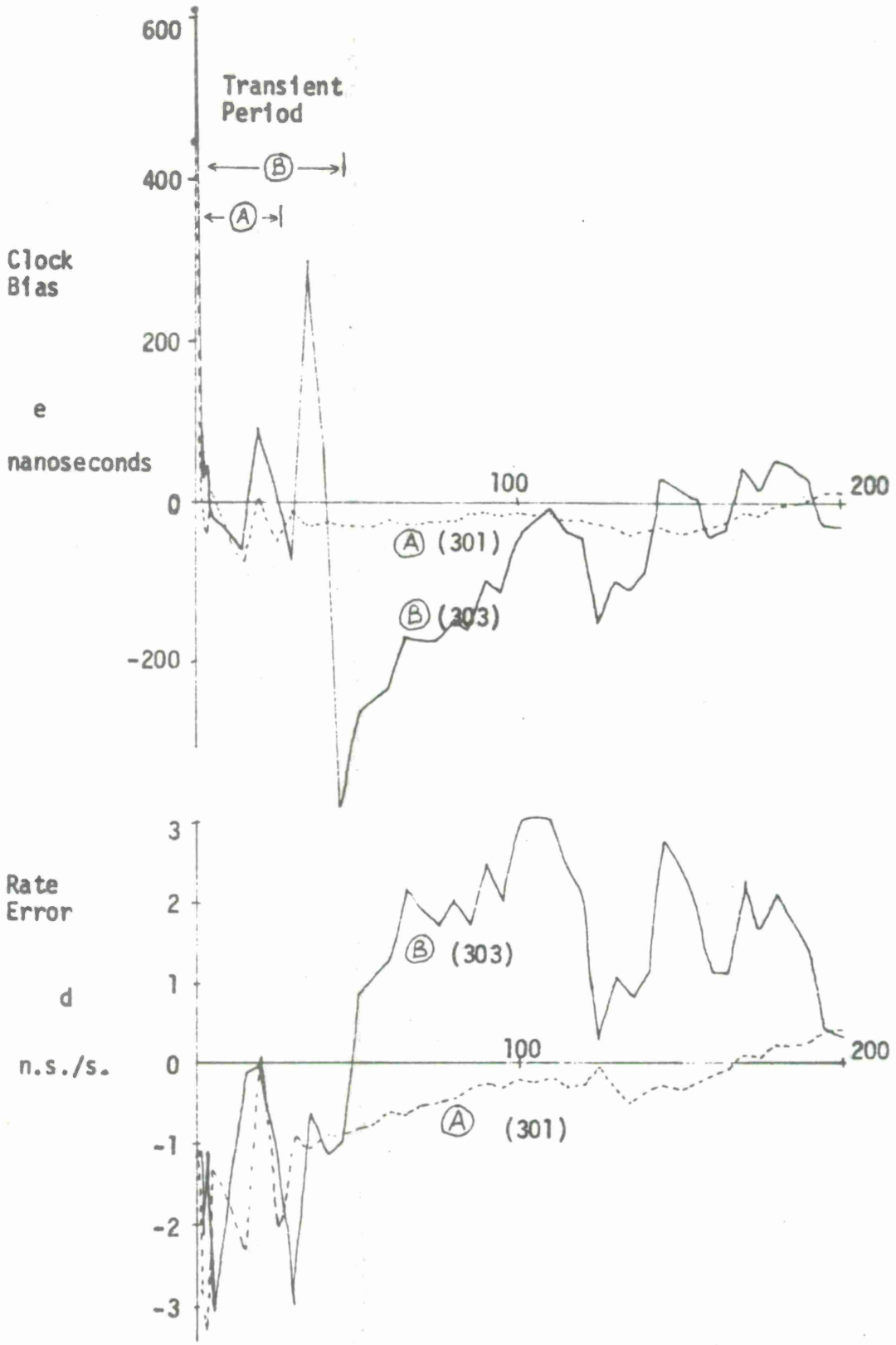

Figure 25. Ground Unit--Initial Synchronization

the position error (and the time error) to settle down to their final values. In fact, it is a moot point whether the final values have been reached on this run. (Further consideration will be given to the steady state ground unit in the next section--run #306.)

Statistical measurements on selected frames from runs #301 and #303 pictured in Figures 24 and 25, is tabulated in Table X. The theoretical data is repeated from Table IX. Predicted biases in time and position are shown as zero, though they are in fact dependent upon the particular conditions of the reference sites (Figure 21, Tables VI and VII).

Table X

GROUND--MEASUREMENTS VERSUS EXPECTATION

Site A

	Transient			Steady State		
	Frames	Theory	Sim	Frames	Theory	Sim
$\bar{e}$	5	0	-28 ns	30	0	-18 ns
r.m.s.(e)	to 25	24 ns	41 ns	to 200	10 ns	22 ns
σt		24 ns	30 ns		10 ns	13 ns
$\overline{ep}$	10	0	45 ft	30	0	26 ft
r.m.s.(p)	to 25	55 ft	51 ft	to 200	17 ft	27 ft
σ_p*		55 ft	23 ft		17 ft	4 ft

Site B

	Frames	Theory	Sim	Frames	Theory	Sim
$\bar{e}$	5	0	-13 ns	100	0	-23 ns
r.m.s.(e)	to 45	156 ns	169 ns	to 200	65 ns	59 ns
σ_t		156 ns	169 ns		65 ns	54 ns
$\overline{ep}$	5	0	146 ft	175	0	103 ft
r.m.s.(p)	to 45	200 ft	163 ft	to 200	22 ft	113 ft
σ_p*		200 ft	119 ft		22 ft	7 ft

Measured data for the root mean square error generally runs higher than predicted due to the non-zero bias, except for the transient position error; the measured standard deviation about the mean time error is generally higher, but there are exceptions in both cases. The measured values of position standard deviation are quite low, but this may be a matter of the definition of σ which is logical in the x or y direction but which loses meaning when combined into the ever positive position error. The r.m.s. position error, however, is still a faithful measure of bias plus standard deviation.

I believe that the important point here is that with one exception--the steady state position of site B which is barely that--the measured values are really quite close to those predicted by theory, especially considering the introduction of bias from the reference sites.

Of interest is the time history of the effective αt of the modified α - β tracker. This is shown in Figure 26 for the two examples. With A, the value proceeds down from one in an orderly manner during transition, then jumps to and maintains a value near .033 indicating a solution rate of about 95%. In case B, after 1 solution several successive failures occur driving α back up to one. Then it appears to get about a 70% solution rate, leveling off near .30 in transition and near 0.06 in steady state.

ENTRY OF AIRBORNE UNIT

Assume that the reference triad plus one mobile ground unit are operating in a steady state condition. We will now consider an incoming airborne unit--at first as a passive system member, performing time synchronization, position location, and velocity adjustment; then as an active system member interacting with ground and master units. The example chosen was run #306 of 3 April 1971.

The scenario for #306 is depicted in the $\dot{g}t$ contour map of Figure 27. (This figure is similar to Figure 23, but with the scale increased by a factor of 3.5--it is roughly 20 n.m. to the inch.) The mobile ground unit labeled G, is located in the vicinity of Cambridge Hill--approximately 16 n.m. north and 5 n.m. west of E Building. At this point $\dot{g}t$ = 3.38 and gp = 4.23 which is similar to the ground unit B in the previous example, #303. As the run starts, it is assumed that the master, two references and the ground unit have been operating for some time and are in a steady state condition. The airborne unit, labeled A, enters the system at a point 65 n.m. north and 15 n.m. west of E Building. It is flying south at 300 knots maintaining 2000 feet altitude. At this point, the aircraft can "see" only the ground unit and two reference sites.

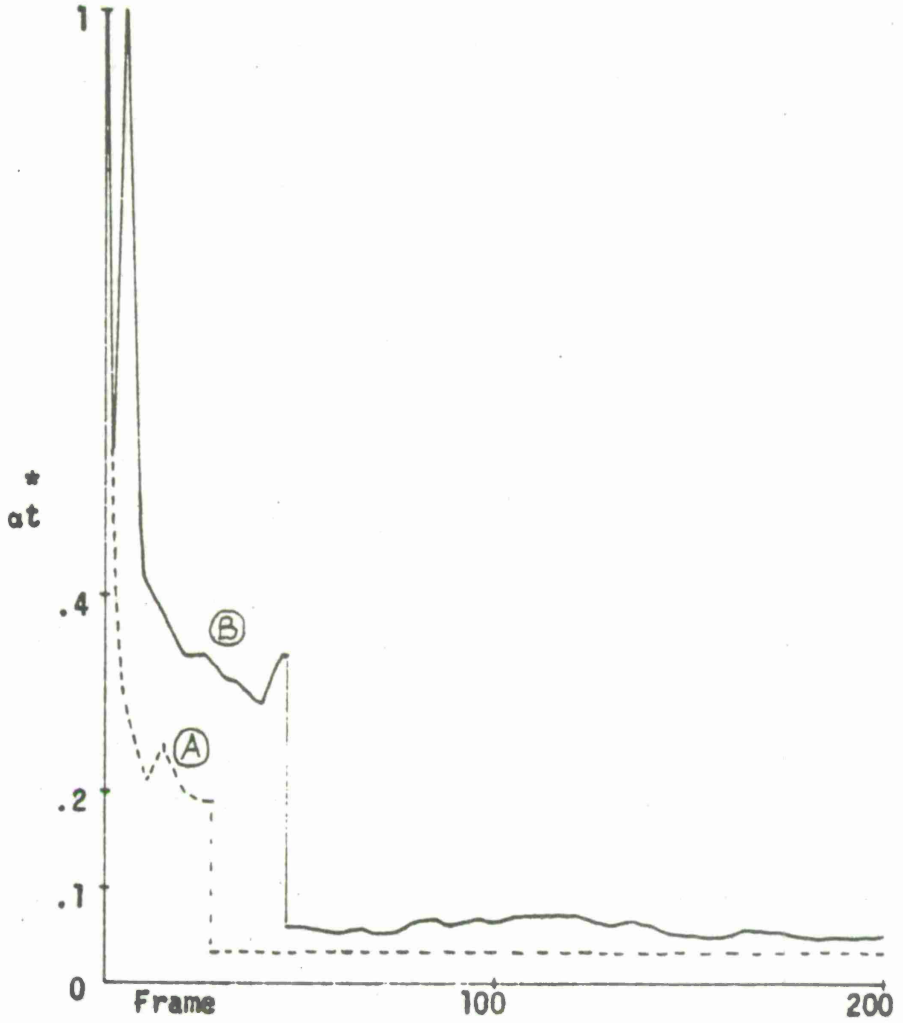

Figure 26. Effective Time Smoothing Constant

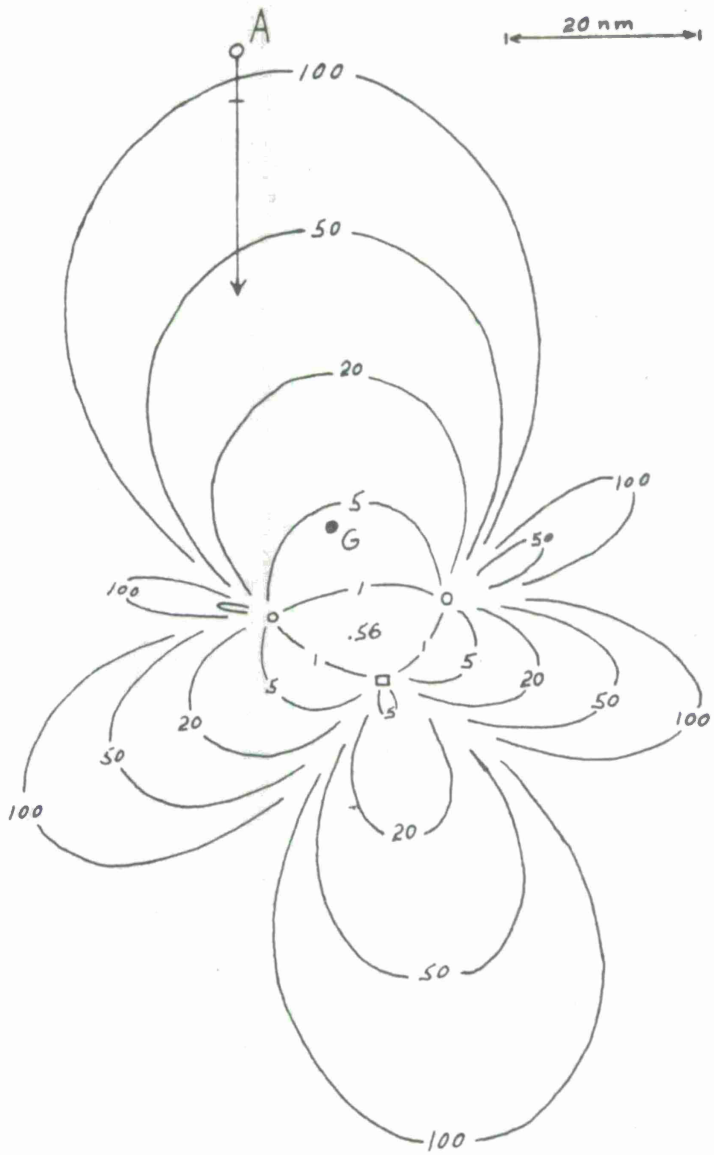

Figure 27. Scenario for Run #306, Showing $\dot{g}t$ Contours

Because the master is not initially in sight, his data priority is 2. His $\dot{g}t$ = 104.7 and $\dot{g}p$ = 105.5. The initial conditions and environmental parameters are shown in Table XI.

The particular initial condition errors shown in Table XI are the result of a random perturbation of specified σ about zero mean. The aircraft continues to be effected by random perturbation, at the start of each frame, in speed, heading and climb rate, about a zero error mean.

It was required that the airborne unit obtain 25 unsuccessful time solutions before becoming active. Because the successful solution rate was just over 50% in the transition phase, this required 48 frames. In Frame 49 then, the time smoothing constant was switched from .18 to .044 and position determination changed from hyperbolation to direct ranging. At this time the master was not yet in sight so the data priority of the airborne unit remained at 2 and while the aircraft utilized ground data, the ground mobile did not yet utilize airborne data. In frame 53, the aircraft picks up the master, changes data priority to 1 and then starts interacting with the ground unit. The run continues through frame 300, by which time the airborne $\dot{g}p$ has been reduced to 32.6.

A plot of the variation in $\dot{g}p$ is shown in Figure 28, for both the air and ground unit. The airborne unit experiences a continuously decreasing geometric dilution of precision except for the discreet jump in frame 53 when the additional source is added. That change is just proportional to $\sqrt{4/3}$, and is due to the change in sample size. The ground unit shifts from a constant $\dot{g}p$ = 4.23 to a constant $\dot{g}p$= 1.08 when it starts using the airborne source. This change is due almost entirely to the sudden improvement in geometry, i.e. picking up a source on the side opposite from the reference triad.

The expected steady state position error, assuming that measurement is the only source of error, is found as before by multiplying $\dot{g}p$ by the measurement error, and the factors rp, rt, and eff as shown in equation (54). As with other runs in this series, the effective measurement error was taken to be the combination of σ_t = 50 and σ_m = 100 nanoseconds. Thus, the effective measurement error is 112 nanoseconds or 0.018 nautical miles. The expected position error is plotted as dashed lines in Figure 29. The actual values of position error obtained in the simulation are shown as solid lines. There curves represent root mean square averages over 25 frame periods.

The ground unit appears not to have started in a true steady state as the position error climbs and seems to be leveling off between 0.005 and 0.006 nautical miles (30 to 35 feet) as opposed to

Table XI

#306 ENVIRONMENT

ktm	.6	master feedback constant (time)
kpm	.6	master feedback constant (position)
DMAX	.5 ns/s	time rate adjustment limit/sec
VMAX	.1 knot	speed adjustment limit/sec
HMAX	.03 degrees	heading adjustment limit/sec

Unit	R1	R2	G	A
α_t (active)	.036	.036	.032	.044
β_t (active)	.00068	.00068	.00052	.001
α_t (passive)	N/A	N/A	N/A	.18
β_t (passive)	N/A	N/A	N/A	.018
α_p	N/A	N/A	.018	.18
β_p	N/A	N/A	N/A	.018
MTA(G)	.05 nm	.05 nm	1.0 nm	1.0 nm
eo	-13 ns	40 ns	77 ns	-99 ns
do	.34 ns/s	-.17 ns/s	1.22 ns/s	1.06 ns/s
exo	.0004 nm	.0072 nm	-.0008 nm	-.0868 nm
eyo	-.0051 nm	-.0100 nm	.0038 nm	.0277 nm
ezo	5 ft	16 ft	-89 ft	-23 ft
σ_{vp}	N/A	N/A	N/A	.5 knots
σ_h	N/A	N/A	N/A	.1 degree
σ_w	N/A	N/A	N/A	.5 ft/sec

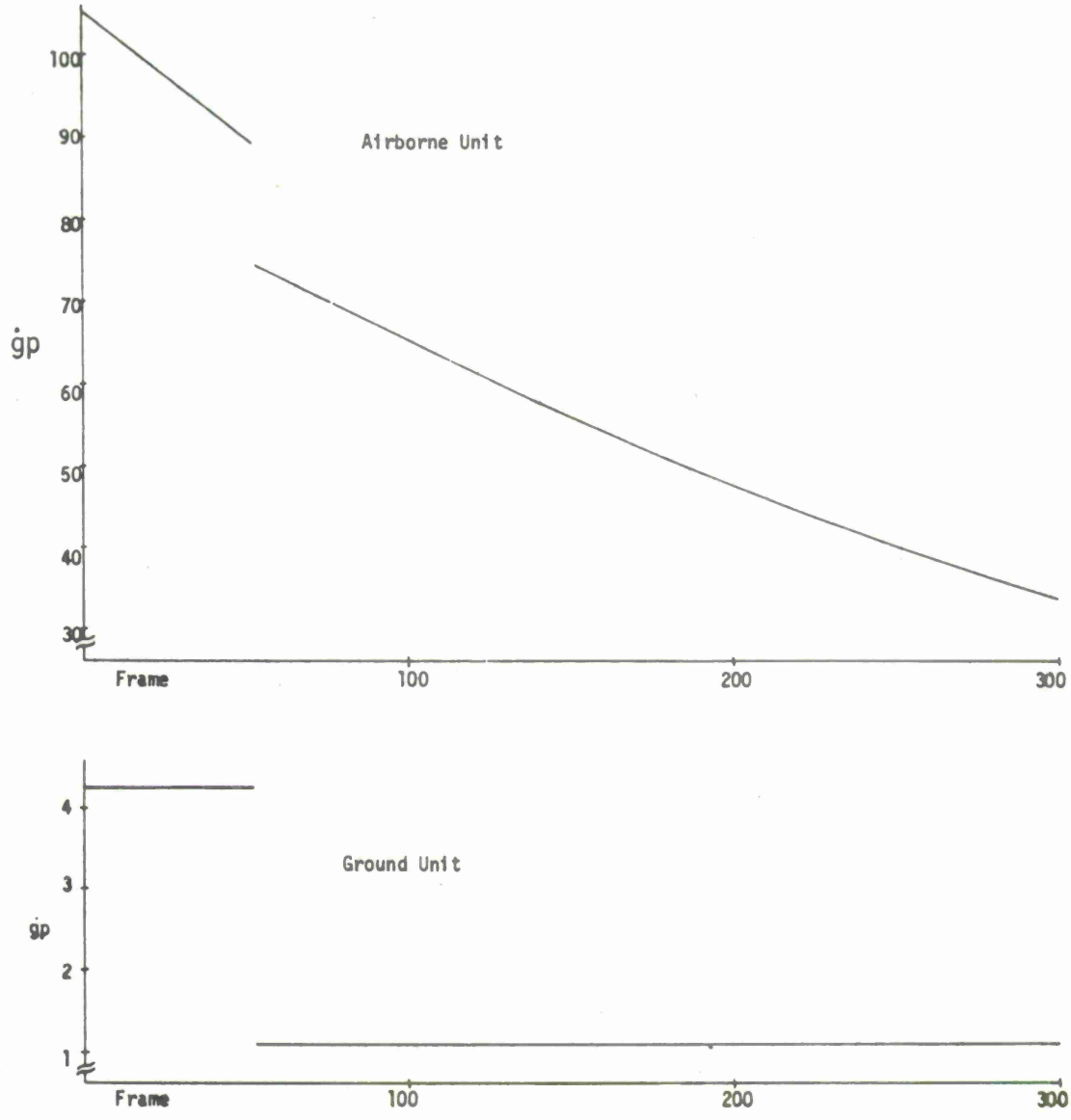

Figure 28. Variation in Geometric Dilution of Precision (Position) ġp for Run #386

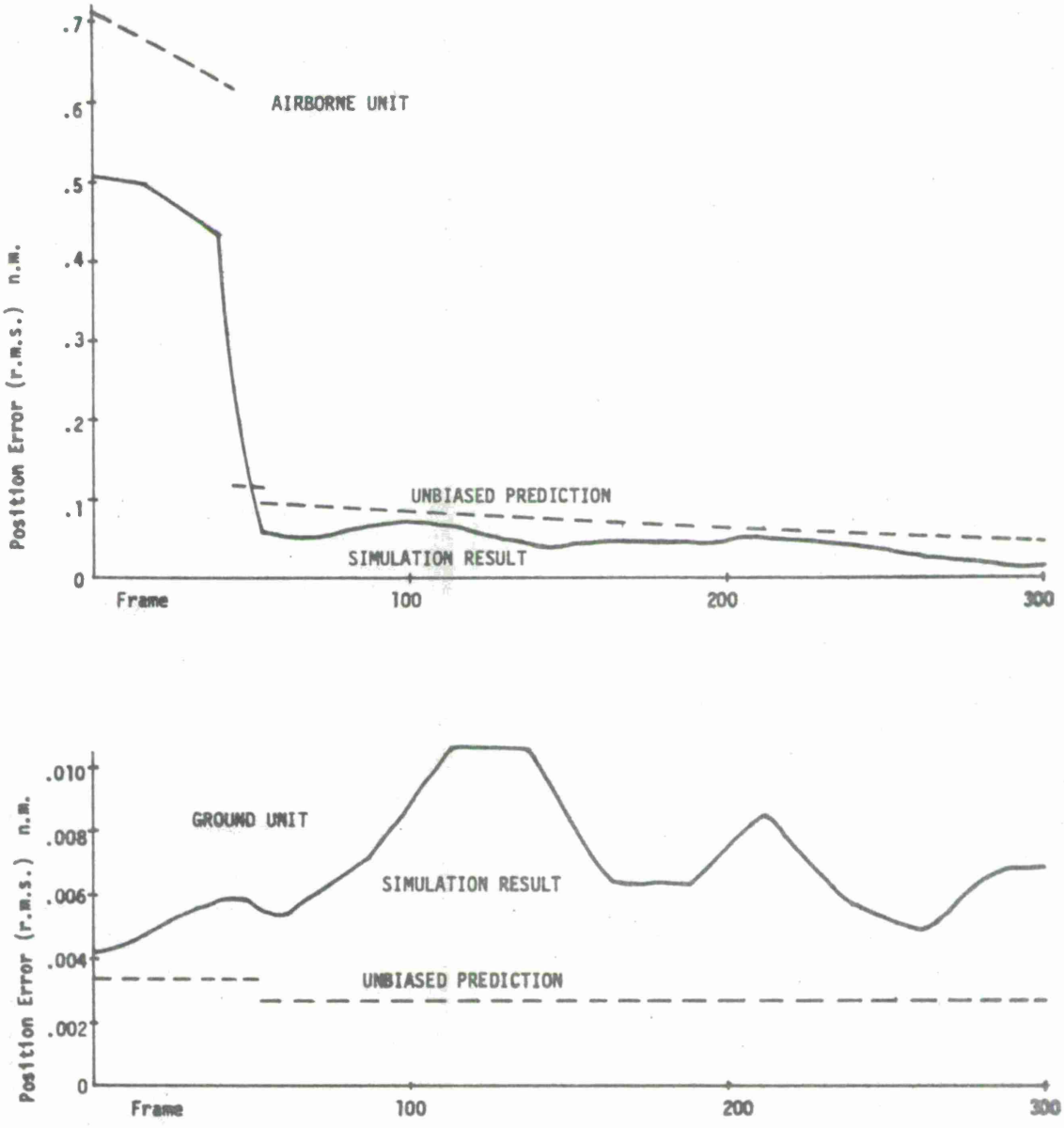

Figure 29. Predicted and Observed Position Error (r.m.s.) Run #306

the expected 0.003 n.m. (20 feet). The larger error must be due the position and timing error of the reference sites. Then, as the airborne source is brought in, the error climbs to between 0.10 and 0.11 n.m. (60 to 66 feet), showing the effect of adding a source with comparatively larger time and position errors. The error then follows a general downward trend corresponding to the improving condition of the airborne source. Toward the end of the run, the position error of the ground unit is not appreciably different from that which existed before acquiring the airborne source.

The airborne unit exhibits a position error some 25% lower than might be expected. There are three probable sources for this:

(a) Successive positions are highly correlated so that the effect of master feedback is to suppress peak error.
(b) The two interacting units are on the same side of the reference triad so that errors at one unit tend to induce a negative reaction at the other, which in turn tends to correct for the original error.
(c) Velocity adjustment was severely limited (see Table XI) so that the expected variance as indicated by equation (49) is not obtained.

The velocity adjustment limiting used in this example could only be used by aircraft with instrument inputs to the computer. This could be either IMU input or speed and heading input. It is assumed such input will accurately sense changes and have only a slowly varying bias that can be tracked with long period integration. Much noisier response would be expected from aircraft trying to track speed and heading.

While Figure 29 provides a nutshell performance picture of run #306, the next three figures provide supportive information on a frame to frame basis. These will be presented with as little verbiage as possible.

Time and time-rate error of the two reference sites is shown in Figure 30. Included is the expected bias due to position error. Because the reference units use an α of 0.036, the tracked clock error (standard deviation) should be 6.06 times smaller than the measurement error. Thus, the one sigma spread shown is 18.5 nanoseconds. At R2, the time error seldom strayed past these limits, while at R1 the time error appears to be biased some 10 to 15 nanoseconds low. At both reference sites the clock rate error appears to oscillate about zero, at least after the first 100 cycles.

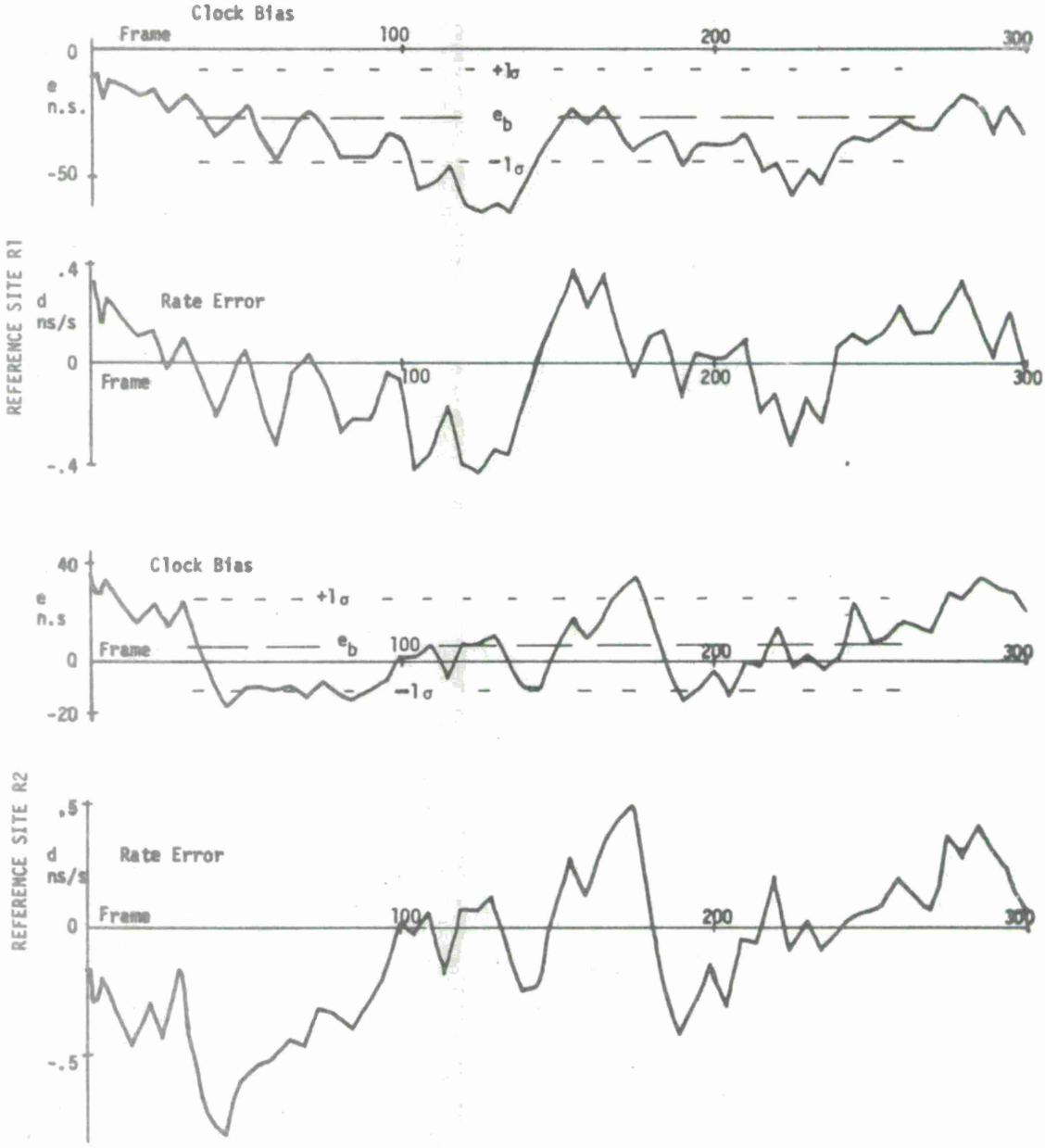

Figure 30. Reference Site Timing Error, Run #306

Time and time rate error of the ground unit (dashed line) and the airborne unit (solid line) are shown in Figure 31. For the first 60 frames, the airborne clock error has been scaled down by a factor of 10 (to fit) so that the maximum negative error hits -6.5 μs.

The time feedback, transmitted by master, is also shown in Figure 31 (dotted line). It is shown negatively as it is subtracted. Comparison will reveal general correlation between system error and feedback.

Position errors, in x and y (west and north) of the ground unit (dashed line) and the airborne unit (solid line) are shown in Figure 32. Again, for the first 60 frames, the airborne position error has been scaled down by a factor of 10 so that, for example, the maximum negative y error is nearly one nautical mile. It is noteworthy that prior to frame 53, the ground unit appears to stabilize at a position error of about 0.005 n.m. in x and y. This bias being induced by reference site error. The airborne unit appears to have a bias of about -0.25 n.m. in y and -0.05 n.m. in x during this period. There is a sudden stop of the wild excursions as the aircraft switches to direct ranging in frame 45, and after interaction starts with ground and master units, the position bias seems nearly to be eliminated. At least there are several zero crossings. The ground unit also appears to have reduced the y position bias, but this fact is somewhat hidden in the noise.

The x and y feedback transmitted by the master, is also shown in Figure 32 (dotted line). The values are generally small prior to frame 53 because the master does not "see" the aircraft. When the aircraft comes in view, the efforts of feedback are obvious as the negative bias is cranked out. Thereafter, there is good correlation.

Finally, of interest is the time history of the variable smoothing constant, αt. This is shown in Figure 33--ground unit dotted line and airborne unit solid line. It was mentioned earlier that the airborne unit experienced a solution rate of about 50% during the transition phase, which results in an effective αt of .36, given kt = .18. During the remainder of the run this appears to average about 45% producing an effective αt = .10 given a kt = .044. The ground unit, which starts in steady state, has a solution rate close to 60% just prior to frame 53, which produces an αt of .05 given kt = .032. Then the addition of the airborne source improves $\dot{g}t$ and sharply increases αt to .225. This then settles down to about 0.035 in the later frames indicating an effective solution rate of about 95%.

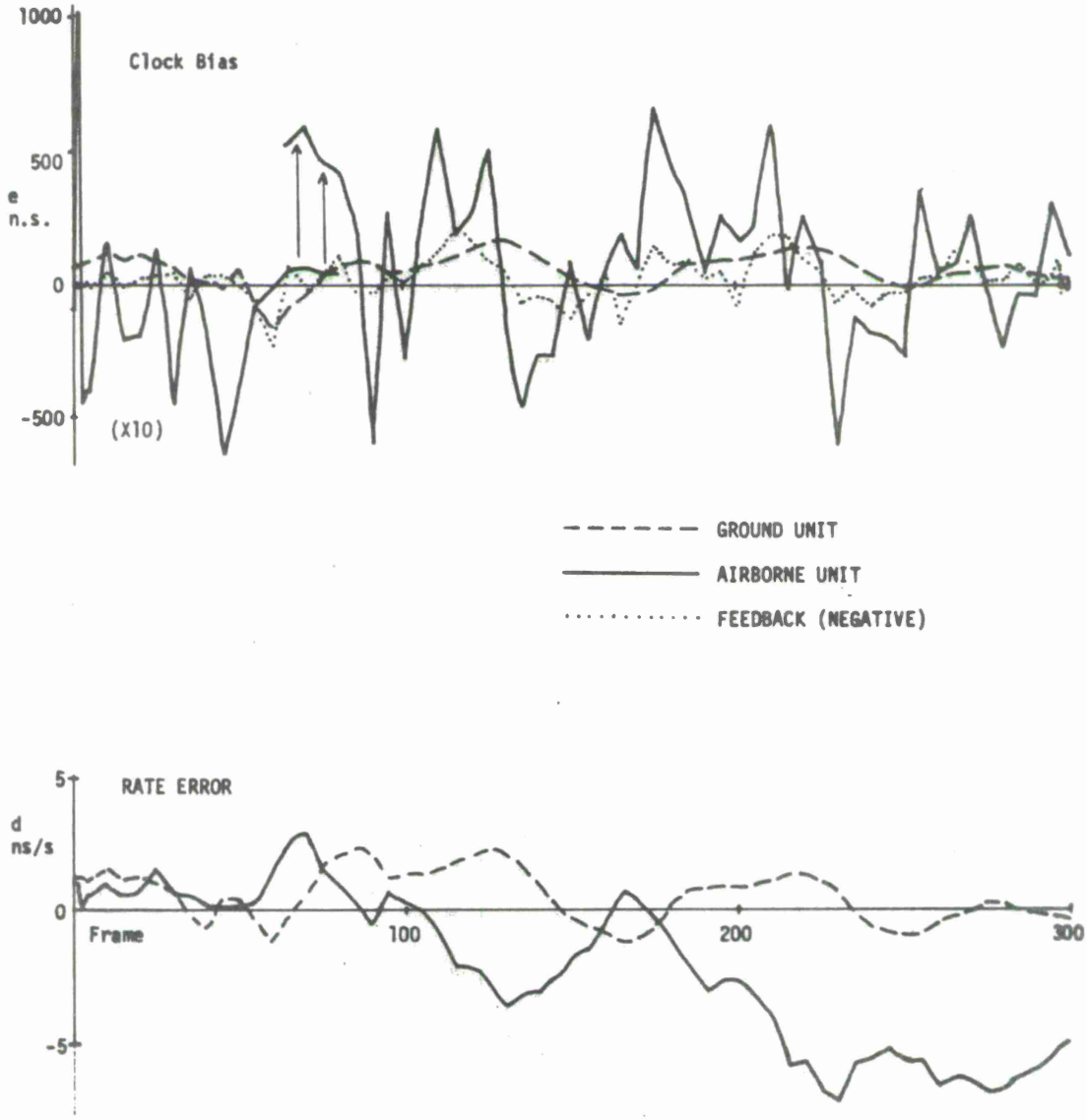

Figure 31. Ground and Airborne Timing Error, Run #306

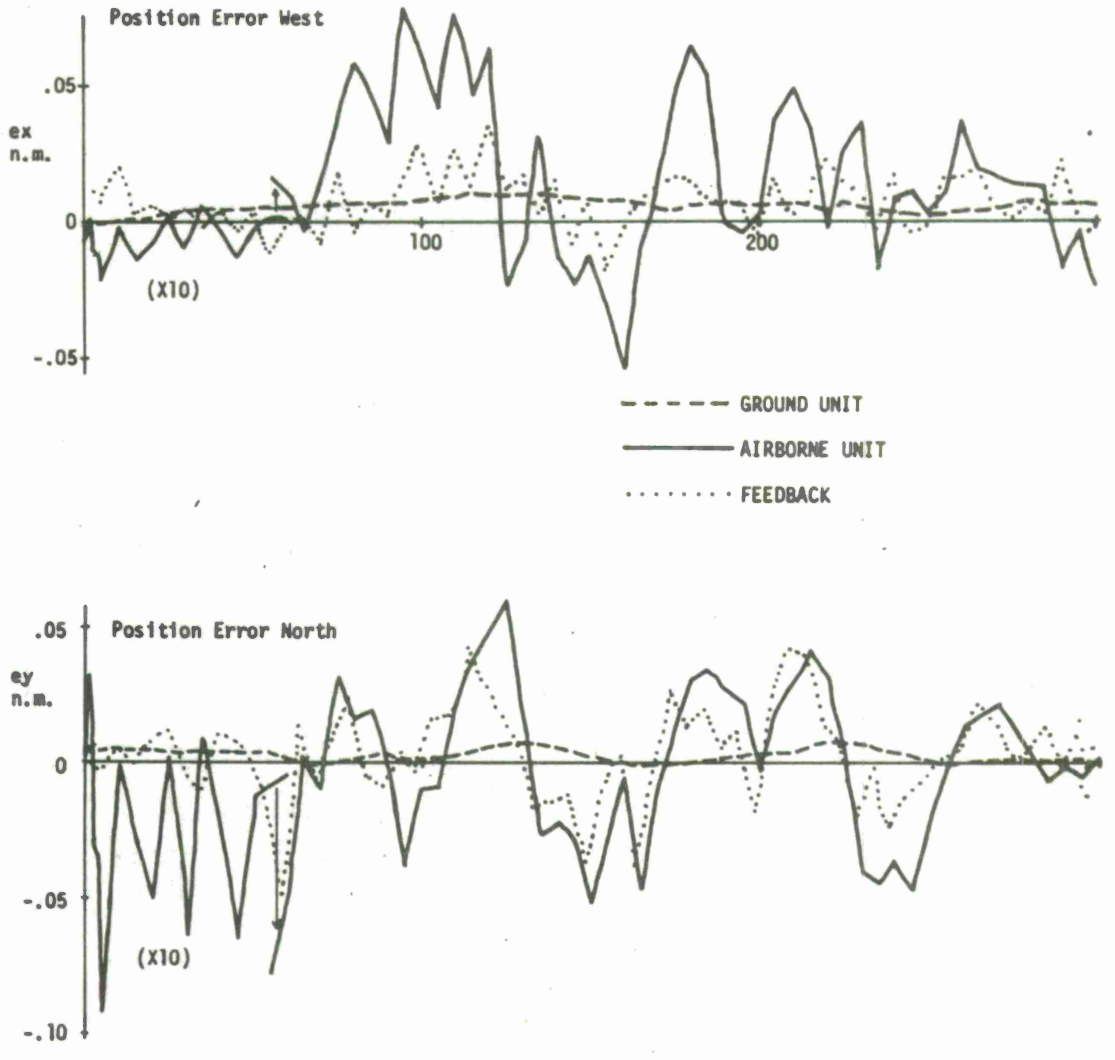

Figure 32. Ground and Airborne Position Error, Run #306

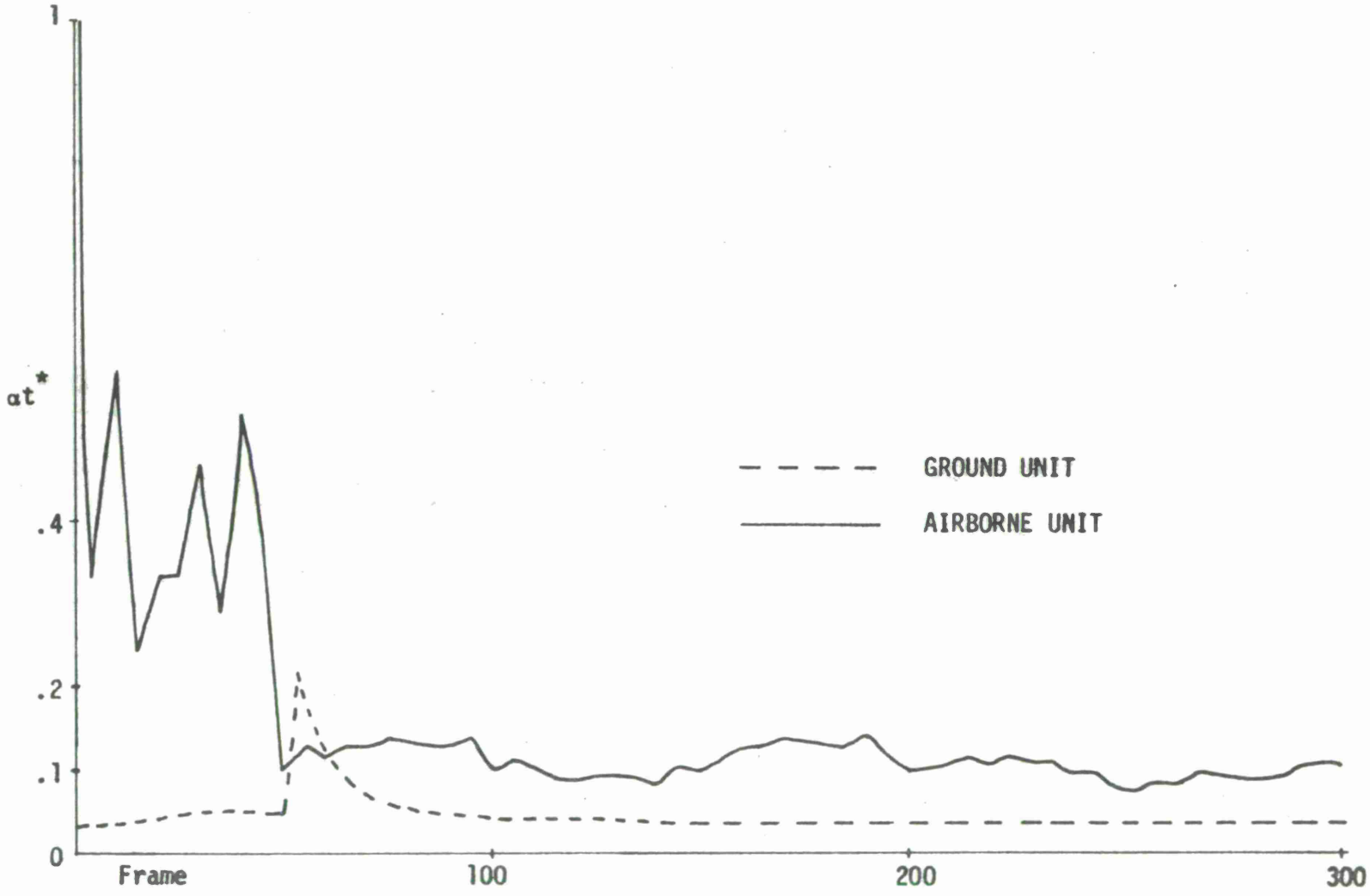

Figure 33. Effective Time Smoothing Constant, αt*, Run #306

AIRBORNE EXTENSION OF COVERAGE

The ability of airborne elements of a PLRACTA network to extend navigation coverage to a remote ground unit will now be considered. The example chosen is simulation run #319 of 2/5/71. This run also shows steady state reference and airborne performance. The aircraft, in this case have particularly large geometric dilution of precision. The ground unit can "see" one reference (Millstone) and the two aircraft. The location of the units is shown on the $\dot{g}t$ contour map of Figure 34. The ground unit, labeled G, is 28 n.m. west and 8 n.m. north of E Building. Initially A1 is 20 n.m. west and 45 n.m. north of E Building, while A2 is 45 n.m. east and 70 n.m. south. (A2 starts with a $\dot{g}p$ of 275.) The aircraft are both flying west at 300 knots.

This particular arrangement was chosen also to demonstrate the capability of the solution check which follows equation (16). Without this filter, such a system, with interacting elements on opposite sides of the reference triad, cannot operate--it tends to blow up. This is because any error induced on one element by measurements on the other is reflected back as positive feedback--just the opposite of the situation in #306 shown previously. The filter takes advantage of the natural system noise and rejects solutions which appear to contain positive feedback.

This run begins with all units in a steady state condition. The ground unit is quite accurately located, initially, so that the effect of 200 frames of tracking off noisy sources can be observed. The initial conditions and other environmental factors are shown in Table XII. It is assumed that A1 and A2 are instrumented such that the navigation program can make use of accurate velocity change information, therefore integrating instrument bias over a number of frames. In this run they are straight line tracks.

The time history of $\dot{g}p$ is shown in Figure 35 for the ground and two airborne units. Because the airborne units also can "see" each other, their effective $\dot{g}p$ is smaller by a factor $\sqrt{3/4}$ than shown in Figure 34, due to the larger sample size. They offer each other no geometric improvement until the last 25 frames. The $\dot{g}p$ at the ground site is quite low because of the wide angle subtended by its data sources.

As before, the $\dot{g}p$ are converted to expected position error, assuming measurement noise is the only input error (equation 54). Expected position error, zero bias, is plotted in Figure 36--the dashed lines--for the three units. These curves just mirror the changes in $\dot{g}p$. The position errors obtained from the simulation are also plotted in Figure 36. Plotted are the 25-frame r.m.s. values of

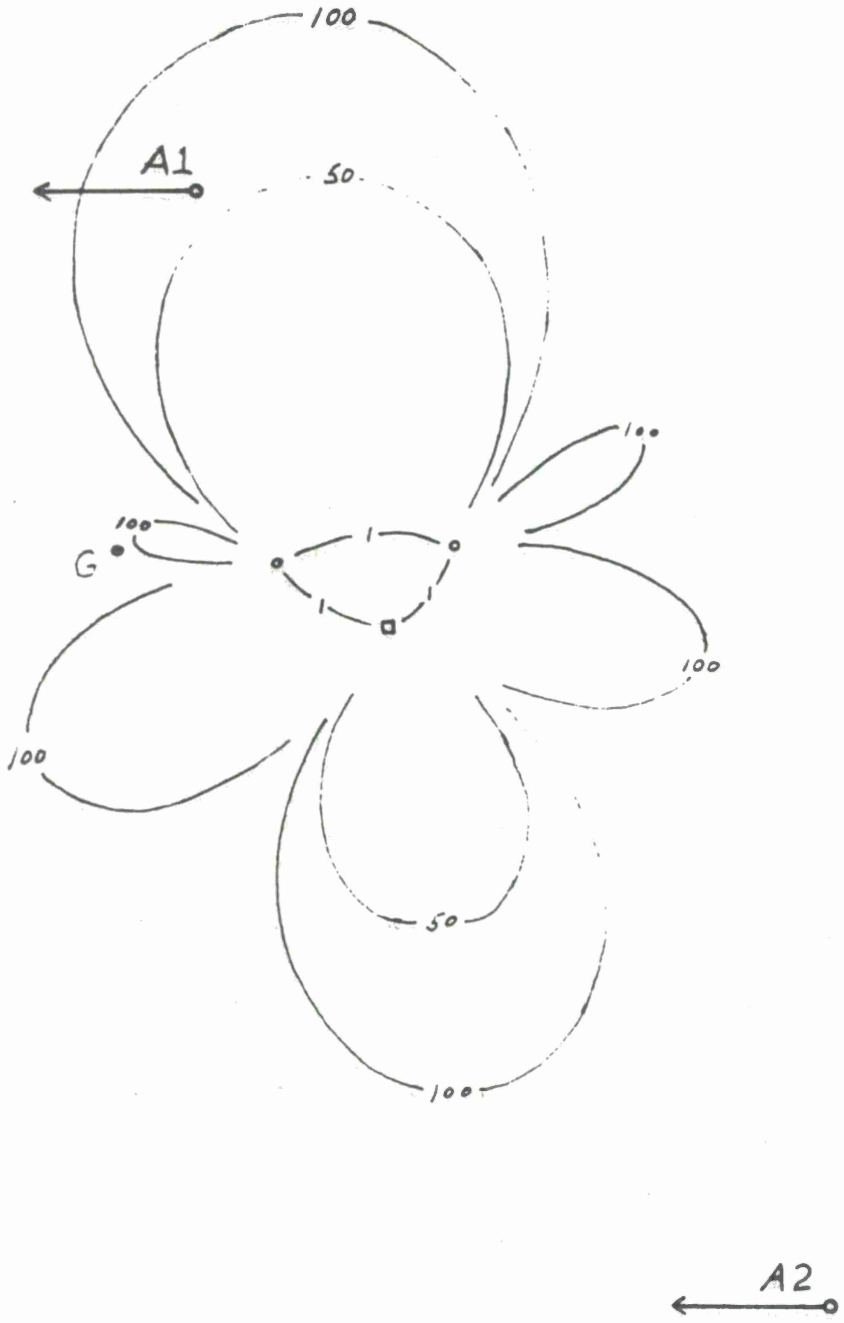

Figure 34. Scenario for Run #319, Showing $\dot{g}t$ Contours

Table XII

#319 - ENVIRONMENT

ktm	.6
kpm	.6
DMAX	.5ns/s
VMAX	1 knot
HMAX	.3 degree

Unit	R1	R2	A1	A2	G
αt	.036	.036	.044	.044	.032
βt	.000684	.000684	.001	.001	.00052
αp	N/A	N/A	.18	.18	.018
βp	N/A	N/A	.018	.018	N/A
MTA(G)(n.m)	.05	.05	.1	.1	.1
eo(ns)	0	-4	-44	87	-45
do(ns/s)	.49	-.84	-.45	1.41	1.35
exo(n.m)	-.0080	-.0100	.0042	.0268	.0005
eyo(n.m)	-.0017	-.0034	-.0375	-.0212	-.0060
ezo(ft)	-.2	9.8	91.5	122.5	27.9
σvp(knots)	N/A	N/A	.5	.5	N/A
σh(degrees)	N/A	N/A	.1	.1	N/A
σw(ft/sec)	N/A	N/A	.5	.5	N/A

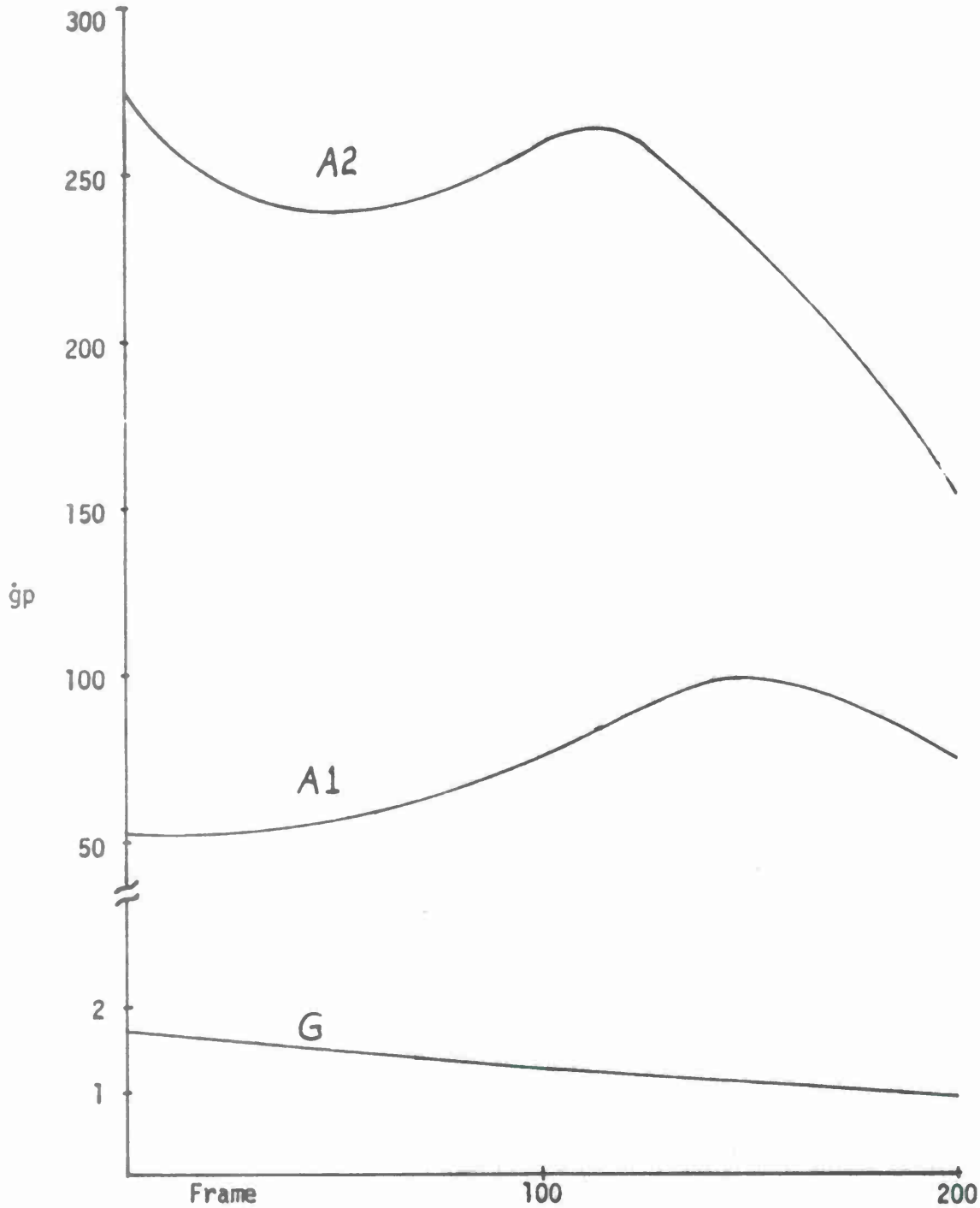

Figure 35. Variation in Geometric Dilution of Precision (Position) ġp

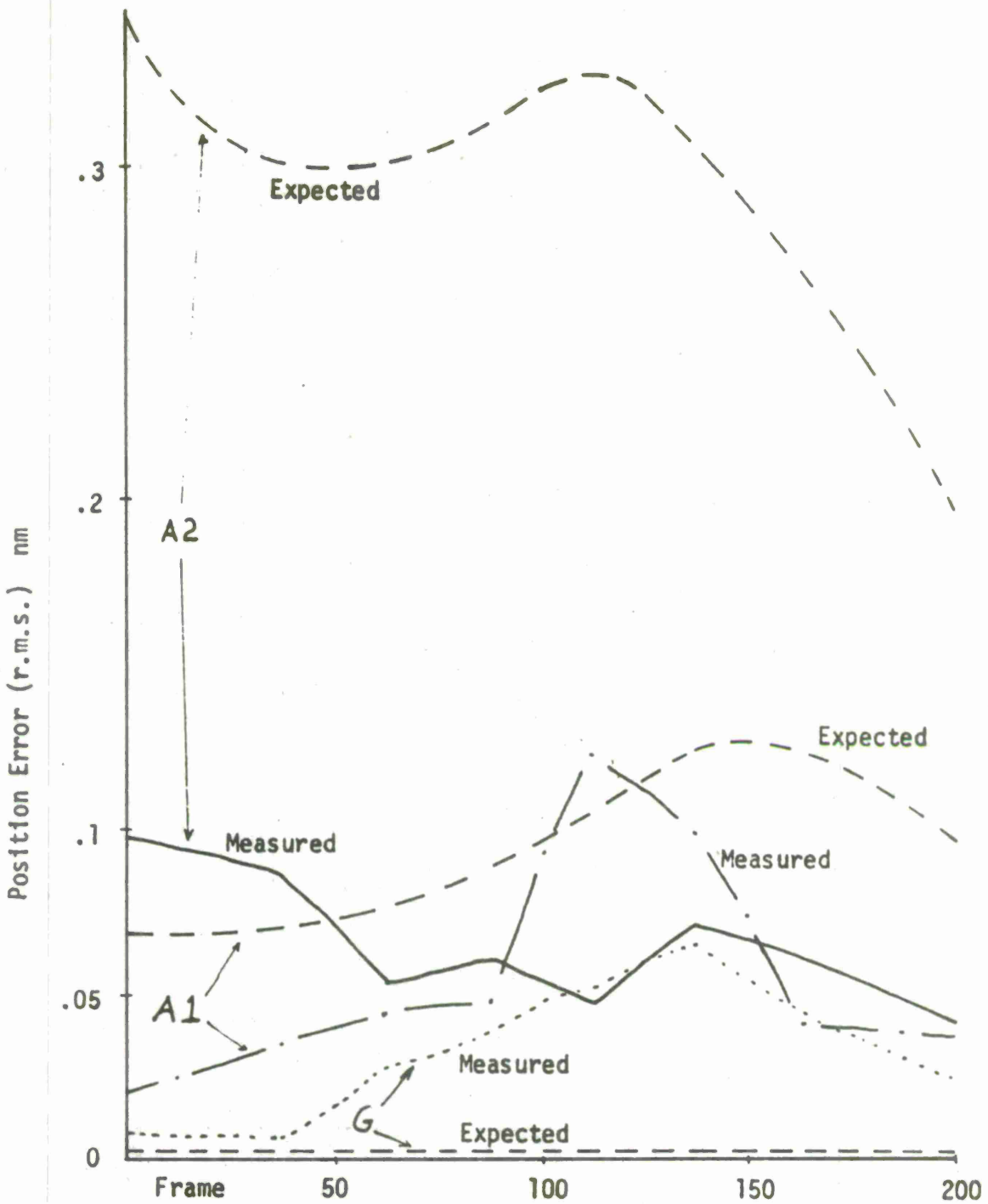

Figure 36. Predicted and Observed Position Error (r.m.s.), Run #319

position error. Here, it is somewhat surprising to find unit A2, the high ġp track, some three times more accurate than expected. What does seem normal is that A1 and A2 tend to assume the same characteristics, and that the ground unit likewise tends to assume the characteristics of its sources. On the latter point, bear in mind that one of G's sources was a reference site. Two reasons for performance exceeding theory were discussed in connection with #306, namely the effect of master feedback on highly correlated position error and the limiting applied to velocity adjustments. The third reason discussed there definitely does not apply here with the units being on opposite sides of the triad. Yet, quite obviously, the airborne units benefit from their data exchange.

Two remaining figures are shown to provide supportive data for run #319. Figure 22 has already shown histories of the time and time-rate error of the two reference sites in connection with the discussion on steady state performance of reference sites.

Figure 37 shows time and time-rate error of the ground unit (dashed line) and the mean of the two airborne units (solid line). Not much can be said except that time error appears to fluctuate about zero. The rise in time rate error toward the end may or may not be significant.

Master feedback of time corrections is also shown (negatively) in Figure 37 (dotted line). There is a strong correlation between the feedback and the airborne mean time error from frame 90 through frame 150.

The x and y components of position error are shown in Figure 38. The mean airborne error is the solid line and the dashed line is for the ground unit. The relative steadiness of the ground unit due to using a much smaller smoothing constant is apparent. Also, interesting is the effect of the net long term error in y, which the airborne units exhibit, upon the ground site--pulling it off to +0.067 nm by frame 135, after which it recovers. At the ground site y was perpendicular to the master, if this has any effect.

The master position feedback is also shown in Figure 38 (dotted line). Here the efforts of the master to correct the system y error up to frame 145 is plain. The x feedback is not particularly correlated with the airborne x error, however.

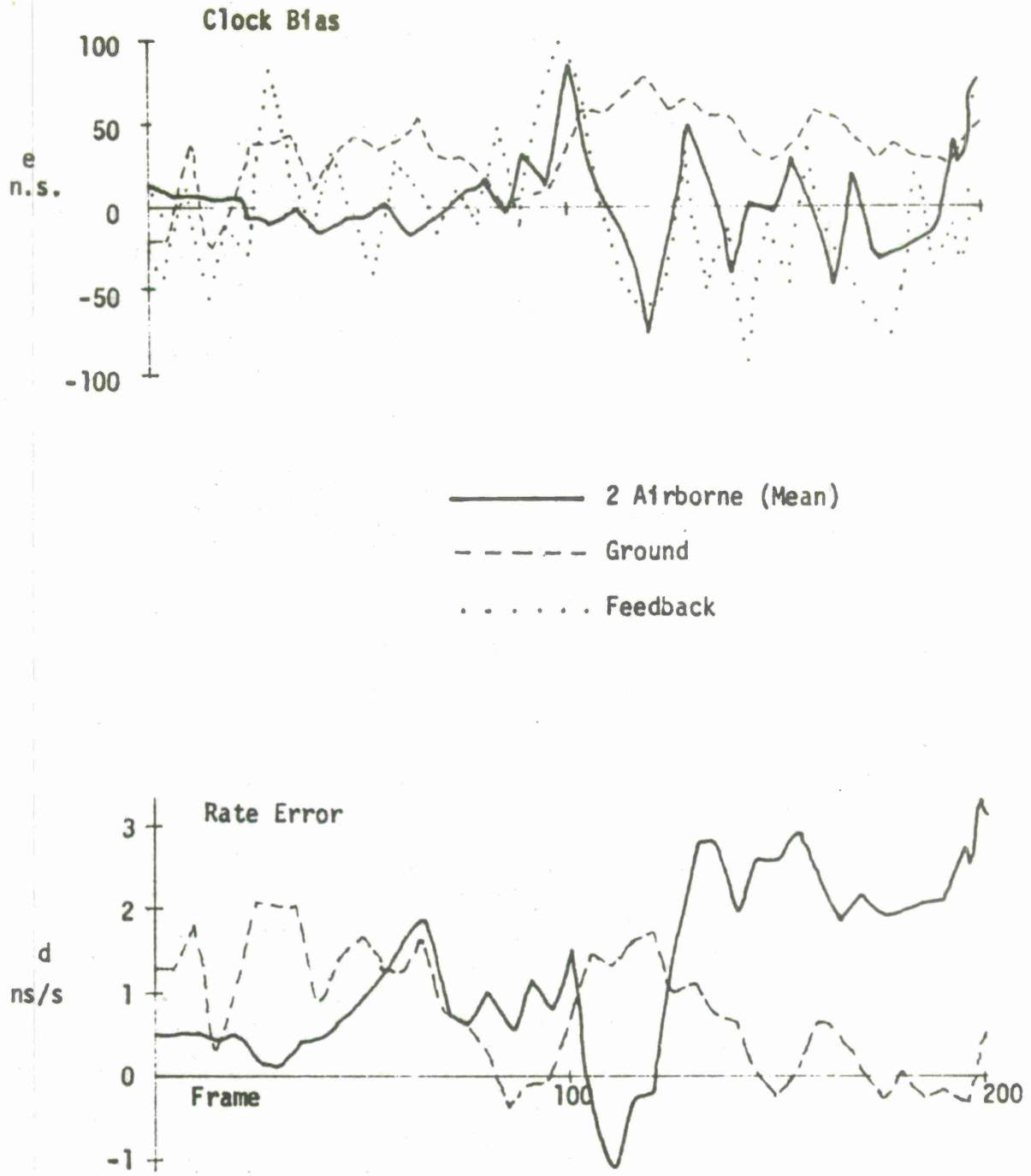

Figure 37. Ground and Airborne Timing Error, Run #319

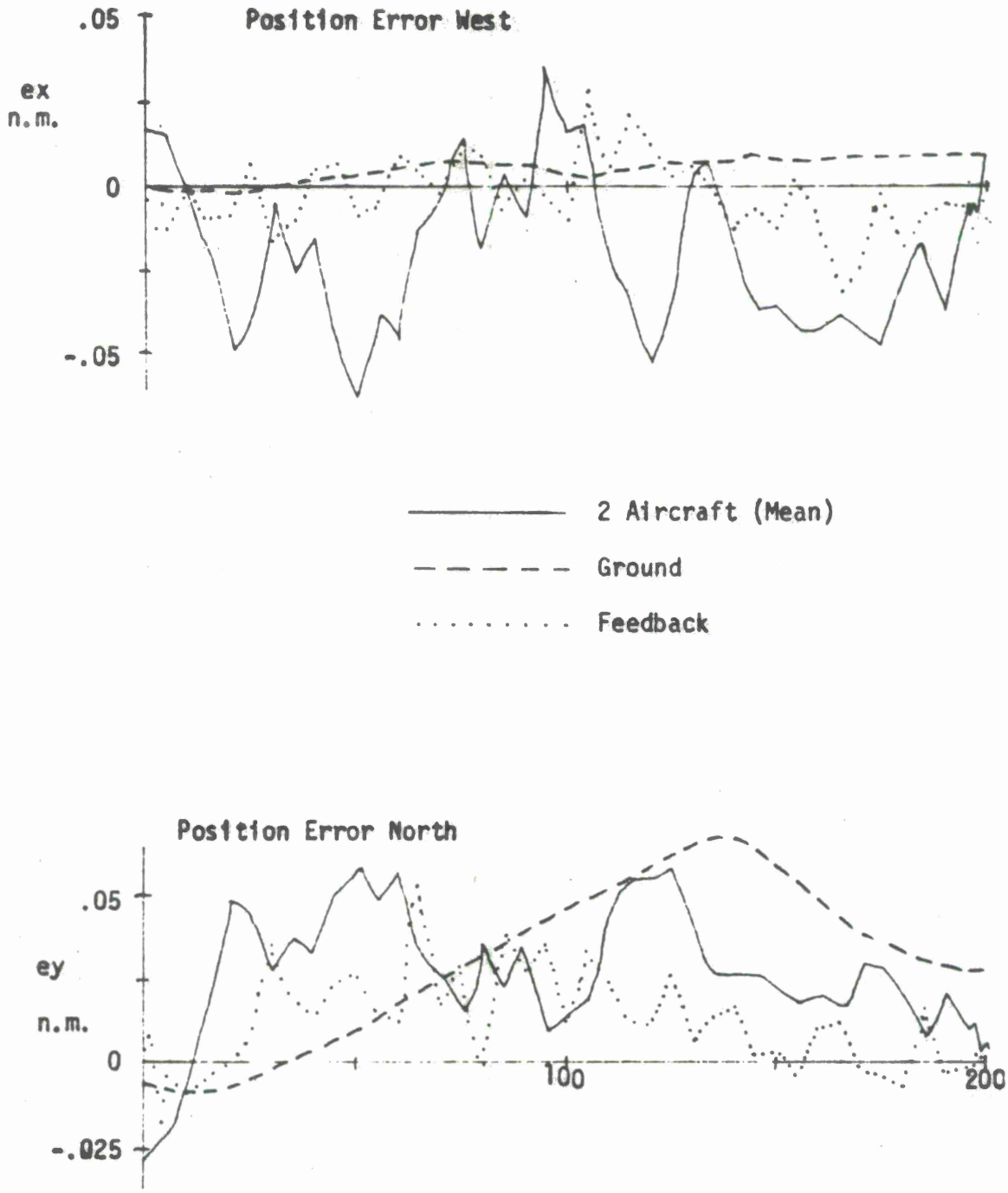

Figure 38. Ground and Airborne Position Error, Run #319

SECTION VI

TACTICAL AREA SIMULATION

In this section, the concept of mutual data exchange for navigation purposes is extended to many aircraft covering a broad area. The results of a single simulation run--#214 of 2/14/71--will be examined in some detail. This run contains thirty airborne elements and three remote ground reference stations (one master and two references, not within line-of-sight). It spans 100 frames--just over 15 minutes in real time--but differences in speed, altitude, navigation capability, geometry, initial conditions and changes with time provide many interesting areas for investigation. The principal items to be observed are:

a. Maintenance of synchronization at remote reference sites by monitoring data priority one aircraft.

b. Steady state error performance of airborne units, and the differences between those of data priority one and data priority two.

c. Synchronization and location of airborne units with very large initial errors.

d. Navigation capability of non-instrumented aircraft.

e. Navigation capability of remote airborne units relying solely on airborne data sources.

The run begins with the two reference sites and sixteen airborne units already in a near steady state condition. Ten of these aircraft are data priority, one--can see the master--and together with the master and two references which transmit five times per frame, provide the data base. The remaining six aircraft are data priority two. Four of the airborne units are maneuvering. Three of these use instrument tracking and one uses data tracking. The data tracker and two of the instrument trackers automatically activate and deactivate their status based on apparent position error. The remaining twelve units follow simple straight line tracks (which should be equivalent to instrument tracks). Aircraft velocity is perturbed in the random walk manner at the start of each frame with sigmas of 1 knot, 0.1 degree and 1 foot per second. The parameter values for this run are shown in Table XIII, and the initial conditions for the nineteen steady state units are given in Table XIV following.

Also, at the start of the run, there are fourteen passive airborne

Table XIII

PARAMETERS FOR #214. 2/4/71

GENERAL

τ	10 seconds	frame time
s	10 milliseconds	slot time
σm	100 nanoseconds	measurement error
σt	10 nanoseconds	transmission error
ktm	.6	master feedback (αt)
kpm	.6	master feedback (αp)
DMAX	1.0 nanosecond	time rate adjustment limit
VMAX	7 knots	speed adjustment limit
HMAX	20.8 degrees	heading adjustment limit

SITE SENSITIVE

	Reference	Airborne (active)	Airborne (passive)
αt	.027	.054	.36
βt	.000378	.0015	.079
αp		.36	.6
βv		.0505	.084
βh		.1150	.192
MTA(G)	.1 nm	.2 nm	
χt	2 frames	2 frames	2 frames
χv		3 frames	3 frames

Table XIV

INITIAL CONDITIONS, STEADY STATE UNITS

	eo (nano-seconds)	do (nano-seconds/sec)	exo (nautical miles)	eyo	ezo (feet)	evp (knots)	eh (degrees)
Master	0	0	0	0	0		
Ref 1	-1	.006	0	.0050	30		
Ref 2	4	.105	.0050	0	-30		
A1	29	1.41	.0045	-.0035	37	-.1	-.05
A2	27	.59	-.0039	.0012	36	.2	-.16
A3	-20	-.14	.0044	-.0077	16	.1	-.11
A4	-9	.22	.0066	.0062	-65	-1.2	.14
A5	32	-.95	.0104	0	-5	-1.7	0
A6	42	-.97	-.0040	-.0031	20	-.3	-.06
A7	4	.64	.0054	-.0129	-7	0	-.07
A8	7	-.81	0	0	0	-1.7	.08
A9	-29	-1.96	0	0	0	1.9	.04
A10	2	.16	0	.0100	0	-.2	.02
A11	4	-1.33	0	-.0100	0	0	.09
A12	-7	.09	0	0	0	1.7	.98
A29	38	-.33	-.0039	-.0112	74	.5	-.06
A30	16	.38	.0070	.0013	14	.5	-.03
A31	22	1.17	-.0026	.0068	-37	-.2	-.03
A32	13	.48	-.0079	-.0094	0	1.9	-.10

units with very large errors in assumed position. These represent units that have completed frame one synchronization--that is, set their clocks to agree with the assumed position--so that each also has a correspondingly large clock bias. Seven of these aircraft are centrally located in the system (low $\dot{g}p$) and seven are "outside" (high $\dot{g}p$). The outsiders are some 200 nm from the nearest priority one unit and in the early stages of the run, as they approach the system, they must track off airborne units only, both priority one and two. In each group there are four maneuvering units, with two on data tracking and two on instrument track, and three straight line tracks. All are automatically activated and deactivated except for one of the straight line tracks which remains passive throughout the run. So, as synchronizing and locating progresses, four units in each group become active (most of the time)--the straight line trackers and the maneuvering units on instrument tracking. The interior ones become data priority one, and the exterior ones become data priority two. As a result, the data base, which drops to eight aircraft in frame 12, builds up to fifteen aircraft in frame 76, dropping again to twelve by frame 100. The initial conditions for the fourteen passive units are given in Table XV.

Figure 39 presents a map of this run, showing the initial positions (priority one, solid; priority two, hollow) and velocity vectors (active, solid; passive, dotted). An indication as to the type of tracking, instrument or data, is also given. (Straight line tracks are assumed to be instrument tracks.)

An idea of tracking capability over this area can be gained by considering, first, the single frame geometric dilution of precision (time) defined here as $\sigma t/\sigma m$ or abbreviated $\dot{g}t$. If only the three ground stations were used as data sources--assuming they can be seen--the contours of $\dot{g}t$ for this area are shown in Figure 40. The nodes and baseline extensions represent areas of no solution. Data for this figure, supplied by Mr. R. J. Kulpinski, has been scaled down to account for the fact that each ground reference station is transmitting five times per frame. Thus $\dot{g}t$ is reduced by a factor $\sqrt{5}$. The tracking accuracy obtainable by tracking the clock with αt, direct ranging for position, and tracking position with αp is shown in Figure 41 as contours of $\sigma PT/\sigma m$ over the area. This assumes that the effective transmission error is σm, and that the unit can "see" all three ground stations. It should be noted that capability is fairly uniform over a broad area, except for the nodes and the baseline extensions.

An immediate advantage of using airborne sources is demonstrated by run #214. A rough average of the $\dot{g}t$ actually experienced by all units over all frames is plotted in Figure 42. I say rough average, however no unit differed by more than a factor of two from this plot.

Table XV

INITIAL CONDITIONS, TRANSIENT UNITS

Insiders	eo (milli-seconds)	do (nano seconds per second)	exo (nautical miles)	eyo	ezo (feet)	evp (knots)	eh (degrees)
A13	.72	1	220	0	0	-.8	.02
A14	.69	-1	-215	0	0	-.8	.07
A15	.72	1	245	0	0	1.1	-.04
A16	.86	-1	245	0	0	.1	.06
A17	.60	1	235	0	0	-.3	.04
A18	.60	-1	235	0	0	.8	.14
A20	.52	-10	-190	0	0	.1	.17
Out-siders							
A21	.98	1	580	0	0	-3.4	.12
A22	1.09	-1	600	0	0	2.3	.04
A23	2.27	1	-390	0	0	.6	-.05
A24	1.15	-1	610	0	0	-1.0	.08
A25	2.21	1	-380	0	0	-2.4	.01
A26	1.04	-1	590	0	0	-1.5	-.18
A28	.92	-10	570	0	0	1.1	-.08

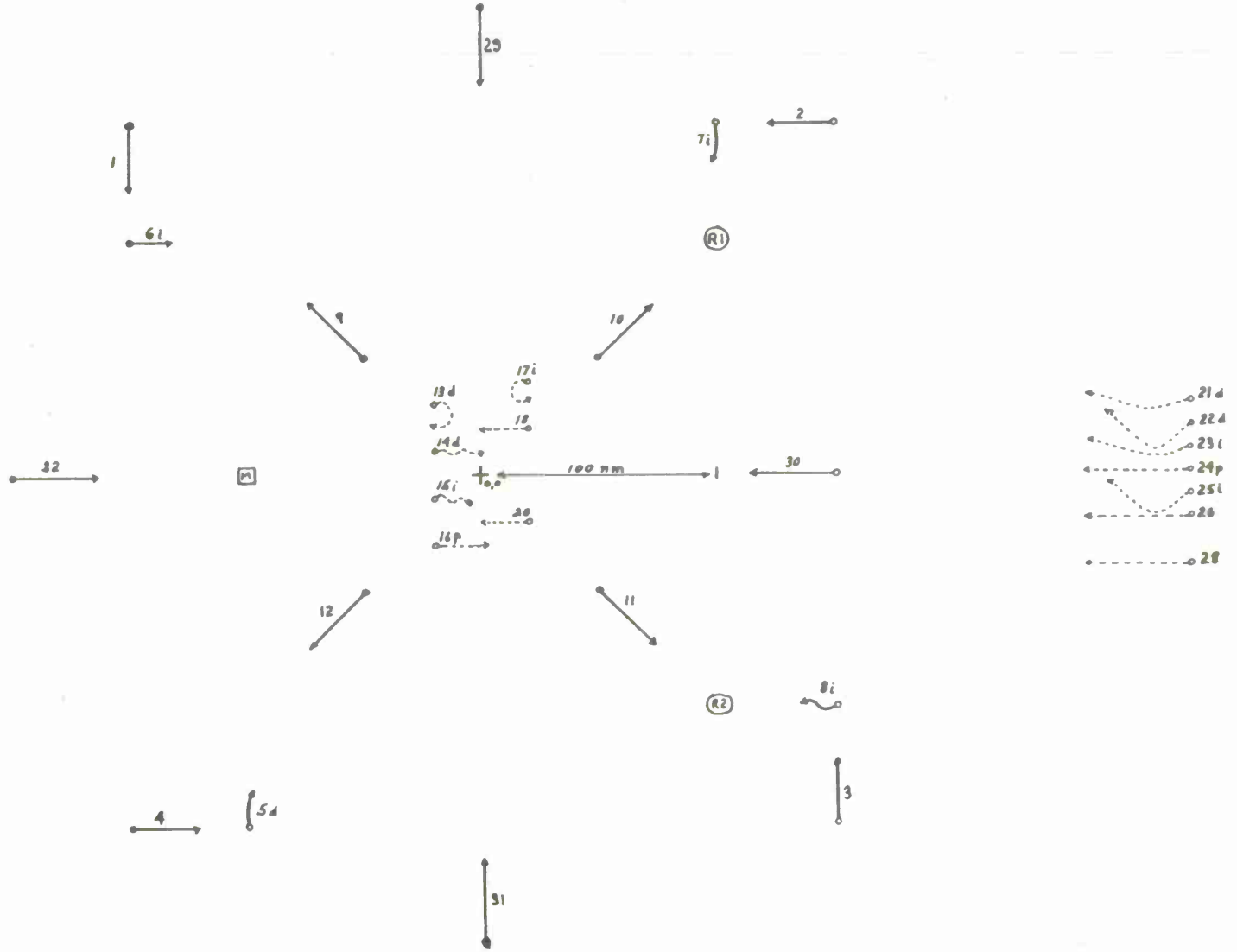

Figure 39. Area Map Showing Initial Positions and Velocity Vectors for Run #214

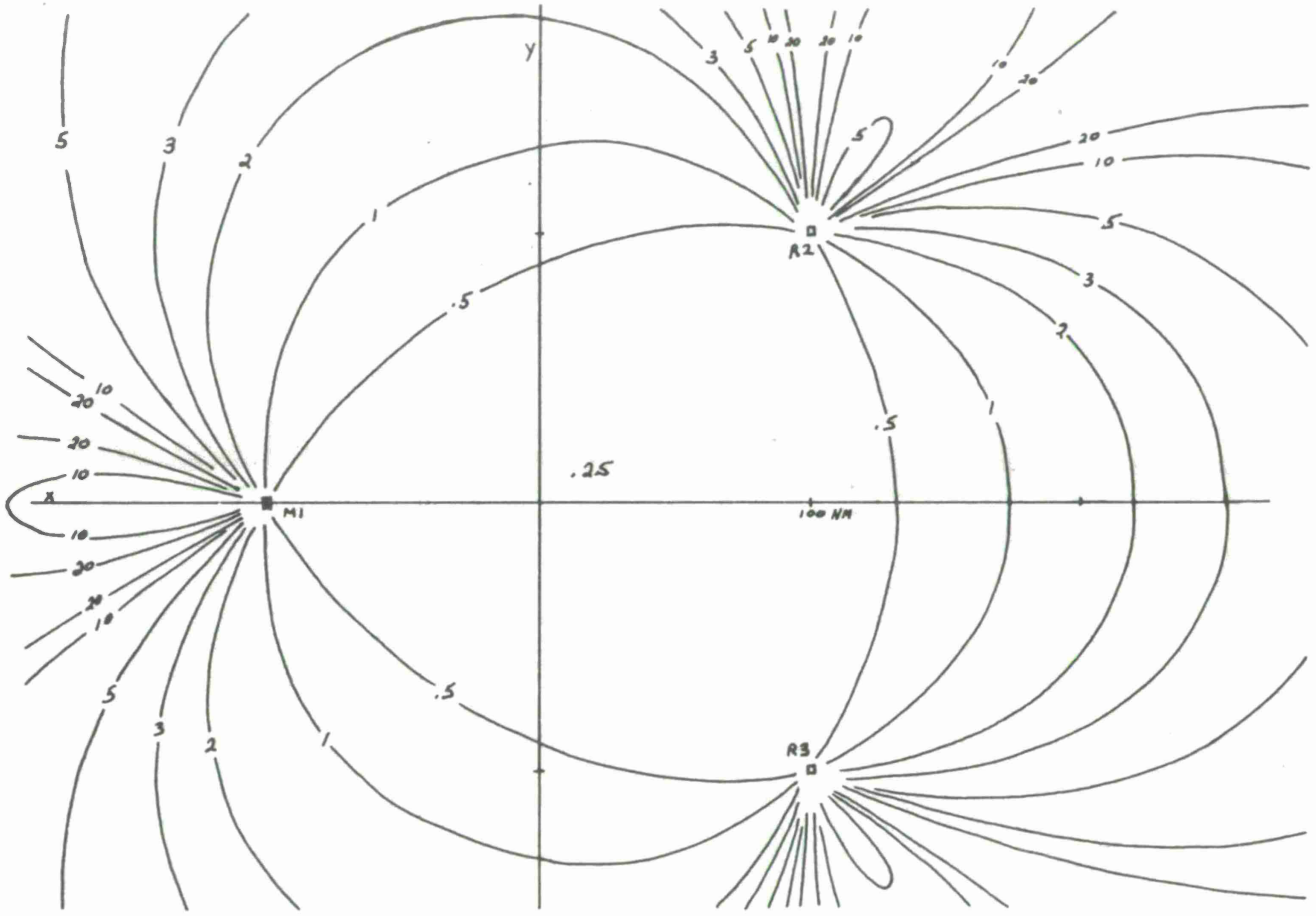

Figure 40. Geometric Dilution of Precision--Single Fix, Time. Five Reports per Frame from Each of Three Perfect References. Showing $\sigma_t/\sigma m$ versus x, y.

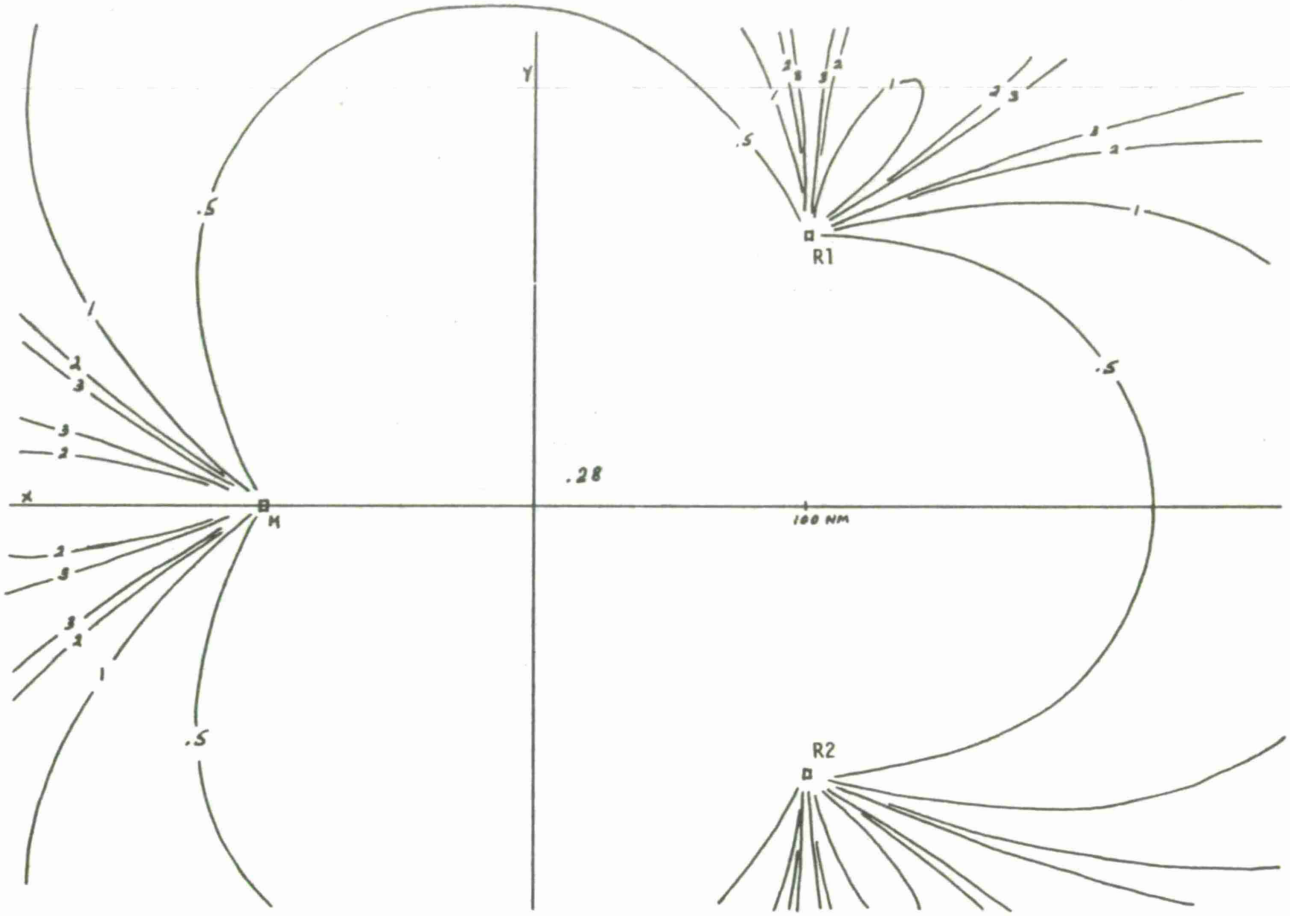

Figure 41. Direct Ranging, Theoretical Tracked Position Accuracy with Three Perfect References. Showing σ_{PT}/σ_m versus x, y. $\alpha_t = .054$, $\alpha_p = .36$

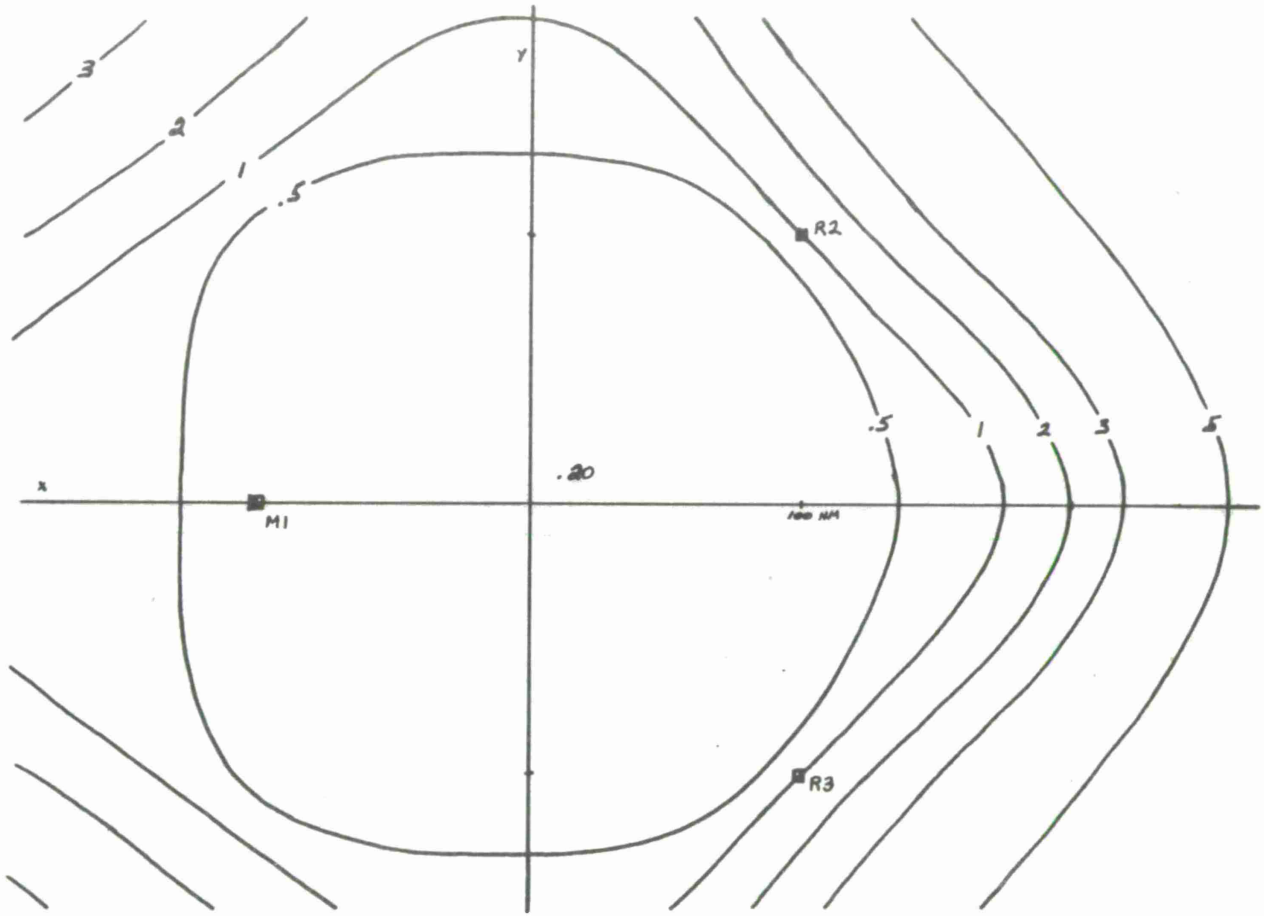

Figure 42. Geometric Dilution of Precision--Single Fix, Time. Five Reports per Frame from Three Imperfect References, plus Fifteen Airborne Sources. σ_t/σ_m versus x, y.

Notably missing are the areas of no solution, and while $\dot{g}t$ is slightly smaller in the center, it appears somewhat larger where the main lobes existed in three station operation. (Compare Figure 40) This is because in practice the majority of the airborne units did not have three station coverage. A unit experiencing a $\dot{g}t$ as shown in Figure 42 should obtain a tracking accuracy (tracked clock, direct ranging, tracked position) $\sigma PT/\sigma m$ as shown in Figure 43. The uniformity is even more pronounced. But bear in mind that the plot shows only a ratio, position error over measurement error, both unbiased. In fact, the σm will include pure measurement error plus source position error from each source. Therefore, while there may be little difference among units due to geography, there will be differences due to the nature of the sources. This may appear quite logical to the reader, but the author took some time in comprehending the situation. The subject will be continued later on in this section.

REMOTE REFERENCES - MAINTAINING SYNCHRONIZATION

Due to the strong interaction, in this run, between airborne units and reference units, it is difficult to consider one without first considering the other. That being impossible, the behavior of the time error at the references will be taken up first.

Both references were given a 30 foot position bias. This, along with other initial data, was shown in Table XIV. The position bias should induce a clock bias which in turn will introduce a bias at receiving airborne units. Because the references depend upon those same aircraft for timing information, the original bias will return as positive feedback. The airborne units, however, are also under control of the master which through feedback commands prevents too large a bias from building up. There should be a stabilization point at which the reference bias, airborne bias and master feedback balance, depending upon the smoothing parameters used. Instead of trying to predict this balance point, let's look at the results and see what happened.

Histories of the clock bias and rate errors for the two reference sites are shown in Figure 44. Both biases build up to nearly 120 nanoseconds before reversing their trend. The rate error appears to be headed back toward zero. The bias may well be stabilizing in the 100 nanosecond range. Is this the clock bias induced by the references' own thirty foot position error? I think so.

Consider the system effect of a 100 nanosecond clock bias (100 feet) plus 30 foot position error--north at R1 and west at R2. This effect, in terms of induced clock error at receiving units, is shown

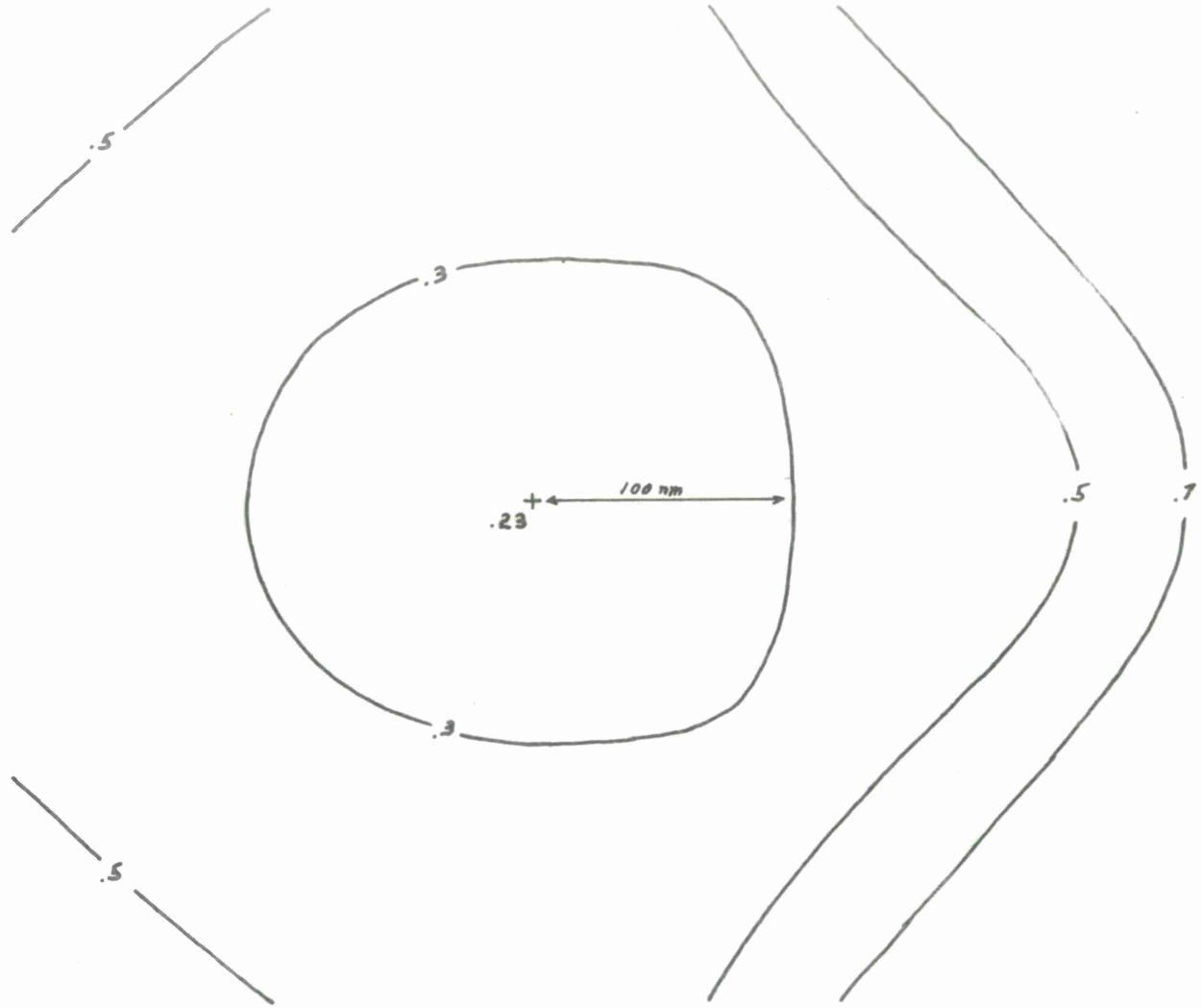

Figure 43. Contours of Tracked Position Accuracy (Direct Ranging), σ_{PT}/σ_m, Run #214 Area.

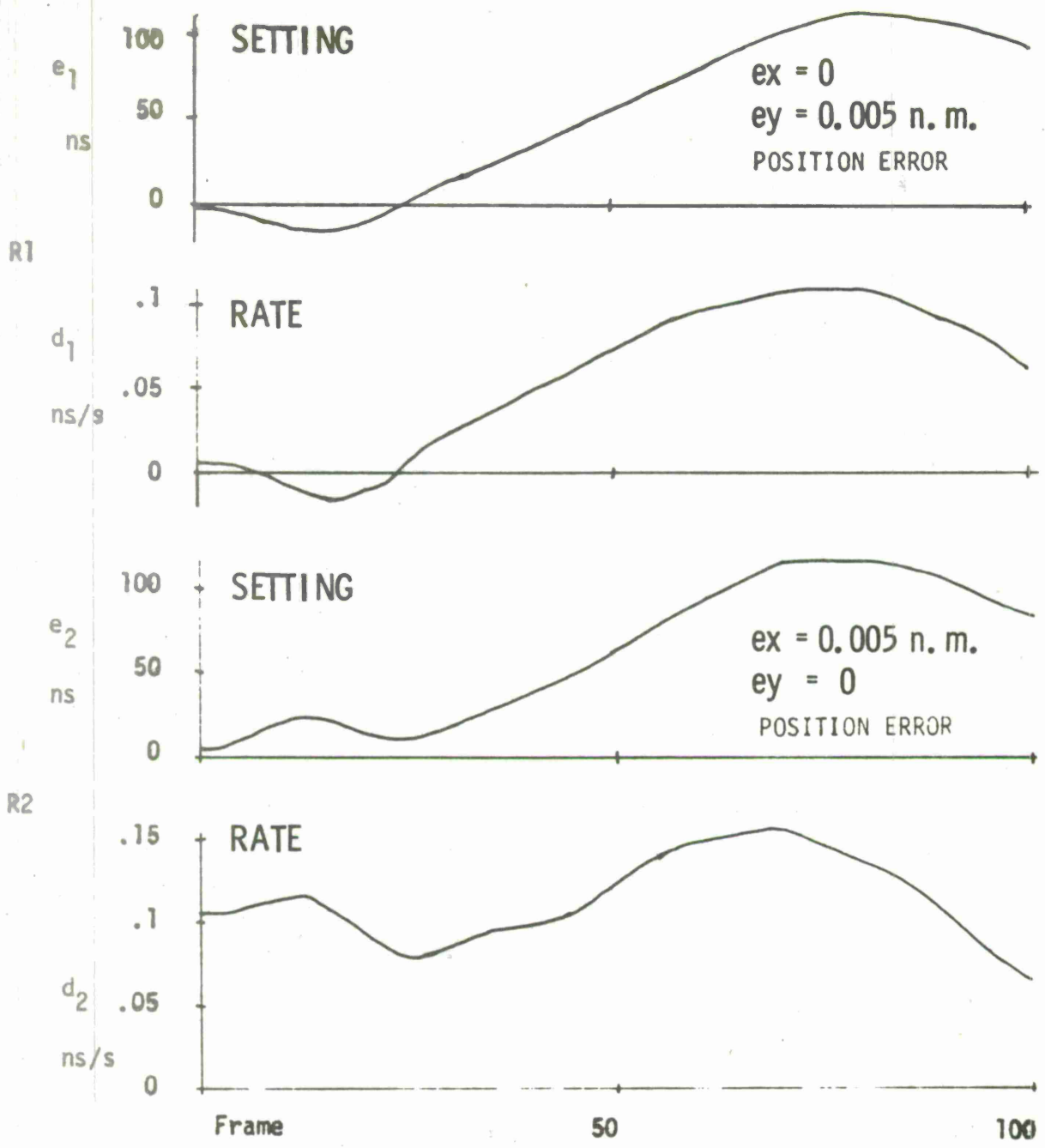

Figure 44. Reference Site Timing Error, Run #214

as a contour map in Figure 45. It can be seen that the induced bias is fairly uniform, ranging from over 85 nanoseconds to the southeast to under 60 nanoseconds to the north. In the areas occupied by data priority one units, the induced bias is between 60 and 70 nanoseconds.

Looking ahead now, the average clock bias and rate errors of all active airborne units is shown in Figure 46. Here it can be seen that the rate error has essentially returned to zero by frame 100, but that from frame 35 on, the average clock bias is in the 60 to 80 nanosecond range, curiously close to that suggested by Figure 45 as the amount induced by reference position bias.

Now if the airborne clocks are 60 to 80 nanoseconds fast (set ahead), among themselves, no error will appear except at the master. Master feedback in time is also shown (negatively) in Figure 46 (dotted line). Except for a spike in frame 25 there was a gradual buildup to -100 nanoseconds in frame 45, then a gradual reduction to about -35 nanoseconds at the end of run.

Looking ahead some more, consider the average position error of all airborne units. This is shown as $\overline{ex}$ and $\overline{ey}$ versus time in Figure 47. The buildup in $\overline{ex}$ is finally reversed in frame 52 crossing zero in frame 78. The reason for the reversal is clearly the effect of master position feedback, shown also in Figure 47 (dotted line). From frame 15 through 65, x feedback from the master was negative--combating a positive x system error.

Now, notice the system position error around frame 80. It is near zero. At this time master time feedback is about -55 nanoseconds, meaning it "sees" some 90 nanoseconds time error, essentially free of position error. This must be the time error of data priority one airborne units. The time error for all airborne units is 80 nanoseconds in frame 80 (Figure 46) and the reference sites are biased by 115. Then as the system x error goes negative the time feedback from master drops.

Thus we can see the position errors varying, and master feedback following to adjust. But the mean system time error remains quite constant. I believe this is induced by the reference bias in position.

STEADY STATE AIRBORNE ERROR PERFORMANCE

We have already seen the average error of airborne units and the effect of master feedback, in Figures 46 and 47. While averages are fine from a system point of view, they obscure individual problems. The root-mean-square position error gives a better picture of individual performance. Figure 48 shows the r.m.s. position error

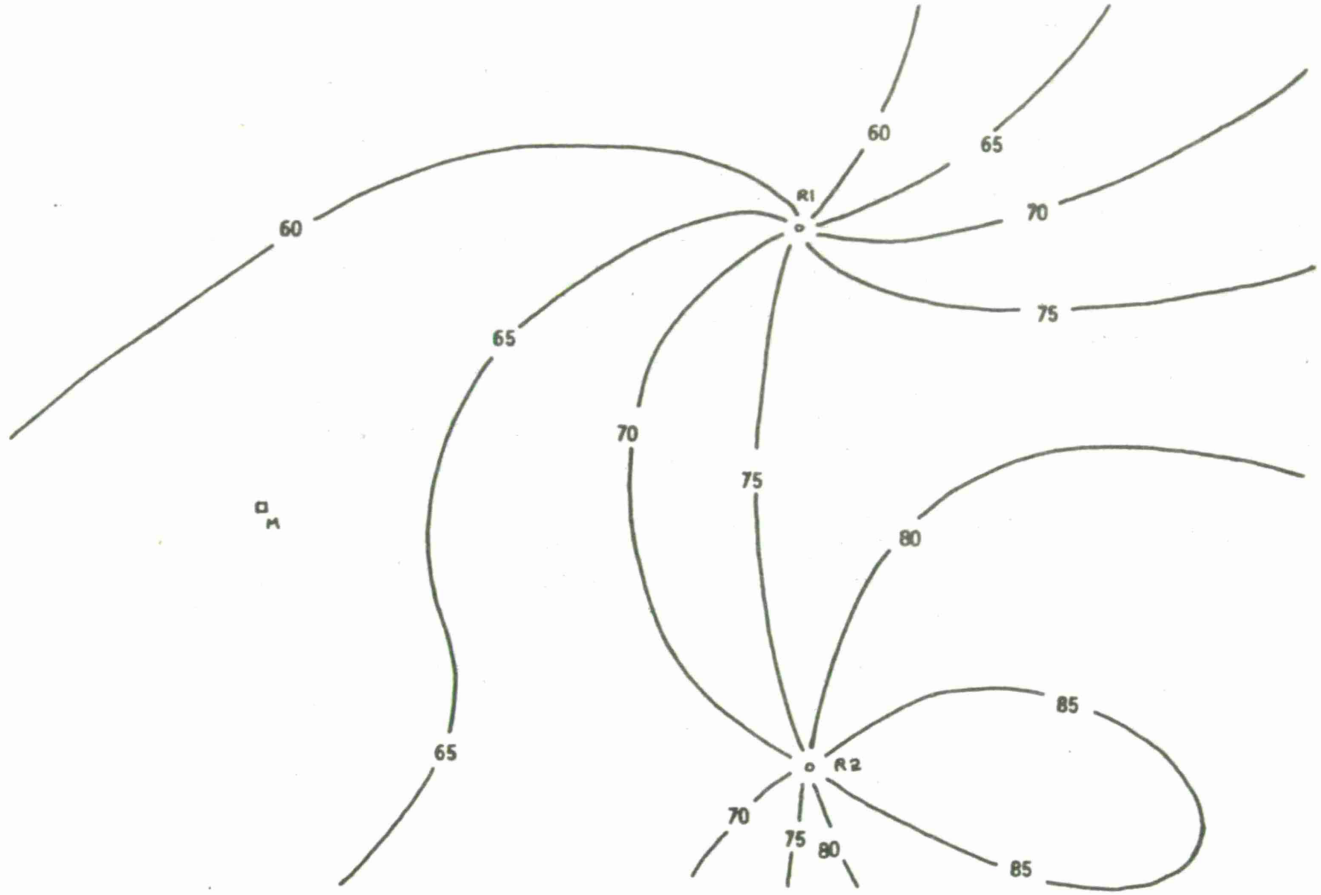

Figure 45. Clock Error Induced at Airborne Units in Triple Ground Cover due to Reference Bias of e_t = 100 n.s. and e_p = 30 feet. Expressed as e (nanoseconds) versus x, y. Run #214.

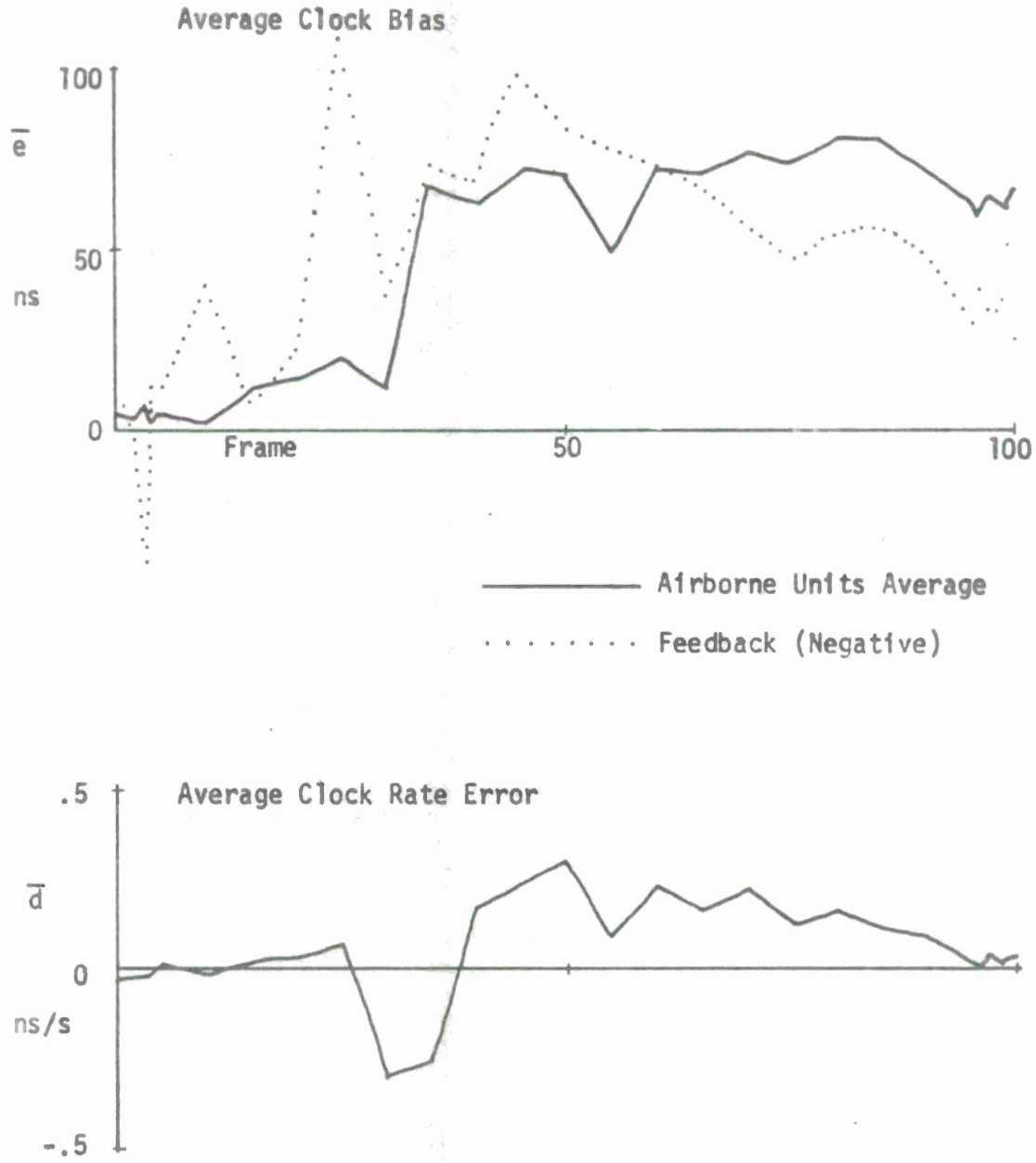

Figure 46. Average Timing Error, Airborne Units, Run #214

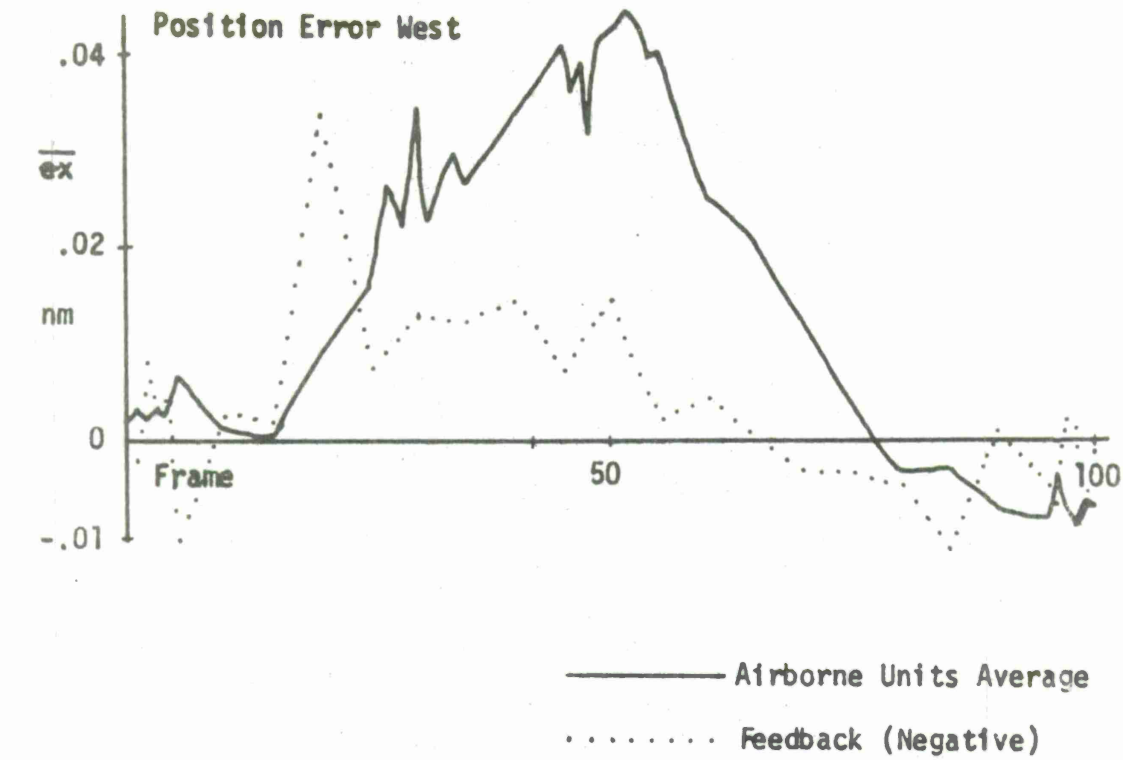

Figure 47. Average Position Error, Airborne Units, Run #214

versus time of all airborne units. In the last forty frames this is split into data priority one and data priority two groupings. Also shown in Figure 48 is the average $\dot{g}t$ versus time obtained for all airborne units and the breakdown to priority one and two. One can also get a rough correlation by referring to the position map of Figure 39 and the average gt contours of Figure 42. While there must be quite a change with time for individual units, on the average there was very little variation in $\dot{g}t$.

As can plainly be seen from this and some of the preceding figures, the run did not, in fact, start out in the steady state. Part of the trouble is due to activating poorly located units between frames 20 and 50. But more than that, the initial conditions were simply "too good." So we don't really see steady state operation until about frame 60 or 80. Certainly the last 20 to 40 frames are indicative of steady state airborne tracking performance.

It might be expected that the r.m.s. position error would be dependent upon the number of reference stations making up the data sources. To this end, the tracks were separated into six groups: priority one with three, two, and one reference sources, and priority two with two, one and zero reference sources. The r.m.s. position error for these six categories is shown in Figure 49, versus the mean $\dot{g}t$ of the group, for the periods frame 61 to 80, 81 to 100, and 61 to 100.

Among the priority one units, those with three reference sources maintained position accuracy about 50% better than those with one or two. There was a definite difference between data priority two and one with the same number of reference sources, the latter being about twice as accurate. Curiously, in both priorities, units with one reference slightly outdid those with two. Certainly with priority one, this is because the one ground source was the master station. The group with zero references sources is misleading because it represents a small sample of two units over five frames that are driving out of the system and have just lost the reference source. The difference between units driving out and carrying good time and units driving in acquiring time, but not yet as good, is demonstrated by a further breakdown of priority one units with three reference sources. It can be seen from Figure 49 that the outbound tracks are some 75% more accurate than inbound tracks, at the same point.

A theoretical position accuracy expectation curve is also shown in Figure 49. This assumes that sources have zero bias and that the only error is due to measurement, σm. The curve has been adjusted to show, roughly, the variation in sample size from 24 on the left to 12 on the right. Obviously there are more errors in the system

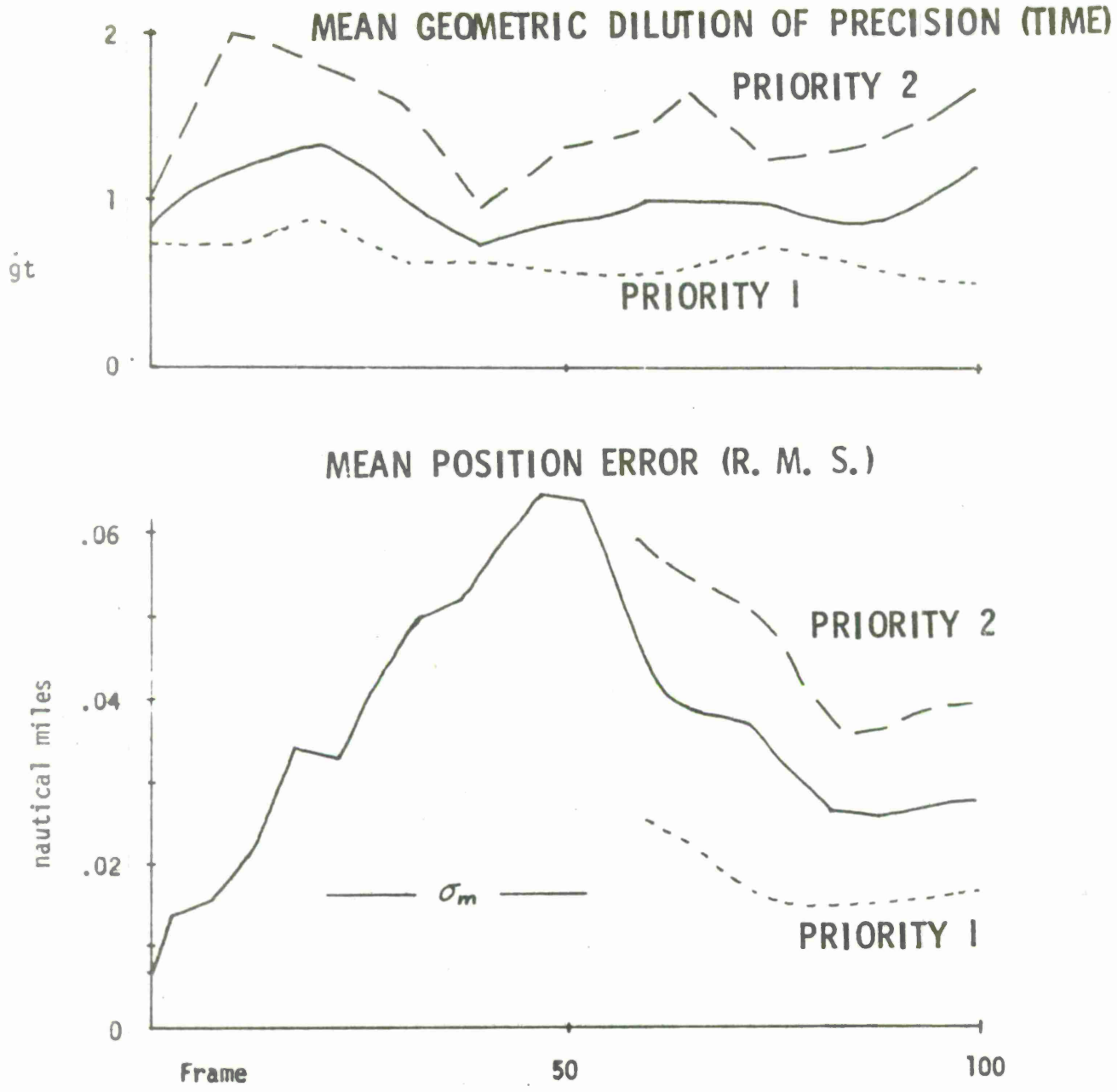

Figure 48. Position Error, Airborne Units, Run #214

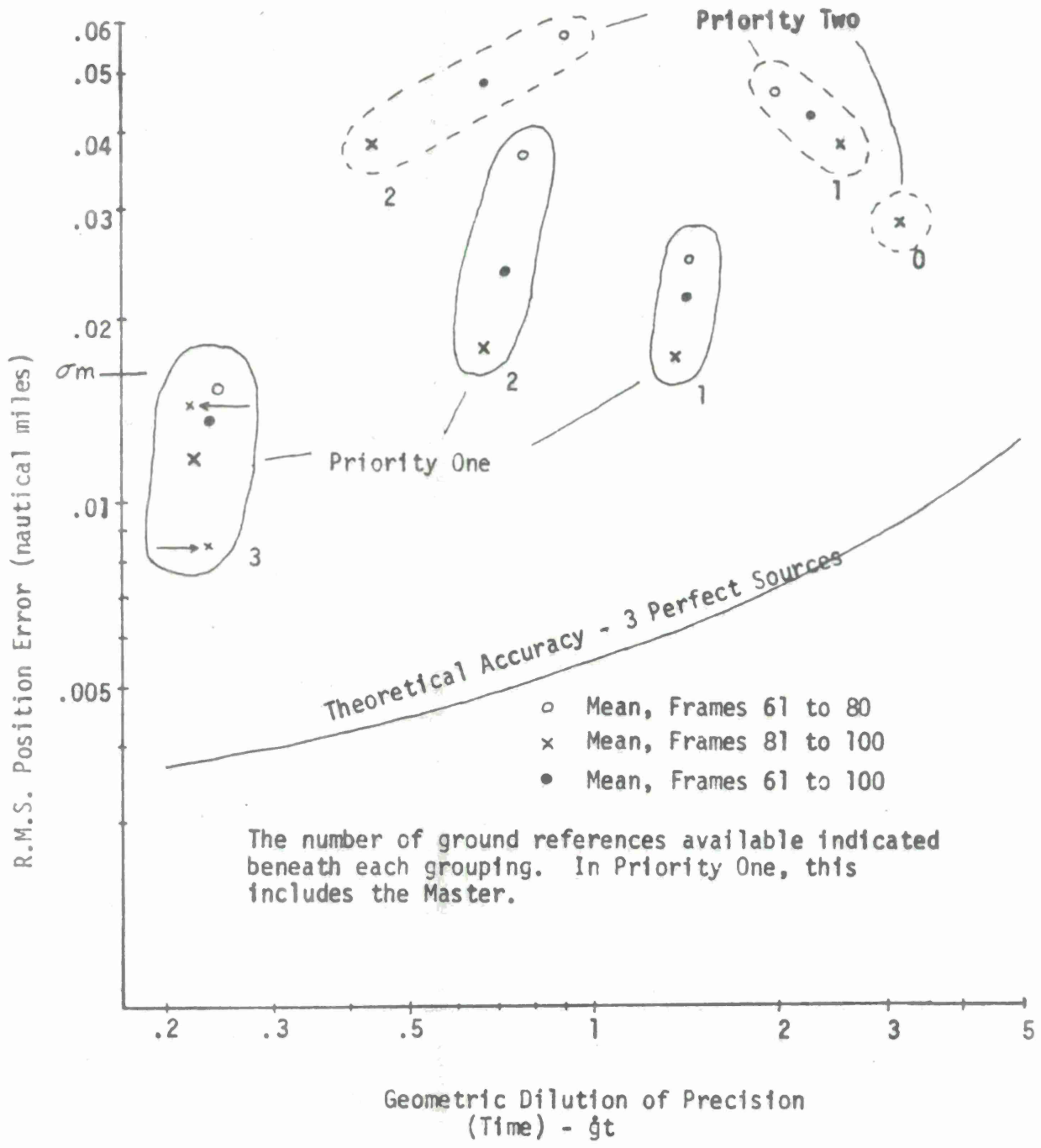

Figure 49. Tracked Position Error (r.m.s.) for several Categories of Airborne Units, versus Mean Geometric Dilution of Precision (Time). Run #214

than the measurement error. In the PLRACTA Demonstration simulations results came quite close to expectations, and were generably better. There are three important differences in the tactical area simulation.

a. References sync off airborne units, and therefore contribute larger error.

b. Random walk speed perturbation plus a ten second frame increased the effects of velocity error.

c. Airborne sources outnumbered reference sources, instead of being a small minority.

It is not known whether these factors increase the effective measurement error σm^* sufficiently to claim that results meet expectation--that is, that tracked position error σPT is the proper factor smaller than some effective σm^*. This would be true of σm^* were three times greater than the pure measurement error, σm.

Perhaps it is sufficient to note that in an apparent steady state condition (the last 20 frames), priority one units with three reference sources have r.m.s. position error significantly less than σm; that priority one units with one or two reference sources have r.m.s. position errors about equal to σm; and that priority two units have r.m.s. position error equal to twice σm.

SYNCHRONIZATION AND LOCATION WITH LARGE INITIAL ERRORS

Simulation run #214 contains fourteen units (initially passive) with very large initial position errors. The initial conditions were shown in Table XV and the starting geometry was shown in Figure 39. The synchronization and location process is illustrated by a tabular presentation of frame by frame error on three selected units. The end of frame errors are tabulated for clock setting, e, clock rate, d, position west, ex, and north, ey, speed, evp, and heading, eh.

Table XVI shows the initiation history of #A13, a maneuvering unit on data tracking. The maneuver consisted of 60 degree turns, at 2 degrees per second, in the same direction separated by 20 second straight legs. The initial error estimate is much too large, but in the right direction. From then on the corrections are orderly and in proportion to the smoothing constants, $\alpha t = .36$ and $\alpha p = .6$. The position is "found" by frame 10, though inaccurate due to being a data track. (See the following section on navigation capability of data track.) The time is "synchronized" by frame 15, though a sizable clock rate error has been induced by the succession of positive adjustments. It takes another 15 or 20 frames to iron out

Table XVI

DATA TRACK INITIATION HISTORY (#A13)

Fr	e (ns)	d (ns/s)	ex (nm)	ey (nm)	evp (knots)	eh (degrees)
0	723588	1.00	220.00	0.00	0	0
1	-2783029	1.00	-169.40	34.72	-0.84	0.02
2	-1466713	1.00	-22.75	5.84	-0.60	-20.02
3	-232992	2.00	-8.94	2.80	-0.28	-40.10
4	-98885	3.00	-3.34	1.92	-7.68	-75.07
5	-51542	4.00	-1.12	1.61	-13.79	-78.67
10	-4153	9.00	-.75	.54	-49.69	-59.44
15	-92	14.00	-.75	-.25	-79.82	-44.50
20	236	11.94	-.16	-.58	-82.22	-37.90
25	11	6.94	.48	-.39	-72.44	-38.79
30	1	3.22	.70	.29	-72.44	-39.81
35	-25	.58	.16	.73	-72.83	-38.81

Table XVII

INSTRUMENT TRACK INITIATION HISTORY (#A15)

Fr	e (ns)	d (ns/s)	ex (nm)	ey (nm)	evp (knots)	eh (degrees)
0	718252	1.00	245.000	0	0	0
1	-1351495	1.00	14.515	-4.374	1.07	-0.04
2	-144584	1.00	5.811	-1.790	.76	-0.05
3	-60384	2.00	2.342	-.730	.24	-0.09
4	-31753	3.00	.735	.040	7.73	-20.41
5	-18124	4.00	.081	.196	13.60	-22.21
10	-1534	9.00	.006	.134	-3.04	-8.69
15	105	12.80	.014	.041	-4.15	-2.25
20	167	7.80	-.040	.022	.64	-.87
25*	249	5.64	.017	.001	-5.68	-.05
30	137	3.45	-.008	.026	-3.67	-.57
35*	87	2.26	.011	.010	-3.01	-.11

* unit was active in these frames

the induced rate error.

The process is shown perhaps more clearly in Table XVII which shows in initiation history of #A15, a maneuvering unit on instrument tracking. The maneuver was alternating 120 degree turns at 4 degrees per second separated by 30 second straight legs. But with instrument tracking the error should be as smooth as a non-maneuvering track. Synchronization looks about the same as with #A13 (the process is independent of position location) synching in at 15 frames and inducing a rate error which is smoothed out in 15 to 20 more frames. In this case it can be seen that position is "found" by frame 5 or so, and that there is a corresponding induced velocity error then of 13 knots and 22 degrees which disappears in 15 frames.

One more example will be shown. This is #A21, a remote maneuvering data track, in Table XVIII. In this case the maneuver was alternating 30 degree turns, at 1.2 degrees per second, separated by 2 minute straight legs. The results are similar except that the initial adjustment is quite large in time, and takes a little longer to settle down.

NAVIGATION CAPABILITY OF AIRCRAFT WITHOUT INSTRUMENT INPUT

In the original PLRACTA concept, at least from this author's point of view, it was assumed that aircraft users who could afford computers could also afford to input velocity change information to the computer. This input could be IMU outputs, or speed and heading instrument readings, etc. Such inputs are desirable because they permit the use of smaller constants (α and β) in tracking the more slowly changing instrument bias rather than the instrument reading itself. And, it may remain a requirement that aircraft which are used as data sources be so equipped. However, the capability exists for an airborne unit to determine its speed and heading without such inputs by integrating over successive positions. In the simulation this has been labeled "data tracking." It is identical to the old SAGE tracking, except for the data sources, and is about as inaccurate. The problem is, an error in position is required to generate a change in speed or heading.

Several maneuvering units which relied on data tracking were included in simulation run #214. Portions of their track histories have been extracted for illustration. All of these were automatically activated and deactivated, which resulted in their being passive 95% of the time. Thus the smoothing constants were $\alpha = .6$, $\beta v = .084$ and $\beta h = .192$, for the most part.

Table XVIII

REMOTE DATA TRACK INITIATION HISTORY (#A21)

Fr	e (ns)	d (ns/s)	ex (nm)	ey (nm)	evp (knots)	eh (degrees)
0	975549	1.00	580.000	0	0	0
1	-6626800	1.00	-208.700	-48.780	-3.40	.12
2	-4513439	1.00	10.968	1.624	-2.60	.12
3	-2041607	2.00	4.482	.687	-4.14	.07
4	-1123412	3.00	1.737	-.032	-12.78	-8.55
5	-666213	4.00	.335	-.279	-19.80	-11.64
10	-67638	9.00	-.104	-.645	-32.05	-18.57
15	-6505	13.00	-.070	-.080	-14.90	-2.74
20	-858	17.00	.101	.029	-4.92	-.70
25	773	18.00	.009	.453	-17.74	13.78
30	202	15.00	.067	.082	-7.19	2.26
35	855	12.00	.031	.019	-1.87	-.05
40	77	12.00	-.042	-.532	-4.16	-12.27
45	192	12.82	.174	-.085	6.21	-1.80
50	-558	7.82	.197	.062	5.97	6.09

Figure 50 illustrates an 800 knot aircraft making a 90 degree, two degree per second turn. True position is shown as a dot, assumed position as a circle. The dashed vector emanating from the circle is the assumed velocity vector. The solid vector is the true velocity, shown coming from the assumed position so that velocity error is more clearly expressed. At the end of the turn, the position error has reached a maximum of 2 nautical miles, and the heading error has reached a maximum of -62 degrees. The speed error peaks out at -20 knots, some three frames later. It takes some ten frames to reduce the position error to less than 0.1 n.m. and twelve frames to reduce the heading error to less than one degree. Instrumented units in the same area were able to average an r.m.s. position error of 0.038 n.m.

Two steady state maneuver conditions are illustrated in Figure 51. The upper curve depicts a 400 knot aircraft making a series of 60 degree, two degree per second turns in the same direction, separated by 20 second straight legs. Heading error varies from a maximum of -53 degrees at end of turn to a low of -26 degrees at start of the next turn, the average lag being 40 degrees. Speed varies only slightly, ranging from a high error of -74 knots at start turn to a low error of -68 knots in the middle of the turns, averaging -71.3 knots. Position error averages .65 nm, varying from .55 nm one frame after turn start to .73 nm one frame after turn end. The steady state condition here then is that the average .65 nm position error is just sufficient to cause a 60 degree heading change in five frames. Tracking keeps up with the amount of turns but lags by 40 degrees.

The lower curve in Figure 51 depicts a similar track except that the turns alternate direction. The average position error of 0.42 nm is somewhat smaller because the true track keeps folding back across the assumed track.

Instrumented tracks in the same area as the two data tracks above had an r.m.s. position error of 0.0145 nm.

AIRBORNE EXTENSION OF NAVIGATION CAPABILITY

The seven aircraft entering the system from the east (see Figure 43) rely entirely on airborne sources for the first 28 to 42 frames of run #214. In the first few frames, they were quite busy just finding themselves, due to large initial errors. But, by frame 17, things were pretty well settled down so that's a good place to start looking collectively at the r.m.s. position error of these tracks. Two of the units were on data tracking, so they will be omitted from this consideration.

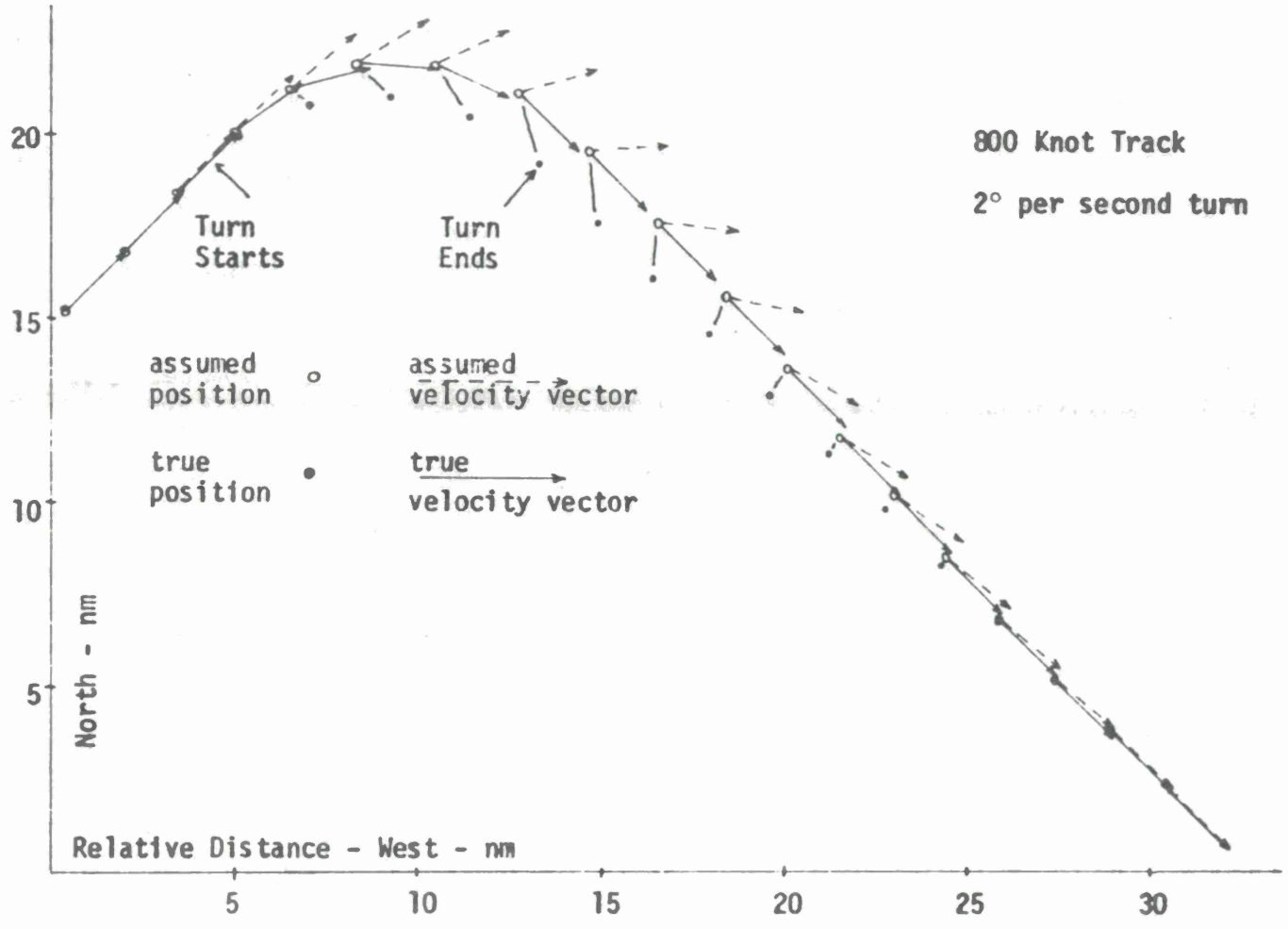

Figure 50. Example of Data Tracking Through 90° Turn

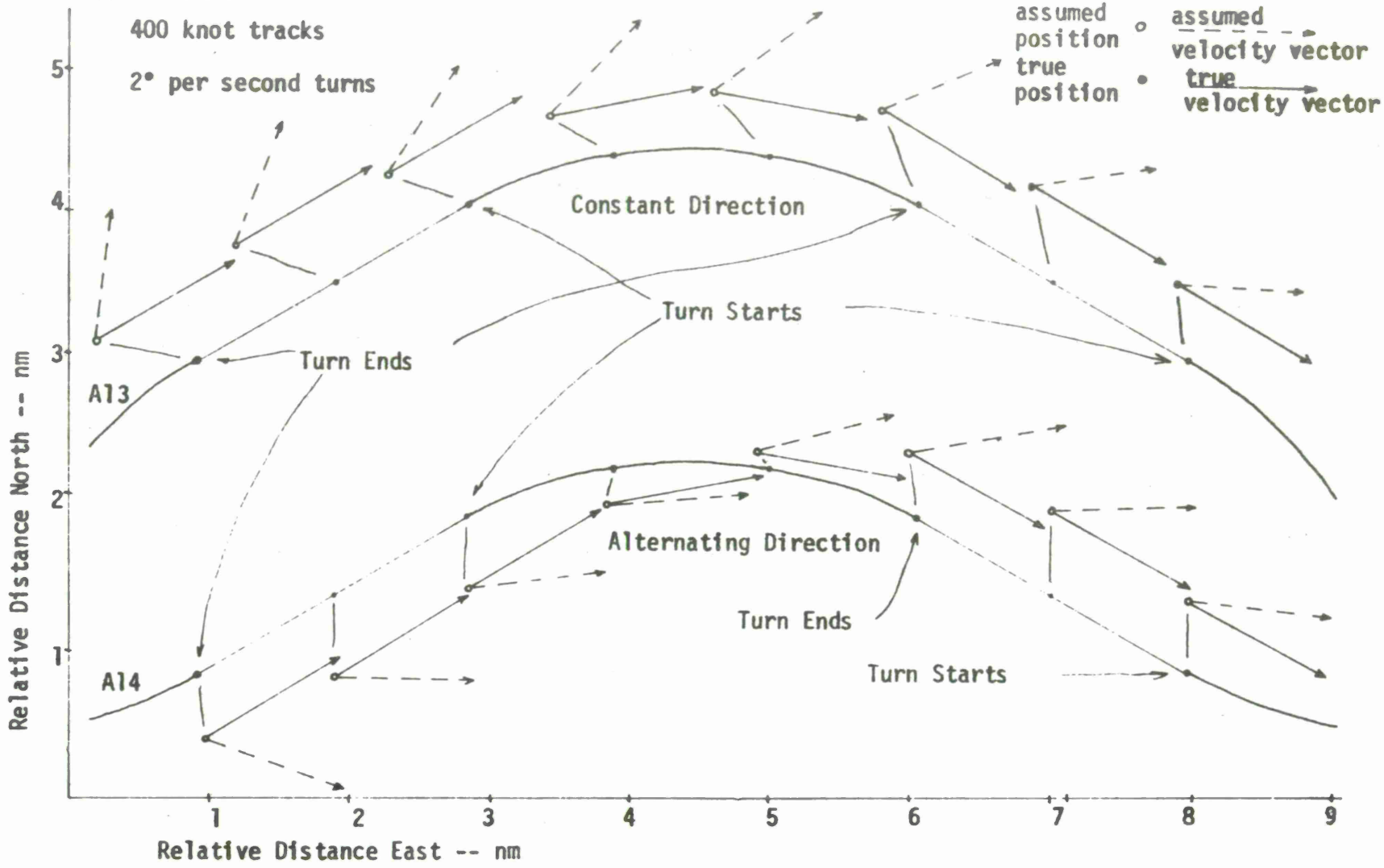

Figure 51. Steady State Tracking Condition -- Maneuvering Units on Data Tracking

In frame 17 then, and continuing for six frames, these units were data priority 3 utilizing 2 to 3 data priority one and 5 data priority two sources. The $\dot{g}p$ averaged 3.57 in this period. This period included one frame of no solution, in which an unsuccessful attempt to switch to data priority two was made. From frame 23 on, the units were data priority two utilizing 3 to 5 sources at first, progressing up to 9 sources by frame 42. The $\dot{g}p$ averaged 6.50 while operating as data priority two. The different $\dot{g}p$ was due to the fact that as a data priority three, units 2 and 3, which were themselves data priority two, could be used as sources providing improved geometry. So, over the period under consideration there was considerable variation in $\dot{g}p$, sample size, and source data priority. Yet there was little correlation between individual position errors and these variations. In fact, the errors were lowest in the early frames despite the fact the initial location had just been accomplished and operation was in data priority three. The errors were highest, however, in the frames immediately following which may reflect the delayed effect.

The r.m.s. position error of units 23, 25, 26, and 28 during frames 17 through 42, while they had available only airborne sources was 0.113 n.m.--that is 690 feet. During this time the average $\dot{g}p$ was 5.35. A smoothing constant of $\alpha = .6$ has a tracking power of $rp = 1.46$. This all implies that these aircraft were "seeing" an effective measurement error, σm^* of 0.031 nm, (from equation 54) taking the r.m.s. as σPT, the tracked position error, and assuming zero bias, which is just about twice the pure measurement error of $\sigma m = 0.0162$ nm (100 ft).

In fact, the sources were not unbiased. Refer back to Figure 47, which shows mean position error of all system tracks. It can be seen that $\overline{ex}$ is nearly zero in frame 17, but grows to 0.036 nm in frame 42. Less of a problem is $\overline{ey}$, which hovers between 0.005 nm and 0.01 nm, as the extension is along the x axis.

The relation between r.m.s. position error, source bias and measurement standard deviation is complex and will not be pursued. However, on the surface it would appear that much of the discrepancy between σm and σm^* (.016 and .031) could be explained by consideration of source bias. If so, the position error of units operating on airborne extension is quite predictable.

REFERENCES

1. R. Deutsch, Estimation Theory, Prentice-Hall, Inc., 1965.

2. R. Page and A. Bridgeman, "Studies in F-99 Command Guidance-III, Smoothing in Track-While-Scan," University of Michigan Engineering Research Institute report 1947-7-T, May 1953.

3. W. J. Nemerever, "Analysis of a Smoothing in Track-While-Scan Process," Boeing Airplane Company Document D5-2361, October 3, 1957.

4. N. P. Nelson, "A Picture of Track-While-Scan Smoothing," MITRE SR-7, Volume II, August 1959.

5. T. R. Benedict and G. W. Bordner, "Synthesis of an Optimal Set of Radar Track-While-Scan Smoothing Equations," IRE Transactions on Automatic Control, July 1962.

Security Classification

DOCUMENT CONTROL DATA - R & D

(Security classification of title, body of abstract and indexing annotation must be entered when the overall report is classified)

1. ORIGINATING ACTIVITY (Corporate author)	2a. REPORT SECURITY CLASSIFICATION
The MITRE Corporation P. O. Box 208 Bedford, Massachusetts 01730	UNCLASSIFIED
	2b. GROUP

3. REPORT TITLE

Recursive Navigation: Program Description and Characteristic Performance, as Indicated by Simulation and Analysis

4. DESCRIPTIVE NOTES (Type of report and inclusive dates)

5. AUTHOR(S) (First name, middle initial, last name)

Robert C. Snodgrass

6. REPORT DATE	7a. TOTAL NO. OF PAGES	7b. NO. OF REFS
OCTOBER 1971	122	4

8a. CONTRACT OR GRANT NO.	9a. ORIGINATOR'S REPORT NUMBER(S)
F19(628)-71-C-0002	ESD-TR-71-362
b. PROJECT NO. 5170	
c.	9b. OTHER REPORT NO(S) (Any other numbers that may be assigned this report) MTR-2143
d.	

10. DISTRIBUTION STATEMENT

Approved for public release; distribution unlimited.

11. SUPPLEMENTARY NOTES	12. SPONSORING MILITARY ACTIVITY
	Electronic Systems Division, Air Force Systems Command, L. G. Hanscom Field, Bedford, Massachusetts 01730

13. ABSTRACT

This document provides a current program description of, and shows the capabilities indicated by, the recursive navigation simulation. Two sets of simulation data are examined in some detail; one resembling the PLRACTA Demonstration testbed and one characteristic of a large tactical area with many aircraft. It will be shown that performance can be predicted with some confidence for certain specific situations.

DD FORM 1 NOV 65 1473

Security Classification

14. KEY WORDS	LINK A		LINK B		LINK C	
	ROLE	WT	ROLE	WT	ROLE	WT
AIRCRAFT POSITION LOCATION						
COMMUNICATIONS						
CONTROL OF TACTICAL AIRCRAFT						
PLRACTA						
POSITION LOCATION, REPORTING AND CONTROL OF TACTICAL AIRCRAFT						
TACTICAL AIRCRAFT COMMUNICATIONS						